INTERACTION OF VANADIUM(V) COMPLEXES WITH RABBIT MUSCLE PHOSPHOGLYCERATE MUTASE STUDIES BY ^{1}H AND ^{51}V NUCLEAR MAGNETIC RESONANCE

by

Susana Liu

B.Sc.(Honors), Simon Fraser University, 1987

A THESIS SUBMITTED IN PARTIAL FULFILLMENT

OF THE REQUIREMENTS FOR THE DEGREE OF

MASTER OF SCIENCE

in the Department

of

Chemistry

SIMON FRASER UNIVERSITY

JUNE, 1989

APPROVAL

Name: Susana Liu

Degree: MASTER OF SCIENCE

Title of thesis: Interaction of Vanadium(V) Complexes with Rabbit Muscle Phosphoglycerate Mutase Studies by ^{1}H and ^{51}V Nuclear Magnetic Resonance

Examining Committee:

Chairman: Dr. E. J. Wells

Dr. M. J. Gresser
Senior Supervisor

Dr. A. S. Tracey
Senior Supervisor

Dr. K. N. Slessor

Dr. T. J. Borgford
Internal Examiner,
Department of Chemistry,
Simon Fraser University

Date of Approval: June 27 1989

PARTIAL COPYRIGHT LICENSE

I hereby grant to Simon Fraser University the right to lend my thesis, project or extended essay (the title of which is shown below) to users of the Simon Fraser University Library, and to make partial or single copies only for such users or in response to a request from the library of any other university, or other educational institution, on its own behalf or for one of its users. I further agree that permission for multiple copying of this work for scholarly purposes may be granted by me or the Dean of Graduate Studies. It is understood that copying or publication of this work for financial gain shall not be allowed without my written permission.

Title of Thesis/Project/Extended Essay

Interaction of Vanadium(V) Complexes with Rabbit Muscle Phosphoglycerate Mutase Studies by ^{1}H and ^{51}V Nuclear Magnetic Resonance

Author: _____
(signature)

SUSANA LIU
(name)

10th July 89.
(date)

ABSTRACT

Proton nuclear magnetic resonance (^{1}H NMR) spectroscopy has been used to investigate the dephosphorylated form of the rabbit muscle enzyme, phosphoglycerate mutase (PGM) (EC.2.7.5.3). By systematically varying the pH, three resonances with a pH dependent chemical shift could be distinguished and these were assigned to histidine residues of the PGM. The behaviour of these histidines was then examined as a function of added substrate and substrate analogues such as 3-phosphoglycerate (3-PGA), 2-phosphoglycerate (2-PGA), 3-phosphonomethylglycerate (3-PMGA), inorganic vanadate (V_i) and vanadate esters of 3-PGA and 3-PMGA at pH 7.7 and 8.5. Upon the addition of aliquots of vanadate or the vanadate ester of 3-PGA to PGM at pH 8.5, two of the histidine residues showed a decrease in intensity while two new resonances appeared. The results were analyzed in terms of the binding of 2-vanado-3-phosphoglycerate (2-V-3PGA), which is postulated to act as a transition state analogue for the phosphorylation of PGM by bound 2,3-diphosphoglycerate (2,3-DPG). The two histidine residues that are affected by the binding of 2-V-3PGA are presumably the pair of histidine residues that are located within the active site of PGM. One NMR signal at 7.70 ppm that did not titrate with pH also showed a decrease in intensity upon the binding of 2-V-3PGA.

This signal was tentatively identified as deriving from an aromatic amino acid of PGM that is remote from the active site. It is suggested that this signal showed a change in resonance position because the binding of 2-V-3PGA caused a conformational change in the enzyme.

Vanadium-51 NMR spectroscopy has also been used to study the binding of 2-V-3PGA to the dephosphorylated PGM. Two molecules of 2-V-3PGA were found to bind to PGM, which consists of two identical subunits. A model of noncooperative competitive binding of divanadate ion (V_2) and 2-V-3PGA to PGM has been proposed. An intrinsic dissociation constant, estimated to be 2×10^{-11} M, was obtained for 2-V-3PGA at pH 7.0. Similar results were obtained using the vanadate ester of 3-PMGA. Weaker binding of a complex of V_i and glyceric acid was observed, and no binding of a complex of V_i and glycolic acid was observed.

DEDICATION

To my dear Mom and Dad

Their love, encouragement and support are my strength and foundation.

ACKNOWLEDGEMENTS

I would like to thank Dr. Michael J. Gresser and Dr. Alan S. Tracey, who gave me the opportunity to work in the field of vanadate as an undergraduate. Throughout the entire experience, they were always available to offer encouragement and support, while providing assistance, and guidance with their knowledge and expertise. Thank is also due to Mrs. Marcelline Tracey who obtained the NMR spectra, and to Dr. Paul Stankiewicz for valuable discussions. Last but not least, Marcia M. Craig, Dr. Huali Li, Dr. David Percival, Nelly Leon-Lai, Mandy Kao and Andrew Ma for their friendship.

TABLE OF CONTENTS

LIST OF FIGURES

LIST OF TABLES

LIST OF ABBREVIATIONS

ADP .....adenosin-5'-diphosphate
Arg .....arginine
BSA .....bovine serum albumin
2,3-DPG 2,3-diphospho-D-glycerate
dPGM .....dephosphorylated phosphoglycerate mutase
DSS .....sodium 2,2-dimethyl-2-silapentane-5 sulfonate
δ_A .....limiting chemical shifts of deprotonated C-2H
δ_{HA} .....limiting chemical shifts of protonated C-2H
EDA .....ethylene diamine
E_T .....total amount of enzyme in the solution
HEPES .....N-(2-hydroxyethyl)piperazine-N'-2-ethanesulfonic acid
His .....histidine
I .....inhibitor (vanadate ester)
K_{id} .....intrinsic dissociation constant
K_m .....Michaelis constant
LDH .....lactate dehydrogenase
Lys .....lysine
NADH .....β-nicotinamide-adenine dinucleotide (reduced)
NMR .....nuclear magnetic resonance
2-PGA D-glycerate-2-phosphate
3-PGA D-glycerate-3-phosphate
PGM .....phosphoglycerate mutase
pH* .....direct pH meter reading that have not been corrected for deuterium isotope effect at the glass electrode
Phe .....phenylalanine
PK .....pyruvate dehydrogenase
3-PMGA .....3-phosphonomethylglycerate (2-hydroxy-4-phosphonobutanoic acid)
PPi .....inorganic pyrophosphate
Ser .....serine
Trp .....tryptophan
Tyr .....tyrosine
UV .....ultra violet
V_i .....inorganic monomeric vanadate
V_2 .....inorganic divanadate
V_4 .....inorganic tetravanadate
V_T .....total vanadate in solution
V_B .....the bound vanadium atoms
$V_{B,inv}$ .....NMR invisible form of bound vanadium atoms
$V_{B,vis}$ .....NMR visible form of bound vanadium atoms
2-V-3PGA 2-vanado-3-phosphoglycerate
2-V-3PMGA 2-vanado-3-phosphonomethylglycerate

CHAPTER I

INTRODUCTION

Vanadium is found in trace amounts in many biological systems.[1] Its concentration in mammalian tissues has been found to be approximately 10^{-7} to 10^{-6}M.[2] Vanadium has beneficial effects at low concentrations in the diet, yet has harmful effects at higher concentrations.[3] The trace quantities of vanadium occuring in living tissues reflect its essential nature in a regulatory role.[3] This may be a consequence of some fundamental effect on cellular activity that represents an expression of the chemical properties of this first series transition metal. Some of the physiological effects that have been ascribed to the presence of vanadium include; its behavior as a diuretic and natriuretic, enhanced contractile ability of heart muscular tissue and increased blood oxygen tensions.[2] A common feature of these effects is that the processes concerned are either directly or indirectly linked to the activity of proteins that catalyze phosphoryl group transfer.

The physiologically relevant oxidation states of vanadium are +4 and +5 (also +3) represented by their thermally stable oxides with electronic configurations of $3d^1$ and $3d^0$ respectively.[4] The vanadium(IV) oxide is very susceptible to air oxidation and as its hydroxide $VO(OH)_2$ is very insoluble (K_{sp} = 1.08 x 10^{-22} M^3)[1] and consequently

when in this form, might not be expected to make a significant contribution to the physiological effects ascribed to vanadium present in living tissue. In the physiological pH range of pH 6 to 8, when the total vanadium concentration is less than 1 mM, the predominant vanadium(V) species in the aqueous solution are the mono, di, and tetrameric vanadates in which the metal is tetrahedrally coordinated.[1] The similarity between the chemistry of the vanadate monomer $H_2VO_4^-$ and that of phosphate is undoubtedly responsible for much of the biological activity of vanadium. V-O bond lengths in vanadate are around 0.17 nm compared to 0.152 nm for the P-O bond in orthophosphate.[5] Molecules containing longer bonds are more susceptible to the close approach of groups on other molecules capable of donating lone pair electron density and are inherently activated towards cleavage in exchange reactions. Vanadic acid H_3VO_4 (pK_a = 3.5, 7.8, 12.5) is a slightly weaker acid than phosphoric acid H_3PO_4 (pK_a = 1.7, 6.5, 12.1) and this could account in part for the preferred binding of vanadate to enzymes.[6]

A variety of mechanisms for phosphoryl transfer have been proposed[7] and are summarized in Figure I.1.

I. The overall reaction to yield products.

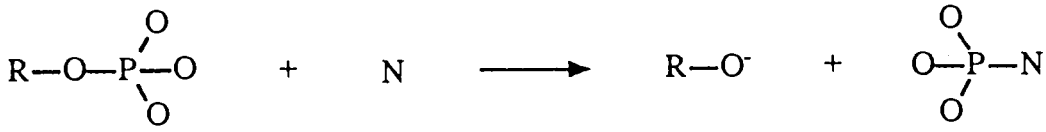

II. Proposed reaction sequences.

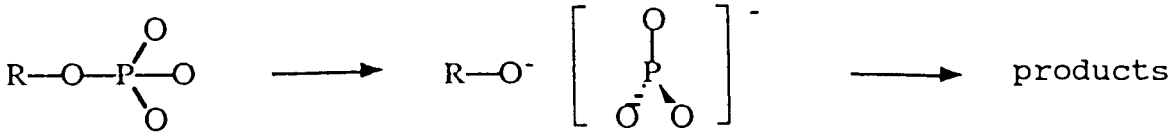

A. Dissociative via a monomeric metaphosphate.

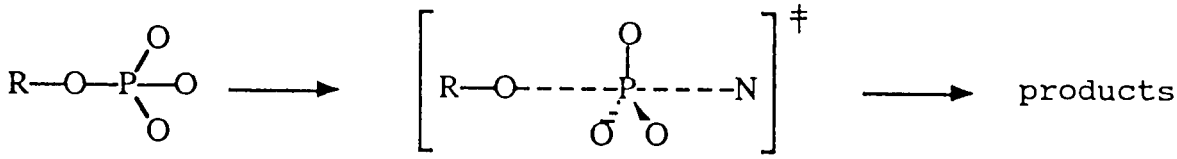

B. Associative via a pentacoordinate transition state.

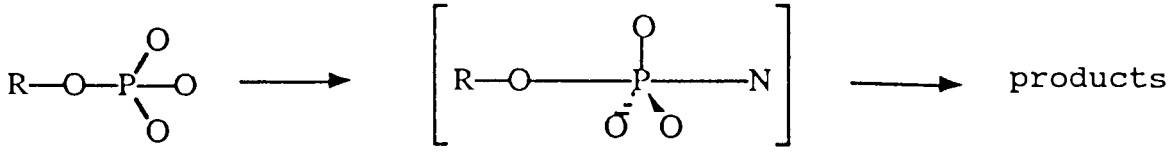

C. Associative via a pentacoordinate intermediate.

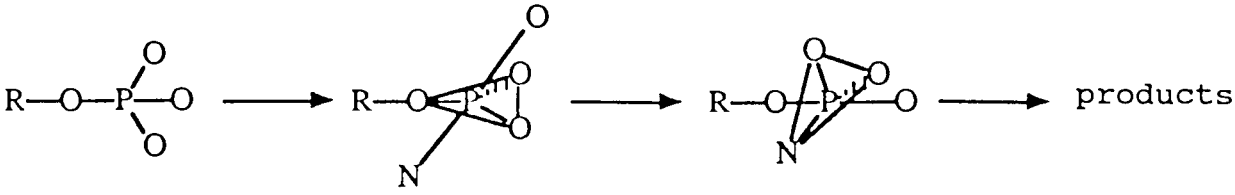

D. Associative via a pentacoordinate intermediate and pseudorotation.

Figure I.1 Proposed mechanisms of phosphoryl transfer.[7]

The metaphosphate mechanism, A, in which bond breaking occurs before bond formation is analogous to that of an S_N1 type of mechanism in carbon chemistry. This

mechanism can in principle proceed with inversion of configuration or racemization, depending on the lifetime of the metaphosphate species. The in-line associative mechanism, B, proceeding via a pentacoordinate transition state, is analogous to the S_N2 type of the mechanism in carbon chemistry. It proceeds via a trigonal bipyramidal species, as do the other associative processes, and leads to inversion of configuration. The second associative mechanism, C, proceeds via a pentacoordinate species which may have a lifetime long enough to undergo one or more pseudorotations before the leaving group departs. A pseudorotation involves a reorganization of the phosphorus ligands to allow the leaving group to take up the apical position. Thus this mechanism can either proceed with retention (if accompanied by a pseudorotation) or inversion of configuration. The adjacent associative mechanism, D, involves attack at a position adjacent to the leaving group. The pentacoordinate intermediate undergoes a pseudorotation and the leaving group departs from an apical position. This mechanism results in retention of configuration. Numerous studies of the stereochemistry of enzymic phosphoryl transfer reactions have led to the proposal that these reactions occur via the in-line associative mechanism whereby the leaving group must leave from an apical position, 180° from the incoming nucleophile with no pseudorotation as shown in mechanism B, Figure I.1.

Vanadate forms stable products with a five coordinate trigonal bipyramidal geometry. This resembles the transition state structure proposed for the phosphoryl transfer reactions as depicted by the in-line association mechanism and is formed by vanadate much more readily than by phosphate. This property has been used to account for the binding of vanadate to enzymes that participate in phosphoryl group transfer.

Vanadate spontaneously esterifies hydroxyl groups in the millisecond timescale.[8-12] Vanadate present at only micromolar concentrations is a potent competitive inhibitor of many enzymes.[13] Interference in a phosphoryl transfer step to a specific active site residue may be what confers upon the enzymes their sensitivity to the presence of vanadate and/or vanadate esters. The low concentrations of vanadate ester spontaneously forming from free vanadate could mimic the normal phosphate ester substrate. The ester, which may be a factor of 10^6 lower in concentration than the substrate, is able to act competively by virtue of binding as a transition state analogue at the enzyme active site.

A vanadate/uridine/ribonuclease complex has been studied by neutron and X-ray diffraction.[14,15] A trigonal bipyramidal structure about the vanadium in the enzyme complex is evident, in accord with the predictions

concerning the role of vanadium oxyanions as transition state analogues.[5]

The oxidation of glucose by β-NADP$^+$ (catalyzed by the enzyme glucose-6-phosphate dehydrogenase) is activated in the presence of vanadate. This observation has been rationalized in terms of the formation of a labile vanadate ester of glucose serving as a better substrate than glucose.[11] Activation of enzyme catalysis by vanadate in conjunction with the dephosphorylated substrate may provide a useful synthetic route to compounds otherwise difficult to obtain simply because their phosphorylated precursors are not available.

The glycolytic enzyme phosphoglycerate mutase (PGM) catalyzes the interconversion of D-glycerate-3-phosphate (3-PGA) and D-glycerate-2-phosphate (2-PGA) as shown in Equation I.1.

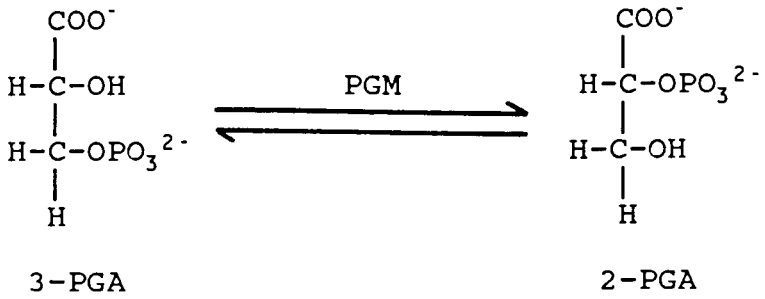

3-PGA 2-PGA

I.1

There are two classes of PGM that can be distinguished mechanistically. The PGM from animal sources and from yeast (EC. 2.7.5.3) show an absolute requirement for the cofactor 2,3-diphospho-D-glycerate (2,3-DPG), and

such enzymes catalyze the intermolecular transfer of phosphoryl groups amongst the two substrates and the cofactor.[17] This class of mutases has been shown to form a phosphorylenzyme, the phosphoryl group of which may be transferred to 2-PGA or 3-PGA or (much more slowly) to water. It appears that the cofactor, 2,3-DPG, is required to maintain the enzyme in its active phosphorylated form.

In contrast to animal and yeast enzymes, the phosphoglycerate mutase from wheat germ and rice germ (EC.5.4.2.1) shows no cofactor dependence, and catalyzes an intermolecular transfer of the phosphoryl group.[17]

The 2,3-DPG dependent mutases, with the exception of yeast enzyme, are dimers of relative molecular mass in the range of 54,000 to 60,000; yeast phosphoglycerate mutase is a tetramer of relative molecular mass 110,000.[18] Thus the molecular masses of the subunits of these enzymes are very similar.

Both the amino acid sequence[19] and the high-resolution X-ray structure[20] of yeast PGM have been determined. The amino acid sequence shows that there are four histidine residues per subunit. The mutase reaction of both the yeast and rabbit muscle enzymes proceeds via a phosphohistidine intermediate[21]. A comparison of the amino acid sequences of the active site peptides from rabbit muscle and to those from yeast PGM shows that the active site peptides, which contain histidine residues, are

virtually identical.[22,23] The structural homology between the yeast and rabbit muscle enzyme active sites is consistent with their having a very similar if not identical reaction mechanism.

Studies of rabbit muscle PGM have shown that there are two active site histidine residues per enzyme subunit.[23] The complete amino acid sequence and the X-ray crystal structure of rabbit muscle PGM have not been published. However, the amino acid compositions of a few closely related cofactor dependent mutases have been studied. The number of aromatic amino acid residues per subunit are summarized in Table I.1. These results suggest that rabbit muscle PGM might contain between 4 and 8 histidine residues per subunit.

Table I.1 Number of Aromatic Amino Acid Residues per Subunit of Cofactor Dependent PGM.

Sources	His	Trp	Tyr	Phe	Ref.
Yeast	4.0	4.5	8.3	5.8	19
Chicken breast muscle	5.3	5.6	8.3	5.8	24
Human Erythrocyte	7.5	4.5	6.5	6.5	25

Abbreviations: His, Histidine; Trp, Tryptophan; Tyr,Tyrosine; Phe, Phenylalanine; Ref, references.

Based on the crystallographic studies of yeast PGM,[21] it is now generally accepted that all cofactor-dependent phosphoglycerate mutases have a unique pair of histidine residues located within the active site that are approximately 0.4 nm apart. The planes of the two imidazole groups are almost parallel to each other and are positioned close to the C-2 and C-3 positions of the substrate as shown in Figure I.2.

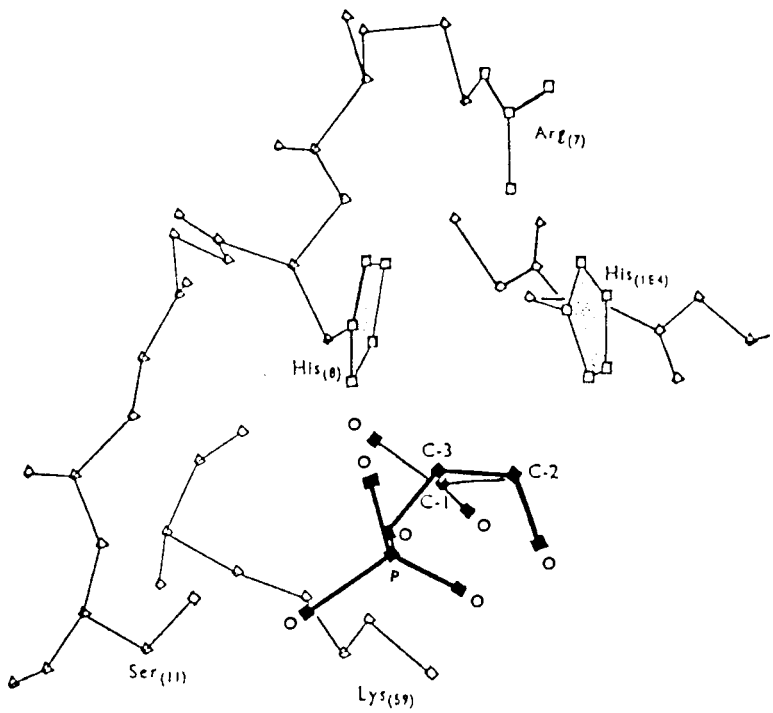

Figure I.2 Drawing of the active site of yeast PGM. A substrate, 3-PGA, and some of the side chains that approach it are shown (reproduced from reference 27).

Rose et.al.[28] were able to isolate only one form of the phosphoryl enzyme. However, the existence of a second

phosphorylated form cannot be excluded as it may have a very short half-life. It has been shown that the PGM reaction catalyzes involves an intermolecular shuttling of phosphoryl groups amongst the two substrates and the cofactor with an overall retention of configuration at the phosphate.[17] As noted previously, phosphoryl transfer in enzyme systems is considered to occur by an in-line associative mechanism and therefore results in an inversion of stereochemistry. Thus the mechanism of phosphoryl transfer catalyzed by PGM can either be (i) a double displacement phosphoryl transfer with one histidine within the active site participating in the phosphoryl transfer via a phosphohistidine intermediate or (ii) a triple displacement phosphoryl transfer in which each of the phosphoryl group transfer reaction between the enzyme and substrate occurs with inversion while the interhistidine phosphate shuttling occurs with retention of configuration. The latter process requires a pseudo-rotation mechanism of phosphoryl transfer. The purpose of this work is to study the histidine residues that are located within the active site of rabbit muscle PGM by ^{1}H NMR spectroscopy.

In addition to the normal catalytic activity, PGM has been reported to catalyze (i) the formation of 2,3-DPG from 1,3-DPG in the presence of 3-PGA,[29] the reaction normally catalyzed by biphosphoglycerate synthase (EC.2.7.5.4) and (ii) the hydrolysis of 2,3-DPG by an intrinsic phosphatase activity (which involves a hydrolysis

of the phosphorylated enzyme followed by the phosphorylation of the dephosphorylated enzyme by 2,3-DPG). These activities apparently are much less important than the mutase activity. The synthase activity, for example, is only about 1% of the mutase actvity.[30] The phosphatase activity has been invoked to rationalize the decrease in 2,3-DPG concentration inside erythrocytes incubated with vanadate.[13] This lowered concentration of 2,3-DPG, a regulator of oxygen transport in erythrocytes, may be the explanation for increased oxygen affinity of whole human blood after incubation with vanadate.[31] A therapeutic agent which leads to an increase in the oxygen affinity of blood may prove valuable in the treatment of the symptoms of sickle cell anemia. Vanadate may therefore be useful in treating this disease, especially in view of the elevated 2,3-DPG level inside red cells.[32]

The molecular mechanism of the vanadate activated 2,3-DPG phosphatase activity of rabbit muscle PGM has been studied and it has been proposed from ^{51}V NMR spectroscopy studies that one divanadate ion (V_2) binds to each of the two identical subunits of PGM in a noncooperative manner.[33] An interesting comparison between V_2 and pyrophosphate as activators of the 2,3-DPG phosphatase activity of PGM can be drawn from enzyme kinetic studies. Both pyrophosphate and V_2 cause similar maximum phosphatase rates, however, the K_m for V_2 is 3×10^{-5} M whereas that of pyrophosphate is 2×10^{-2} M.

These K_m values possibly do not correspond to dissociation constants, but they probably do give a measure of the relative affinities of V_2 and pyrophosphate for PGM. The nearly 10^3 fold lower K_m for V_2 is consistent with the adoption of a trigonal bipyramidal structure by at least one of the vanadium atoms. Thus, the phosphoenzyme form of PGM has a high affinity for transition state analogs of the phosphorylation reaction. This indicates that PGM, in addition to maintaining an active site phosphorylhistidine, has another functional group at the active site which can stabilize the pentacoordinate structure of vanadate. This is consistent with the triple displacement mechanism of the phosphate group transfer in which both histidine residues in the active site are involved.

The pre-steady state inhibition studies of rabbit muscle PGM show that vanadate inhibits mutase activity in a time dependent manner, requiring several minutes for the establishment of a steady-state level of inhibition.[34] Only pre-incubation mixtures containing vanadate, 3-PGA and PGM produce a maximal level of inhibition at the start of the reaction. This strongly indicates that both vanadate and 3-PGA are required in order to form a strong inhibitor species. Steady-state kinetic studies show that inhibition of the mutase activity is enhanced by either increasing the concentration of vanadate or 3-PGA, and that the inhibition is competetive with 2,3-DPG. This inhibition data and the

corroborative NMR results, which show there is spontaneous ester formation between vanadate and 3-PGA,[35] are consistent with the hypothesis that the true inhibitor is 2-vanado,3-phosphoglycerate (2-V-3PGA). This species is competetive with 2,3-DPG. Double reciprocal plots of kinetic data are linear in the absence of 2-V-3PGA, but are markedly curved in the presence of the inhibitor. This curvature has very recently been traced to an effect of 2,3-DPG concentration on the V_i-catalyzed oxidation of NADH (Kathryn Skorey, Paul Stankiewicz and Michael Gresser, unpublished results). Including superoxide dismutase in the reaction mixture to inhibit the V_i-dependent NADH oxidation eliminated the curvature of the double reciprocal plots. This will make it possible to interpret the kinetic studies, when they are repeated with superoxide dismutase present.

The purpose of this study is to investigate the binding of 2-V-3PGA and other vanadate esters to rabbit muscle PGM by ^{1}H and ^{51}V NMR spectroscopy.

CHAPTER II

^{1}H NMR STUDIES ON HISTIDINE RESIDUES OF RABBIT MUSCLE PHOSPHOGLYCERATE MUTASE

II.A THE USE OF ^{1}H NMR SPECTROSCOPY TO INVESTIGATE ENZYME STUCTURES AND MECHANISMS

Over the past few years, the use of ^{1}H NMR spectroscopy as a tool for determining the structural characteristics of small proteins has increased dramatically.[36] In a typical experiment, spectra are obtained from D_2O solution so that the exchangeable protons are replaced by deuterium. This procedure simplifies the spectra to a significant extent. High field spectrometers (corresponding to a proton resonance frequencey of 400 MHz or higher) and the advent of 2D-NMR techniques have allowed the amino acid sequence and 3-dimensional structures of many small proteins to be determined.[36] However in proteins having a molecular weight of above 20,000, the ^{1}H NMR spectrum, even at high field, generally consists of a broad envelope between 0 and 7 ppm. On the low field side of that envelope, the histidine C-2H resonances are often well resolved.[37] The functional significance of histidine residues and the ease with which they are resolved has led to a large number of studies of this spectral region. The pH dependences are observed in the spectral features of

amino acids with ionizable side chains.[38] An important example in practice is the pH dependence of the chemical shift of the imidazole ring proton as described by Equation II.1.

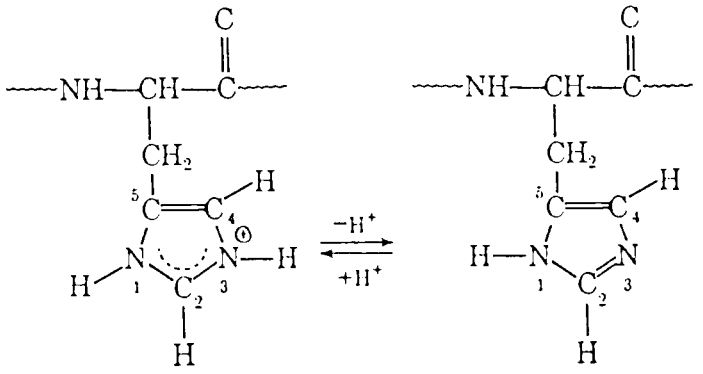

II.1

The pK_a values for the imidazole ring fall within the physiological pH range and protonation-deprotonation reactions of histidine appear to be essential for numerous enzyme reactions.[39] Among the methods available for identifying a particular amino acid,[39] the best known is the identification of the C-2 and C-4 proton resonances of histidine by the upfield shift which occurs on ionization of the histidine side chain. Monitoring the ^1H NMR spectrum as a function of pH allowed identification of all the histidine signals from those histidine residues that are accessible to water. Subsequent titration of the enzyme with substrate analogues indicated the histidine signals that are derived from those histidine residues in the active site of PGM.

II.B EXPERIMENTAL PROCEDURES

II.B.1 Materials

All reagents used were reagent grade chemicals and were used without further purification. The following chemicals and enzymes were obtained from Boehringer Mannheim: PGM, enolase, pyruvate kinase (PK) and lactate dehydrogenase (LDH) are ammonium sulfate suspensions from rabbit muscle; β-nicotinamide-adenine dinucleotide (reduced) (NADH) (disodium salt, grade II); 3-PGA (trisodium salt, grade I); 2-PGA (trisodium salt); 2,3-DPG (pentacyclohexylammonium salt); glycolate-2-phosphate (tricyclohexylammonium salt); and N-2-hydroxyethylpiperazine-N'-2-ethanesulfonic acid (HEPES).

Adenosine-5'-diphosphate (ADP) (sodium salt, grade IX from equine muscle); bovine serium albumin (BSA) (crystallized, lyophilized); DCl (20% solution in D_2O); NaOD (30% solution in D_2O); imidazole (crystalline, grade I) and glycolic acid (free acid) were obtained from Sigma Chemical Co..

Sodium pyrophosphate; ethylene diamine (EDA); phenol reagent solution (Folin-Ciocaiteau, 2N); and cupric sulfate were obtained from Fisher Scientific Co.. NaOH and KCl were obtained from BDH Chemicals.

Glyceric acid (calcium salt dihydrate) and vanadium (V) oxide (99.999%, gold label) were obtained from Aldrich Chemical Co.. Ethylene diamine dihydrochloride, sodium

vanadate (meta) and $MgSO_4$ were obtained from Matheson, Coleman & Bell.

Sodium tartrate and Na_2CO_3 (anhydrous) were obtained from G.Frederick Smith Chemical Co.. D_2O was obtained from two sources: MSD Isotopes and ICN Biomedical, Inc.. 2-Amino-4-phosphonobutyric acid (dicyclohexylammonium salt) was a gift from M.Gelb and E.Black of The University of Washington.

II.B.2 Preparation of Vanadate Stock Solutions

Stock solutions of 0.1 M NaH_2VO_4 were prepared by dissolving vanadium(V) oxide in 1 molar equivalent per vanadium atom of 1.0 M aqueous NaOH. The resulting orange solution was allowed to stand overnight during which time it become colorless. It was then diluted to 0.1 M vanadium atom concentration with distilled H_2O.

II.B.3 Preparation of 2-vanado-3-phosphoglycerate

The interaction of vanadate and 3-PGA has been studied by ^{51}V NMR spectroscopy[35] and the formation of 2-vanado-3-phosphoglycerate (2-V-3PGA), as described in Equation II.2, was observed. The formation constant determined for this reaction was 2.5 M^{-1}.

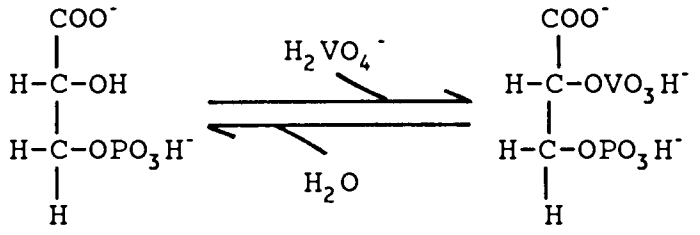

II.2

3-PGA 2-V-3PGA

Stock solutions of 2-V-3PGA were prepared by combining appropriate quantities of vanadate and 3-PGA stock solutions to give the desired final concentrations of 2-V-3PGA as required by Equation II.3. The solutions were then diluted to near the final volume and the pH was adjusted to the desired value by addition of 0.1 M NaOD solution. This procedure avoided exposure of the vanadate solution to acid conditions and the subsequent formation of decavanadate which undergoes only slow hydrolysis under neutral pH conditions.

$$[\text{2-V-3PGA}] = 2.5\ M^{-1}\ [\text{3-PGA}][V_i] \quad \text{Equation II.3}$$

II.B.4 Instrumentation

^{1}H NMR spectra were obtained with a Bruker WM-400 NMR spectometer. Sweep widths of 4000 Hz, 60° pulse angles,

256 scans and 32K data sets were used for all spectra. The strong signal from residual HDO was removed by using a gated decoupling technique.

Samples were contained in Wilmad 5 mm precision bore nuclear magnetic resonance tubes with coaxial inserts containing the external standard, DSS (sodium 2,2-dimethyl-2-silapentane-5 sulfonate) in D_2O. All chemical shifts are given in ppm from this external DSS reference. All spectra were obtained at ambient temperature.

II.B.5 Preparation of Phosphoglycerate Mutase for ^1H NMR Studies

A suspension of PGM in aqueous ammonium sulfate was centrifuged, the supernatant discarded, and the pellet dissolved in 0.5 ml buffer containing 20 mM ethylene diamine dihydrochloride (EDA) and 1.0 mM glycolate-2-phosphate in D_2O to give a concentration of PGM of about 10 mg/ml. The resulting solution was then dialyzed for 6 to 8 hours at 4°C against a similar buffer containing no glycolate-2-phosphate. Several changes of dialysate over a period of 3 days served to replace the exchangeable protons by deuterium. Protein concentration was determined before and after the experiments by either absorbance index (1.0 mg/ml at 280 nm) of 1.48/cm[26] or by the method of Lowry.[40] The enzymes were assayed, as decribed in the Appendix I, before and after the NMR experiments.

II.B.6 pH Titration

pH measurements of PGM solutions were made at room temperature using an Accumet 910 pH meter from Fisher Scientific with an extra long calomel microcombination electrode. The meter was calibrated with two freshly opened pH standards bracketing the pH reading. The pH values given are the actual meter readings and have not been corrected for the deuterium isotope effect at the glass electrode. The notation pH^* is used to indicate direct pH meter reading.

pH adjustments were made by adding 0.05-0.1 N NaOD and 0.05-0.1 N DCl delivered from a micrometer syringe. The pH was measured both immediately before and immediately after obtaining the NMR spectra. The values reported are the average of the two measurements. If the difference in pH^* reading of a sample before and after recording a spectrum was greater than 0.05 pH^* unit, the results were not accepted. In general the agreement was better than 0.04 pH^* unit.

II.B.7 Ligand binding studies

Solutions were made by introducing the appropriate amount of a freshly made ligand stock solution in buffer (D_2O) into a 10 mg/ml PGM solution by a micrometer syringe. The pH of these solutions were adjusted carefully to the

desired values and the mixtures were stirred for 45 minutes before the NMR spectra were obtained.

II.C Result and Discussions

II.C.1 pH Titration of the Phosphoglycerate Histidine Residues

Figure II.1.A shows a full ^1H NMR spectrum of dephosphorylated PGM (dPGM) at pH* 7.70. The part of the spectrum of interest here is the aromatic region, lying between 6 and 9 ppm, and in particular the region in which the C-2H histidine signals resonate. These are found downfield of the main aromatic envelope at about 7.5 - 8.0 ppm and are typically recognized by their downfield shifts of about 1 ppm as the imidazole ring becomes protonated. The expansion of the low field region in Figure II.1.B shows the C-2H resonances of the histidine moieties. The C-4H resonances of histidine occur in the region of high aromatic signal intensity and are buried under the large envelope of phenylalanine, tyrosine, and tryptophan resonances.

Figure II.2 shows that the region 7.0 - 9.5 ppm of the ^1H NMR spectrum of dPGM contains three C-2H resonances whose position depends upon pH. Since the complete amino acid sequence of rabbit muscle PGM has not been studied, the assignment of the histidine resonances cannot be made from the amino acid's position in the amino acid sequence. The histidines therefore are referred to as His A, B and C

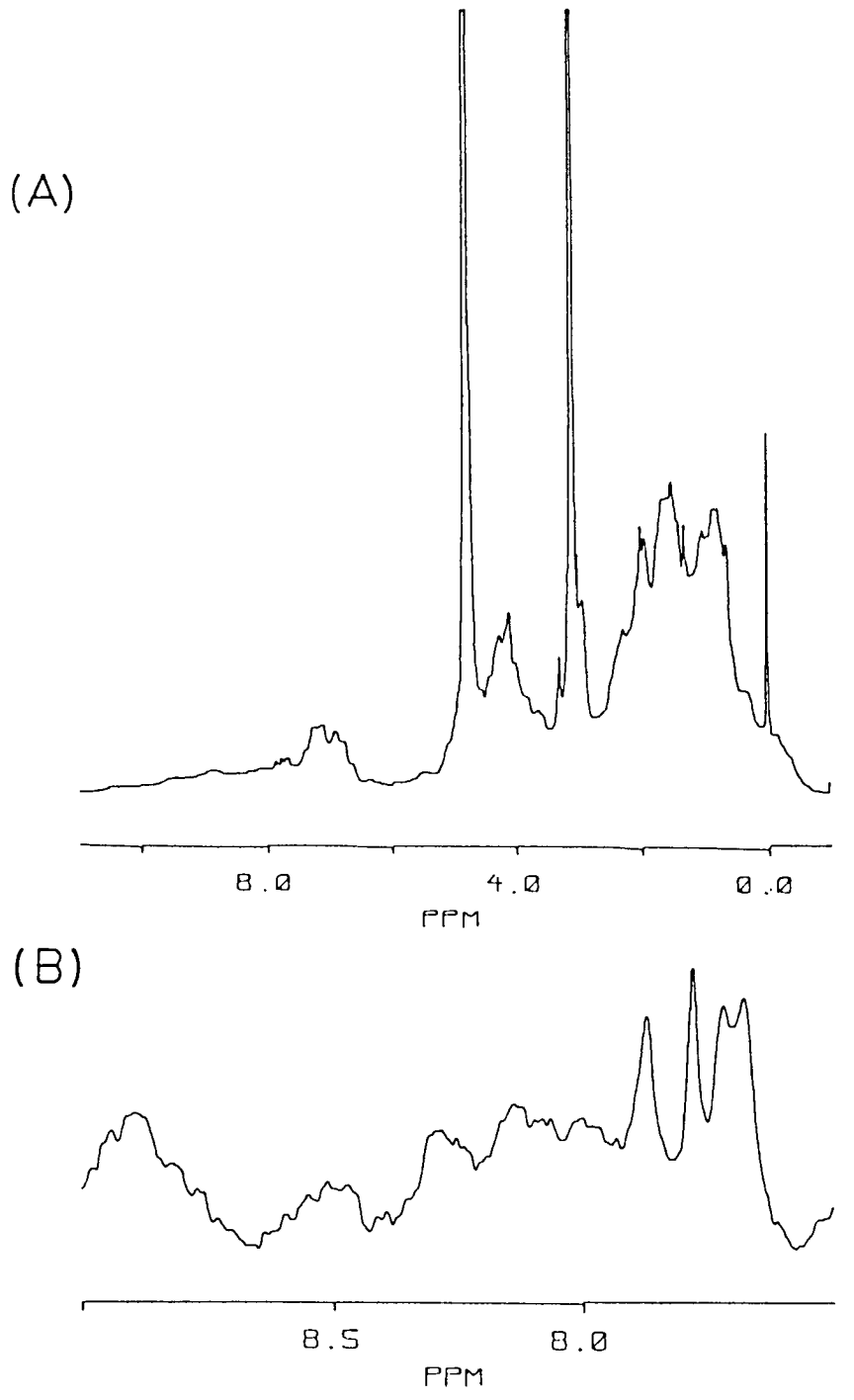

Figure II.1

The ^1H NMR spectra of dephosphorylated rabbit muscle PGM at 400 MHz. The solution contained 0.21 mM dPGM and 20 mM EDA buffer in 99.8% D_2O at pH* 7.70.

(A) Full spectrum;

(B) Expansion of the low field region showing the C-2H histidine resonances.

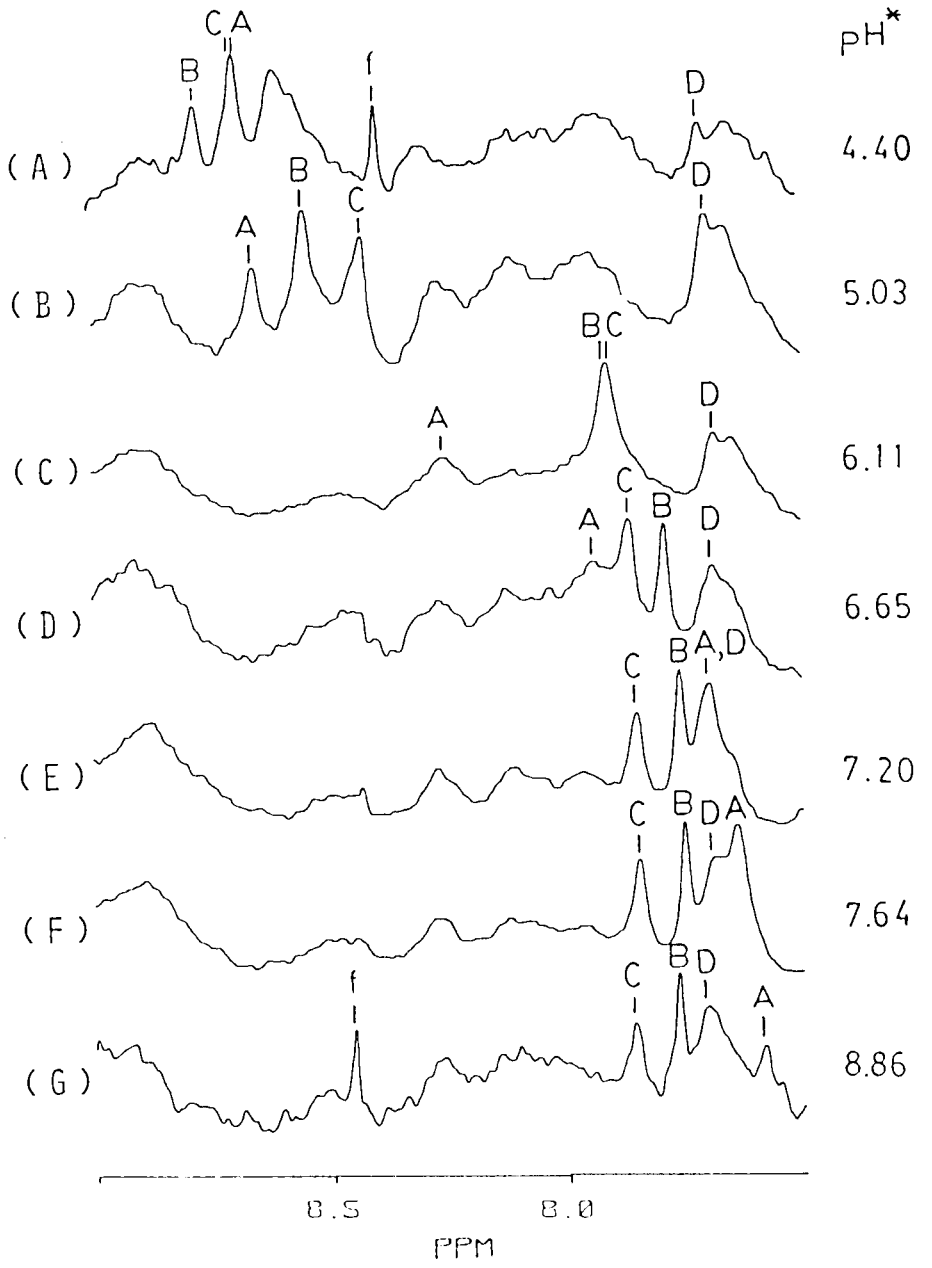

Figure II.2 The 400 MHz partial ^{1}H NMR spectra of the aromatic region of rabbit muscle dPGM at various pH* values showing pH dependent chemical shifts. The resonances assigned to the C-2H protons of histidines are shown as A, B and C. A sharp signal is also assigned as D. The resonance at 8.44 ppm designated by "f" is due to contamination by formic acid. The resonance at 8.61 ppm at pH* 4.40 is due to denatured enzyme.
The conditions of the experiments were 0.2 mM PGM, 20 mM EDA in 99.8% D_2O. pH* refers to the direct pH meter reading in D_2O.

respectively. Apart from the these three histidine resonances there is one clearly recogizable resonance that occurs in the aromatic region of ^1H NMR spectra and does not titrate with pH. It seems unlikely that signal is from a histidine residue that is buried in the interior of the molecule since the resonance is at least as sharp as those of the other histidine protons. This signal might result from a tryptophan or phenylalanine residue on the PGM. Whatever its identity, this signal is assigned as resonance D. Broad peaks are notable at chemical shifts of 8.85, 8.30, 8.20, 7.71 and 7.66 ppm and these do not change position appreciably in the pH* range 4.4 - 9.0. These most probably correspond to peptide N-H groups that are buried in the folded structure of the protein so that their exchange with the D_2O solvent are substantially inhibited.[37] At pH* values below 4.40, dPGM starts to denature and a precipitate forms. Therefore, a histidine with a pK_a below 4.40 would go unrecognized; the same also applies to one with pK_a above 9. Observations, thus, centre on histidine residues which are assessable to water and titrate within these pH* limits.

The presence of the non-titrating peaks, the rather poor signals-to-noise ratio of the spectra, and the fact that the imidazole C-2H peaks themselves overlap at some pH* values combine to make accurate determination of the position of the histidine peaks difficult. Having estimated the position of the peaks at various pH* values, the next

problem was to join the points to give titration curves. Because of the extensive overlap of peaks, it was not possible to do this completely unambiguously. The curves shown in Figure II.3 were chosen on the basis of area measurements and the somewhat different line width of the peaks. In this figure, the positions of the nontitrating peaks have been omitted for clarity.

As seen in the Figure II.3, the experimental data fit very well with the Henderson-Hasselbalch titration curves as shown in Appendix II, and there is no marked deviation of the experimental data from the theoretical curves. Drawing the titration curves through the points in a number of other ways was tried; these uniformly gave a poorer fit to the theoretical curves. The values of δ_{HA}, δ_{A}, and pK_a which define these curves are shown in Table II.1.

Table II.1: ^{1}H NMR Studies: pH Titration Parameters for Histidine Residues in Rabbit Muscle dPGM

Resonance	pK_a	δ_{HA} (ppm)	δ_{A} (ppm)	slope* (see appendix II)
His A	6.54±0.04	8.69	7.57	1.03±0.03
His B	5.24±0.04	9.00*	7.77	1.00±0.05
His C	5.20±0.05	8.80*	7.85	1.04±0.05

* refers to calculated values
δ_{HA} = limiting chemical shifts of protonated C-2H
δ_{A} = limiting chemical shifts of deprotonated C-2H

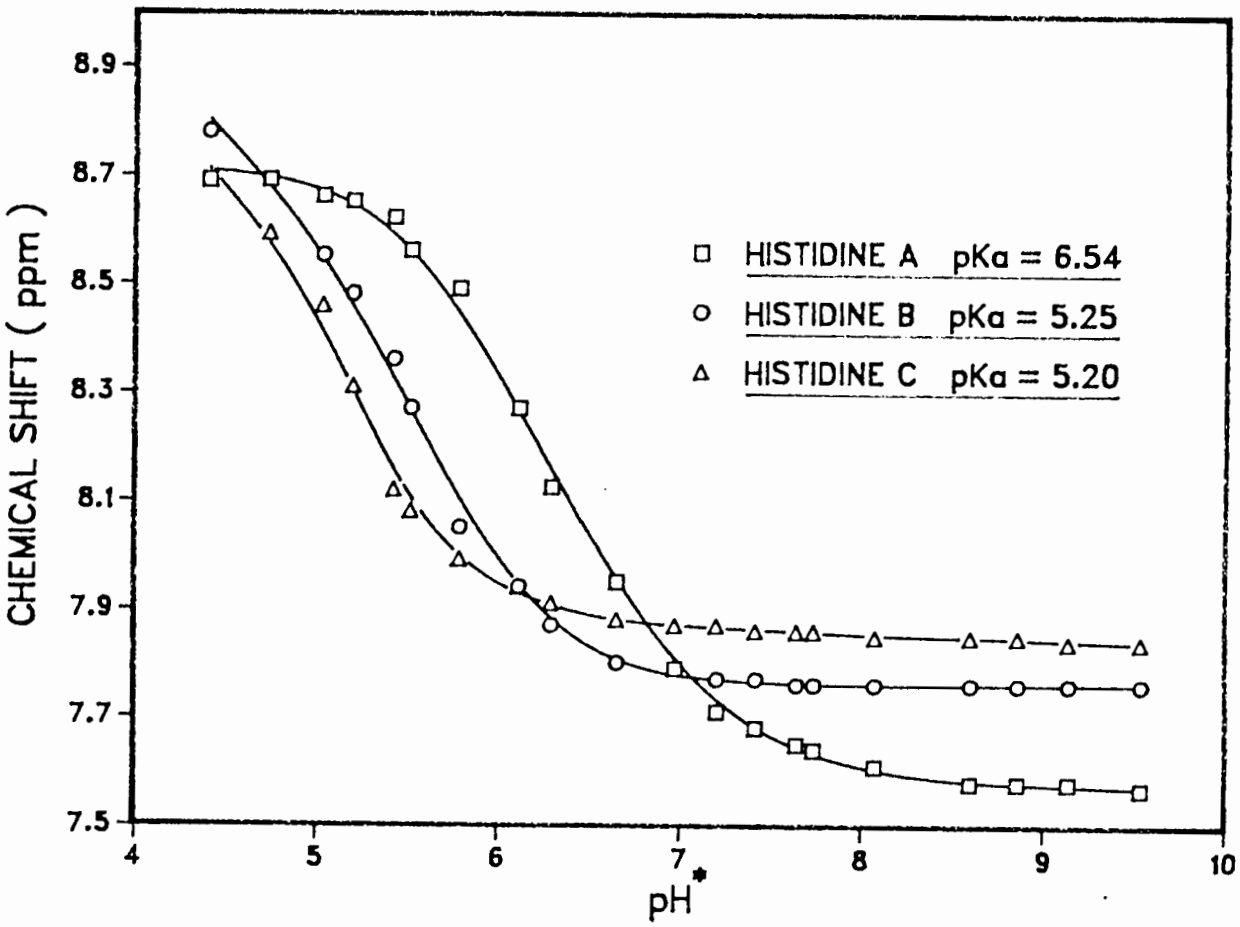

Figure II.3 The ^1H NMR titration curves of the histidine C-2H protons of dPGM. The curves labelled A, B and C correspond to peaks A, B and C in Figure II.2 respectively. The curves calculated from the experimental points as in Appendix II are shown by the solid lines.

The pK_a values are slightly higher in D_2O and D_2O/H_2O mixtures than in water.[41] Therefore, the increase in pK_a approximately balances the decreased reading from the glass electrode (pH = pD + 0.4) and the measured pK_a in D_2O is assumed to essentially be the true pK_a in water.

It is worth emphasizing that, since all the points on the curve contribute to the determination of the pK_a values, their accuracy is substantially greater than that of individual points on the curve.

The same pH titration experiment was repeated in the absence of the EDA buffer. No marked deviations was observed from the one obtained in the presence of the buffer.

As is indicated by Figure II.3 and Table II.1, the C-2H of His A is in quite a different magnetic environment from those of the other two histidine residues. Its chemical shift, 0.2 - 0.4 ppm upfield from the other C-2H resonances, and a considerably higher pK_a suggests that this histidine is in the vicinity of a negatively charged residue that helps to stablize the positively charged imidazole ring. It is never possible to define unambiguously the environment of a histidine residue from its chemical shifts and pK_a alone, though many possible environments would be incompatible with these values.

The line widths of proton resonances in low-viscosity solvents are effectively determined by the

rotational correlation time of the protein. An imidazole group buried within a compact globular protein can rotate only when the whole molecule rotates. Consequently, its correlation time is determined by the rotational diffusion time of the macro-molecule. If the line width for such a buried group is more than 0.1 ppm, with comparsion to the apparent half-width of the other histidine which is about 0.02 to 0.04 ppm, under our present experimental conditions it would not be distinguishable from the base line. On the other hand, the imidazole group of a histidine residue inwhich rotates relatively rapidly about the $C\alpha$-$C\beta$ bond would show an appreciably narrower resonance. There are a few examples even in diamagnetic proteins in which the unusual environment of a histidine leads to its C-2H resonances being shifted upfield into the main aromatic region of the spectrum or appreciably broadened.[37] Therefore, we conclude that in rabbit muscle dPGM, there are three histidine residues in which rotation about side-chain bonds is relatively unrestricted and which are therefore probably at or near the surface or in the active site of the enzyme. There might also be histidine residues which are not free to move rapidly with respect to the rest of the protein molecule.

II.C.2 Studies of the Interactions of Substrate and Substrate Analogues with PGM at pH* 7.70 and 8.50

Figure II.4 shows the spectrum of dPGM as well as the spectra taken in the presence of increasing amounts of vanadate. The C-2H resonance of His C shows a small downfield shift of 0.01 ppm, probably a result of a change in the local environment of this histidine side chain. The resonances of His A and B show a decrease in intensity as the concentration of vanadate increases while a new resonance at 7.61 ppm grows slowly in intensity. The changes in areas of the histidine signals are small and are, unfortunately, superimposed on one another. As a result, quantitative analysis cannot be carried out.

The pyrophosphate and divanadate ions (V_2) which are structurally similar, might be expected to mimic 2-PGA by occupying the anion-stabilizing positions normally occupied by the phosphate and carboxylate moieties when 2-PGA is bound.[32] Studies of the interaction of pyrophosphate with the histidine resonances of dPGM at pH* 7.70 reveal that only His B undergoes a very slight decrease in intensity while the rest of the aromatic envelope is unaffected even at the highest concentration of pyrophosphate (30 mM). Kinetic studies of the phosphatase activity of PGM have shown that both pyrophosphate and V_2 similarly affect the maximum phosphatase rates, however the K_m for V_2 is 3×10^{-5} M, while that for pyrophosphate is

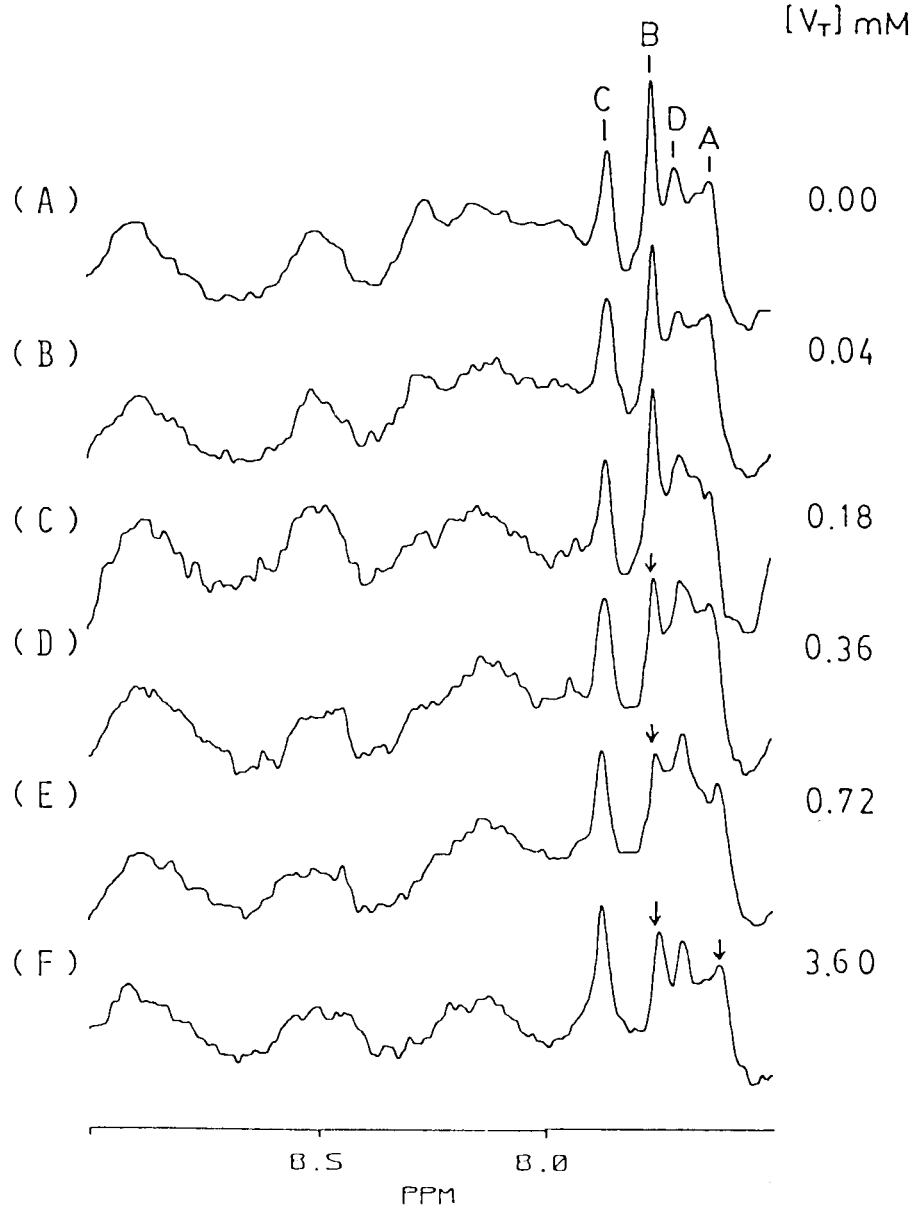

Figure II.4 The aromatic region of 400 MHz ^{1}H NMR spectra of 0.18 mM dPGM in 20 mM EDA buffer (99.8% D_2O) at pH* 7.70±0.04.

(A) Spectrum of free dPGM showing signals of His A, B, C and resonance D.

(B-F) Spectra illustrating the effects of successive additions of vanadate on the signals of the histidine resonances. The downward arrows indicate the signals which decrease in intensity.

$2x10^{-2}$ M.[33] The results obtained from these ^1H NMR studies are consistent with the nearly 10^3 fold lower K_m for V_2 and this is consistant with the hypothesis that the catalytic site of PGM is designed to stabilize the transition state for phosphoryl transfer. As previously mentioned the structure of the transition state is thought to resemble a pentacoordinate trigonal bipyramid and such a structure is more readily adopted by vanadate than by phosphate.[5]

Figure II.5 shows a spectrum of dPGM and compares this with the spectra taken in the presence of successive additions of 3-PGA at pH* 7.70±0.05. It can be seen that the C-2H resonances of His A and C are not affected by the successive additions of 3-PGA while His B shows a decrease in intensity. Growth of a new resonance was not observed in the spectrum probably because either the the new signal is too small to be seen because of the low signal to noise ratio or it is obscured by other aromatic amino acid signals in this part of the ^1H NMR spectral envelope. Analysis of spectra taken in the presence of progressively increasing amounts of 2-PGA at pH* 7.70±0.03 did not reveal any differences deriving from this structural form of phosphoglyceric acid.

The ^1H NMR spectra of dPGM taken in the presence of a constant amount of vanadate but varying concentrations of 3-PGA show dramatic differences from the spectra of Figures II.4 and II.5. The effect is demonstrated in Figure II.6

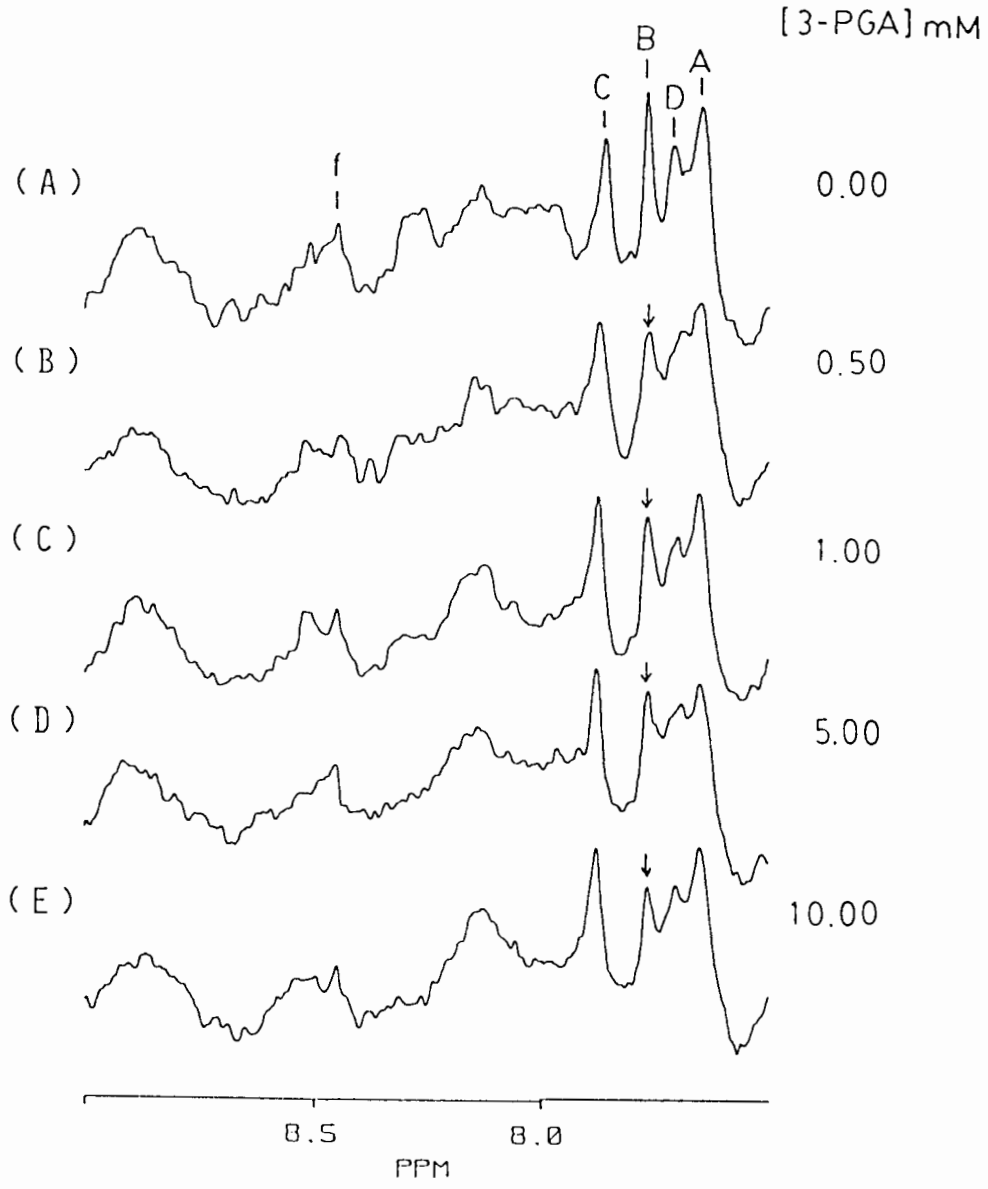

Figure II.5 The aromatic region of 400 MHz ^{1}H NMR spectra of 0.25 mM dPGM in 20 mM EDA buffer (99.8% D_2O) at pH* 7.70±0.05.

(A) Spectrum of free dPGM showing His A, B, C and resonance D.

(B-E) Spectra illustrating the effects of successive additions of 3-PGA on the signals of the histidine resonance.

The downward arrows indicate the signals which decreases in intensity. The peak at 8.44 ppm designated by "f" is due to the contamination of formic acid.

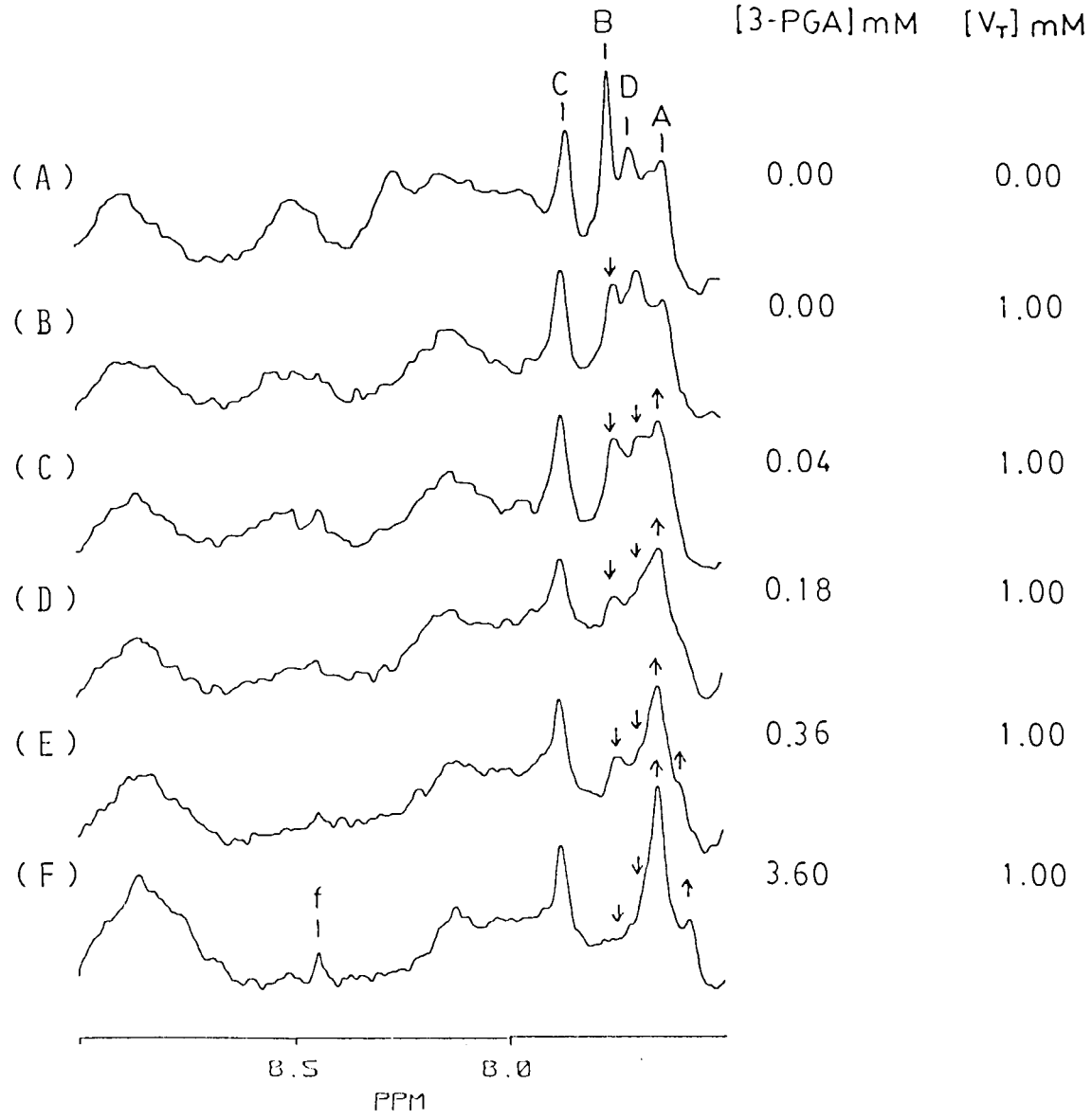

Figure II.6 The aromatic region of 400 MHz ^{1}H NMR spectra of 0.28 mM dPGM in 20 mM EDA buffer (99.8% D_2O) at pH* 7.70±0.05.

(A) Spectrum of free dPGM showing His A, B, C and resonance D.

(B) Spectrum illustrating the effects of addition of 1 mM vanadate to (A).

(C-F) Spectra illustrating the effects of successive additions of 3-PGA to (B).

The downward arrows indicate a reduction while the upward arrows indicate a growth of signal intensity. The peak at 8.44 ppm designated by "f" is from the contaminant, formic acid.

which shows the effect on the C-2H resonances upon addition of 1 mM of vanadate and successive aliquots of 3-PGA at pH* 7.70±0.05. With the initial addition of aliquots of vanadate, His A and B both show a small change in signal intensity. Upon the addition of 3-PGA in the subsequent steps, both His B at 7.76 ppm and resonance D at 7.71 ppm decrease markedly in intensity and this disappearance is accompanied by the appearance of two new signals at 7.65 and 7.60 ppm. These new signals grow in intensity as the concentration of 3-PGA is increased. Detailed analysis of the effect of the presence of 3-PGA and vanadate on the His A resonance at 7.63 ppm is not possible as it is being obscured by the new signals that appear as the concentration of 3-PGA is increased.

^{1}H NMR spectrum were also taken after addition of 4 mM of 3-PGA to dPGM followed by aliquots of vanadate at pH* 7.70±0.05. The effects on the ^{1}H NMR spectra are shown in Figure II.7. Analysis of these spectra does not reveal any differences when compared to those spectra taken in the presence of 1 mM of vanadate followed by aliquots of 3-PGA at pH* 7.70. These result have shown that both the decrease in intensities of the NMR signals of His B and resonance D and the increase in intensities of new signals at 7.65 and 7.60 ppm are a function of both the concentration of vanadate and of 3-PGA. Other work has shown that there is spontaneous ester formation between vanadate and 3-PGA[35]

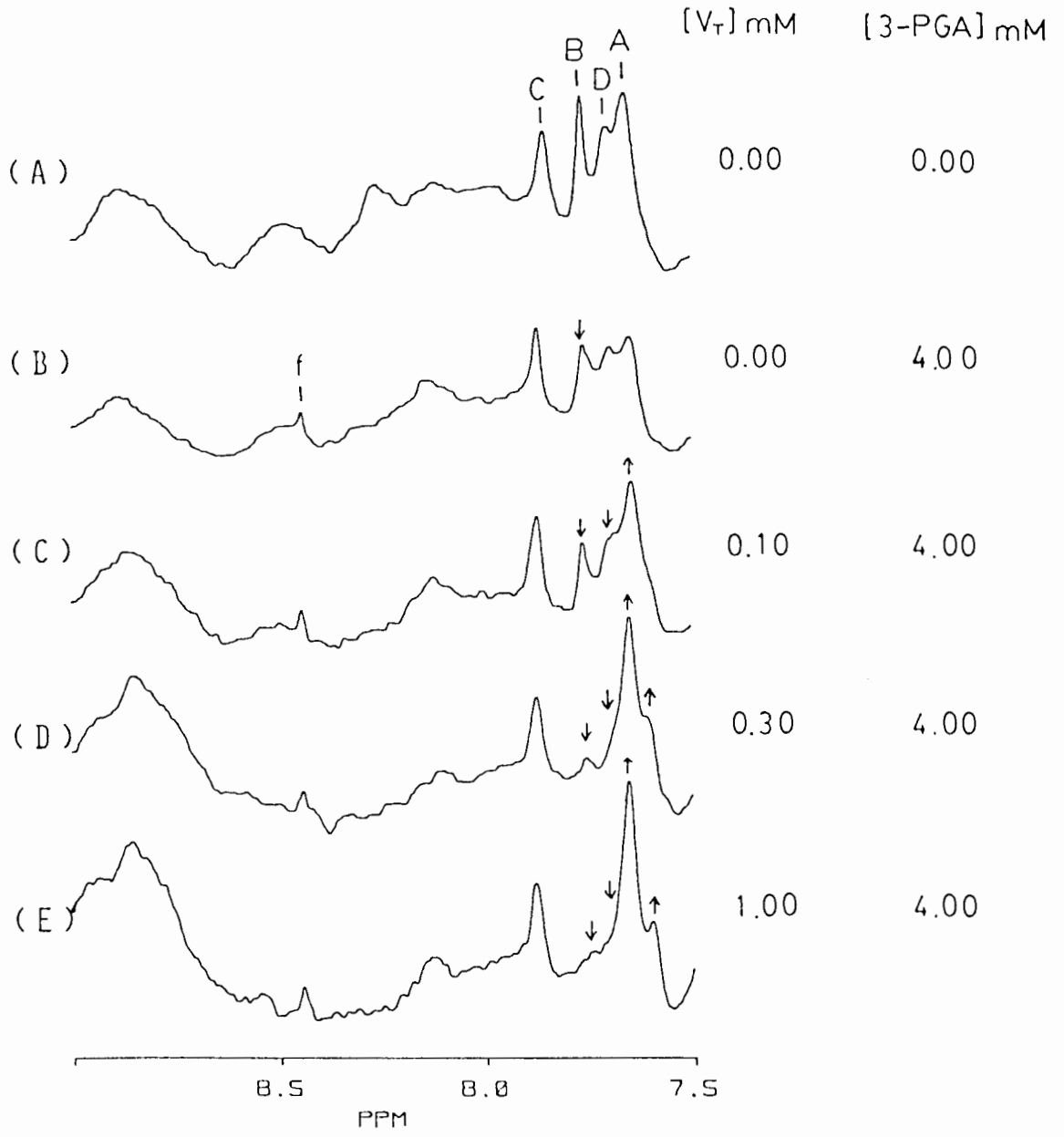

Figure II.7 The aromatic region of 400 MHz ^{1}H NMR spectra of 0.20 mM dPGM in 20 mM EDA buffer (99.8% D_2O) at pH* 7.70±0.05.

(A) Spectrum of free dPGM showing His A, B, C and resonance D.

(B) Spectrum illustrating the effects of addition of 4.0 mM 3-PGA to (A).

(C-E) Spectra illustrating the effects of successive additions of vanadate to (B).

The downward arrows indicate a reduction while the upward arrows indicate a growth of signal intensity. The peak at 8.44 ppm designated by "f" is from the contaminant, formic acid.

while steady-state kinetic experiments have shown that inhibition of mutase activity is dependent on both vanadate and 3-PGA and that this inhibition is competitive with 2,3-DPG.[34] This suggests that it is 2-V-3PGA, a transition state analogue of PGM, that binds to the catalytic site of the enzyme and affects various resonances in the ^1H NMR spectrum. Figure II.8 shows the ^1H NMR spectra of dPGM in the presence of increasing amounts of a 2-V-3PGA stock solution which was make up by combining appropriate quantities of vanadate and 3-PGA. The concentrations of 2-V-3PGA shown in the figure were calculated by using Equation II.3 given in section II.B.3. The spectra show exactly the same results as those obtained from the separate additions of vanadate and 3-PGA. Additional studies showed that the ^1H NMR spectra do not distinguish between the addition of either 3-V-2PGA or 2-V-3PGA. This last result was not expected, however, recent kinetic studies have shown that, contrary to current concepts, mammalian PGM is capable of exerting suboptimal catalysis of monophosphoglycerate isomerization in the total absence of 2,3-DPG.[42] Bearing in mind that the concentrations of PGM used in these ^1H NMR studies (0.17-0.22 mM) are much higher than those used in the enzyme kinetic studies (0.04 μg/ml), the dephosphorylated enzyme will exhibit significant mutase activity in the absence of 2,3-DPG. It is therefore not suprising that when either 3-PGA of 2-PGA was added to dPGM,

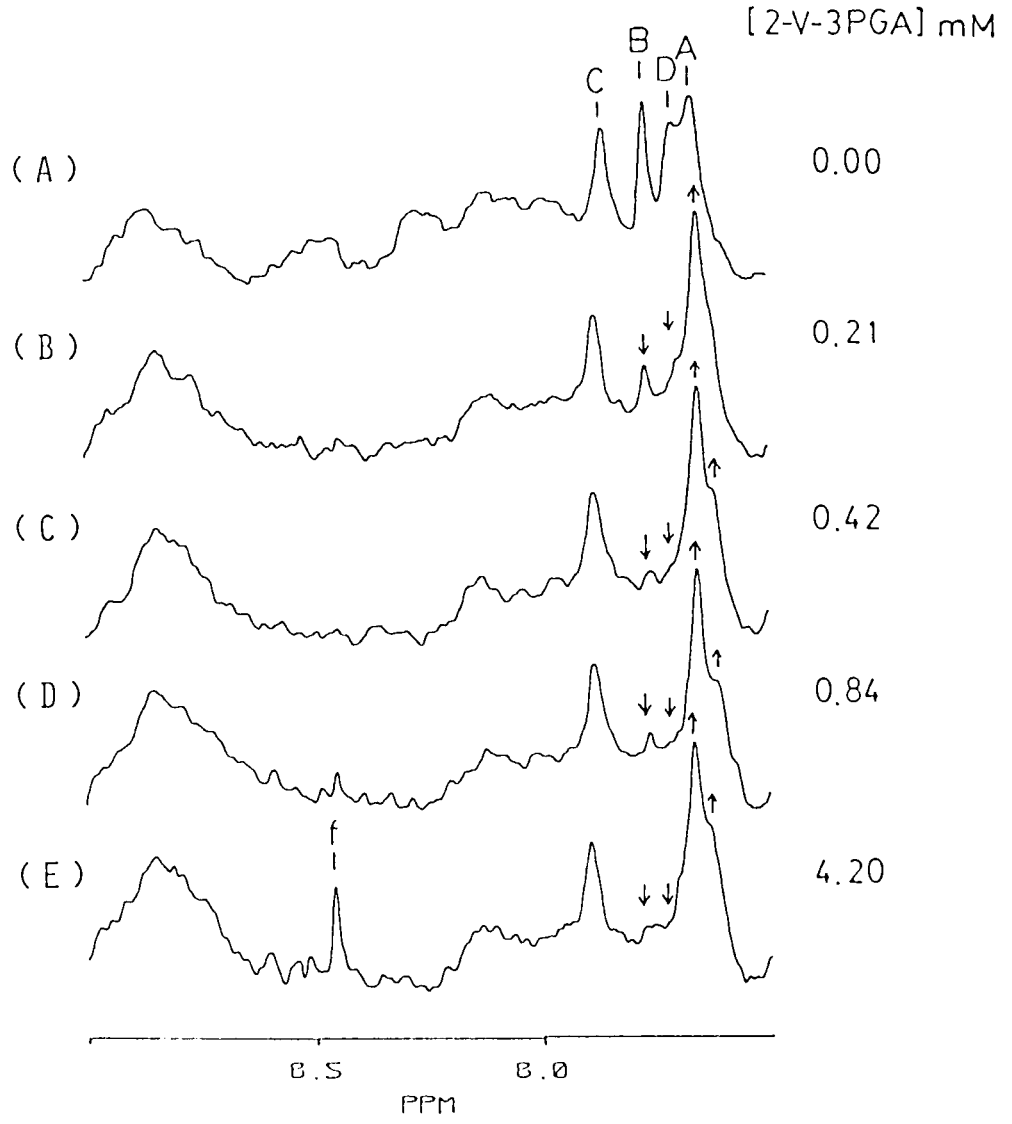

Figure II.8 The aromatic region of 400 MHz ^1H NMR spectra of 0.21 mM dPGM in 20 mM EDA buffer (99.8% D_2O) at pH* 7.70±0.03.

(A) Spectrum of free dPGM showing His A, B, C and resonance D.

(B-E) Spectra illustrating the effects of successive additions of a stock solution of 2-V-3PGA to (A).

The downward arrows indicate a reduction while the upward arrows indicate a growth of signal intensity. The peak at 8.44 ppm designated by "f" is from the contaminant, formic acid.

the same histidine residues were affected. The effect on the histidine signals may actually be due to a mixture of 3-PGA/2-PGA in the certain ratio established by the mutase itself. The possibility that both 3-PGA and 2-PGA interact with the same histidine residue cannot be ruled out.

The phosphonomethyl analogue of 3-phosphoglycerate, DL-2-hydroxy-4-phosphonobutanoic acid (for simplicity referred to as 3-PMGA) is isosteric with 3-PGA and involves only the replacement of $-O-PO_3H_2$ by $-CH_2-PO_3H_2$ as shown below.

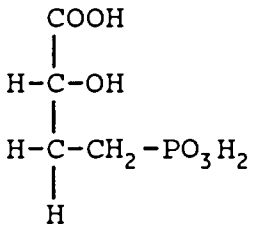

3-PMGA

3-PMGA is known to be a potent competitive inhibitor of cofactor-dependent PGM from yeast and of cofactor-independent PGM from wheat germ.[43] The advantage of utilizing the phosphonomethyl analogue is the extreme stability of the P-C bond which precludes any enzymic (or accidental) cleavage. It presumably binds to the enzyme in the same manner as the substrate.[44] As a result no phosphoryl transfer will occur. Thus, 3-PMGA is a useful

tool for NMR spectroscopic studies on the mechanism of action of PGM.

The 3-PMGA used was a racemic mixture. The concentrations of 3-PMGA reported in the present study refers to the concentration of the D-isomer only as it is known that phosphoglycerate with an L-configuration is a very poor substrate.[45] Figure II.9 shows a spectrum of dPGM and a spectrum taken in the presence of a saturating amount of 3-PMGA at pH* 7.70. On addition of aliquots of 3-PMGA, the C-2H resonance of His B shows only a small decrease in intensity when compared to the decrease in intensity shown with addition of 3-PGA. This indicates that 3-PMGA binds to the catalytic site of PGM the same way as 3-PGA, but in a weaker manner.

Figure II.10 shows the spectra of dPGM as well as successive spectra taken in the presence of 1.5 mM vanadate and with increasing amounts of 3-PMGA. Thus a vanadate ester of 3-PMGA (2-V-3PMGA) is expected to form in the aqueous solution. The resulting spectra are very similar to those obtained in the presence of 1.0 mM vanadate and with increasing amounts of 3-PGA (Figure II.6) except that a higher concentration of 3-PMGA was required to cause an equivalent change of intensity. This indicates that 2-V-3PGA binds much more tightly to the dPGM than 2-V-3PMGA. In fact, as shown in Section III, the intrinsic dissociation

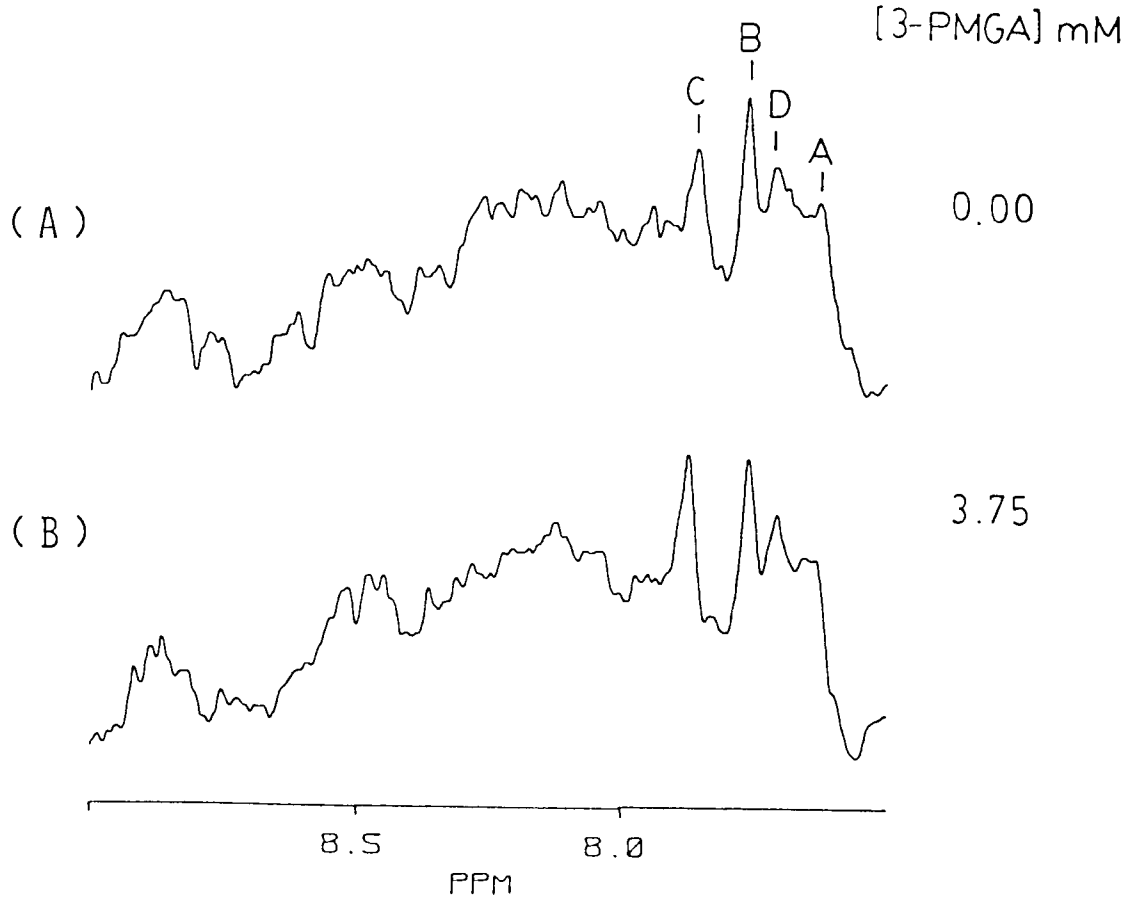

Figure II.9 The aromatic region of 400 MHz ^{1}H NMR spectra of 0.19 mM dPGM in 20 mM EDA buffer (99.8% D_2O) at pH* 7.70±0.07.

(A) Spectrum of free dPGM showing His A, B, C and resonance D.

(B) Spectrum illustrating the effects of addition of 3.75 mM 3-PMGA.

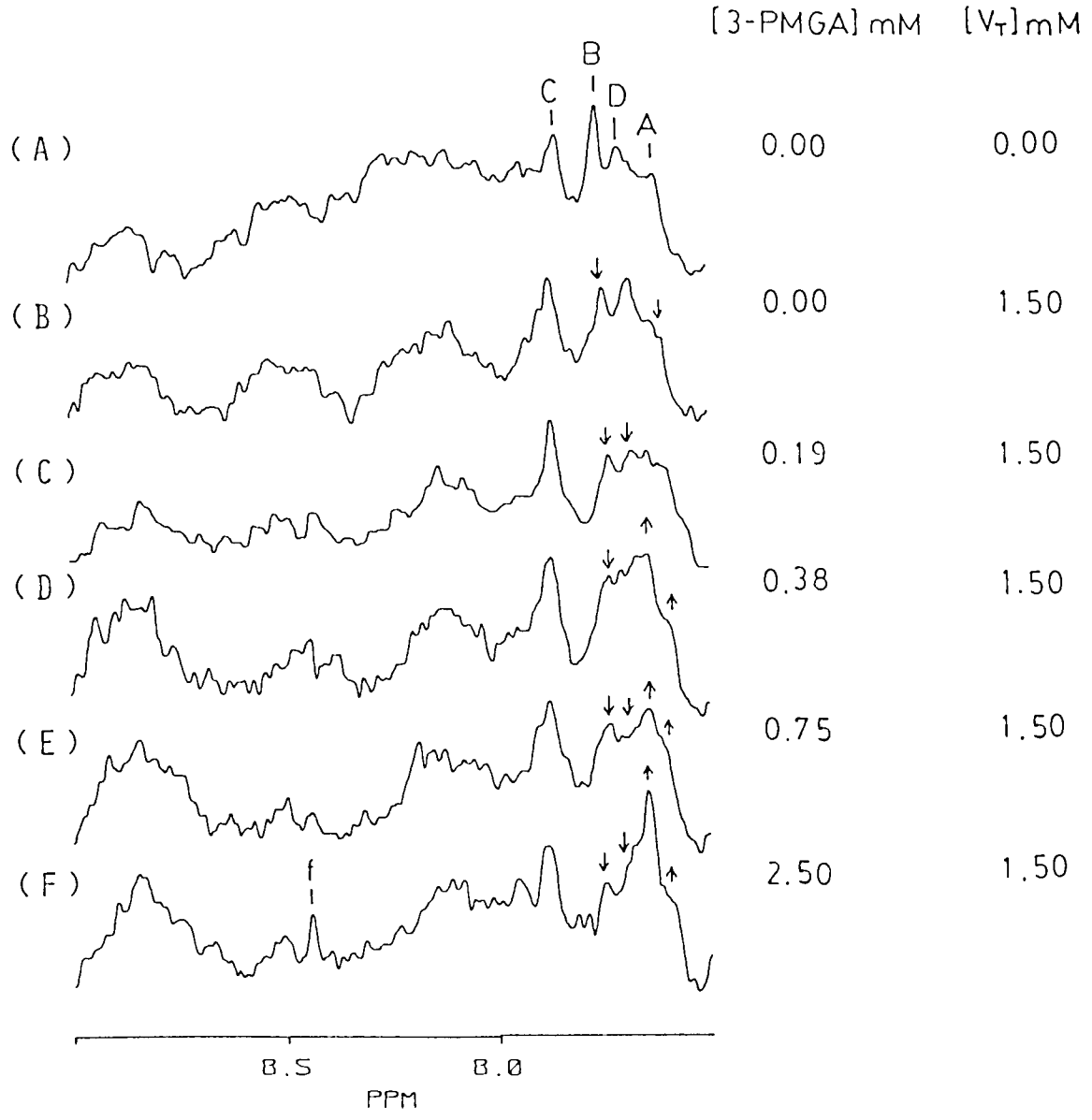

Figure II.10 The aromatic region of 400 MHz ^{1}H NMR spectra of 0.19 mM dPGM in 20 mM EDA buffer (99.8% D_2O) at pH* 7.70±0.07.

(A) Spectrum of free dPGM showing His A, B, C and resonance D.

(B) Spectrum illustrating the effects of addition of 1.5 mM vanadate to (A).

(C-E) Spectra illustrating the effects of successive additions of 3-PMGA to (B).

The downward arrows indicate a reduction while the upward arrows indicate a growth of signal intensity. The peak at 8.44 ppm designated by "f" is from the contaminant, formic acid.

constants for the vanadate esters of 3-PMGA and of 3-PGA are 1.4×10^{-8} M and 2×10^{-12} M, respectively.

Binding of 2,3-DPG to dPGM has also been studied by ^{1}H NMR spectroscopy at pH* 7.70. Figure II.11 shows the spectrum of PGM as well as a spectrum taken in the presence of 10 mM 2,3-DPG. When 2,3-DPG is added, the enzyme becomes phosphorylated and in a subsequent step the monophosphoglycerate dissociates. In the mutase reaction, either 2-PGA or 3-PGA binds to the phosphorylated enzyme (EP), and subsequently the phosphate is transferred and the other isomer is released. Occasionally, the phosphate group on PGM is transferred to the availabe hydroxyl group of D-phosphoglycerate and bound 2,3-DPG is generated. If 2,3-DPG dissociates from the enzyme in this step, dephosphorylated enzyme (E) will then be formed. Therefore, it is expected that a mixture of the species E, E(2,3-DPG), E(2-PGA), E(3-PGA), EP(D-glycerate) and EP is formed. The effects on the C-2H resonances are therefore an average of all these species. The NMR signal from His C shows a downfield shift of 0.02 ppm while His B shows a decrease in intensity which was accompanied by the appearance of a new signal at 7.68 ppm. Changes in intensity of the signal from His A and that of resonance D were not observable as they were buried under the new signal at 7.68 ppm.

At this point, one might conclude that His B is the only histidine residue occuring in the catalytic site and

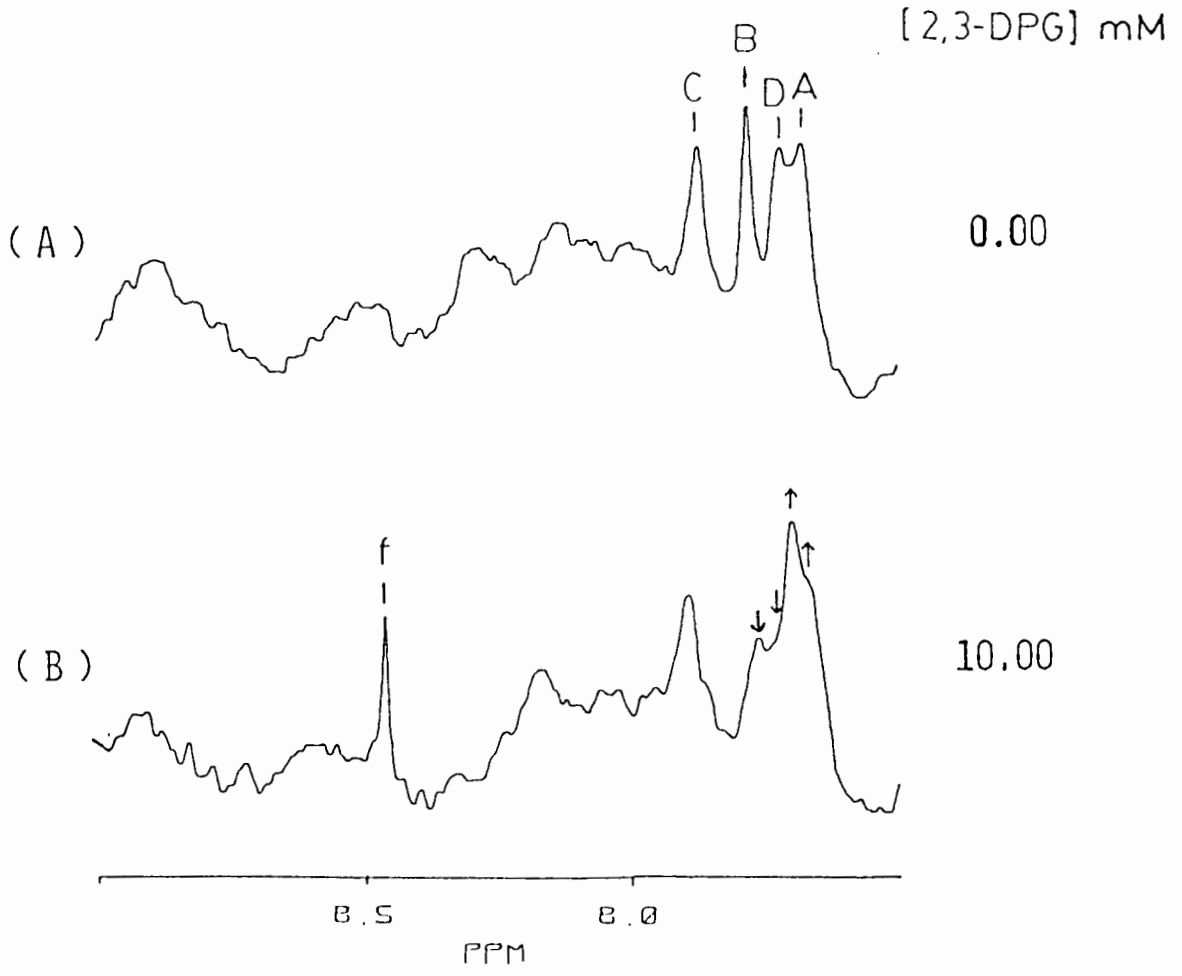

Figure II.11 The aromatic region of 400 MHz ^{1}H NMR spectra of 0.21 mM dPGM in 20 mM EDA buffer (99.8% D_2O) at pH* 7.70±0.01.

(A) Spectrum of free dPGM showing His A, B, C and resonance D.

(B) Spectrum illustrating the effects of addition of 10 mM 2,3-DPG to (A).

The downward arrows indicate a reduction while the upward arrows indicate a growth of signal intensity. The peak at 8.44 ppm designated by "f" is from the contaminant, formic acid.

participating in the phosphoryl transfer reaction. It has however been shown that both His A and B decrease in intensity as V_2 binds to the catalytic site. The new resonance appears very close to the resonance of His A and makes it difficult to observe the change in intensity of the His A. A similar situation might arise when 2,3-DPG, 2-V-3PGA and 2-V-PMGA binds to PGM and the change of intensity of His A will not be observed. In order to test whether the His A signal undergoes a change in intensity, the binding of vanadate and 2-V-3PGA to dPGM has been studied at pH* 8.50. The spectra are shown in Figures II.12 and II.13. It can clearly be seen that both the His A and B signals decrease in intensity upon addition of vanadate. With increasing proportions of 2-V-3PGA in the aqueous solution, both the His A and B resonances decrease in intensity and this decrease is accompanied by the appearance of new signals at 7.66 and 7.56 ppm. Resonance D which occurs normally at 7.71 ppm apparently undergoes a small change in chemical shift and lies underneath the new resonance at 7.66 ppm. Thus it is reasonable to interpret these data as meaning that both His A and B occur at the catalytic site of PGM and participate in the phosphoryl transfer reaction.

Table II.2 gives a summary of the results obtained using various ligands which bind to rabbit muscle dPGM and the various resonances in the aromatic region that were affected at pH* 7.70 and 8.50. Addition of aliquots of

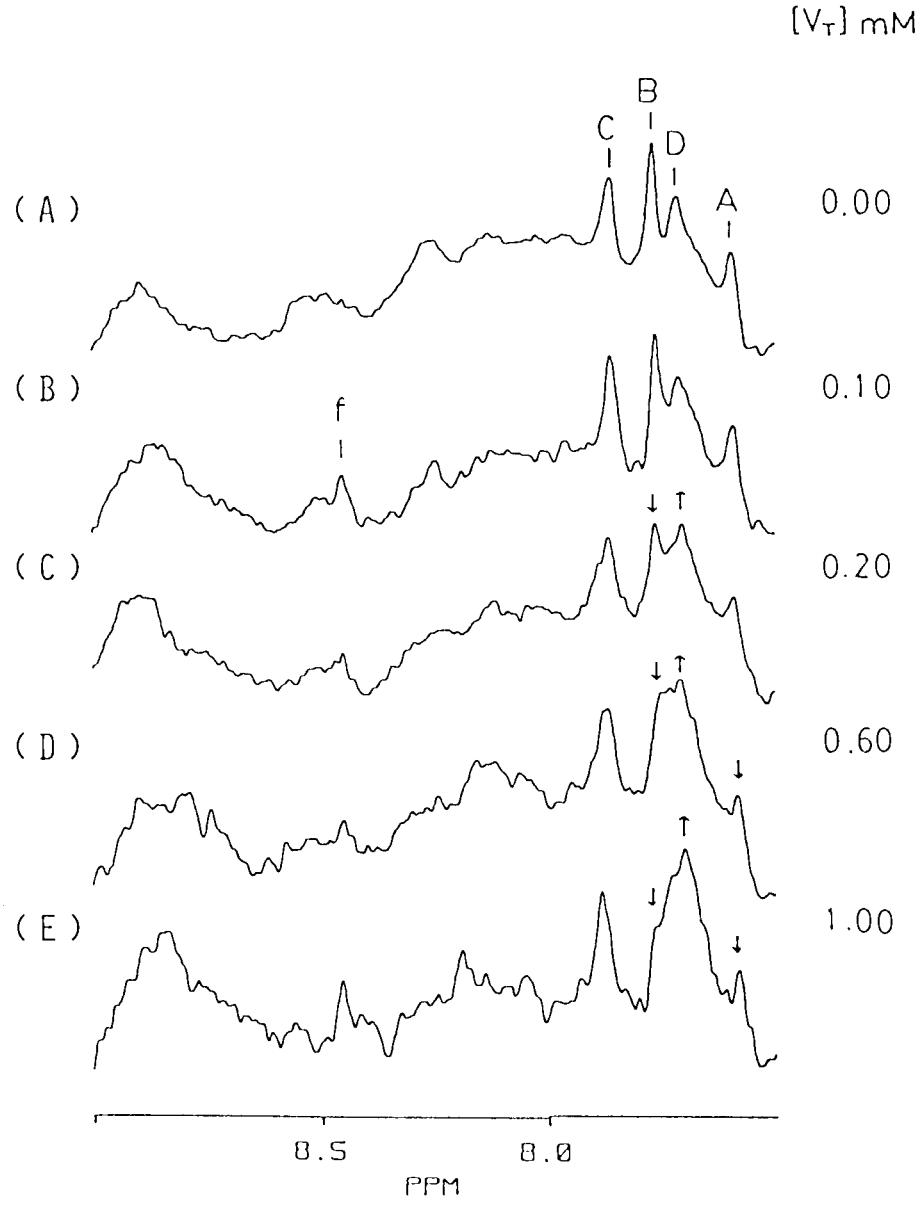

Figure II.12 The aromatic region of 400 MHz ^{1}H NMR spectra of 0.25 mM dPGM in 20 mM EDA buffer (99.8% D_2O) at pH* 8.50±0.06.

(A) Spectrum of free dPGM showing His A, B, C and resonance D.

(B-E) Spectra illustrating the effects of successive additions of vanadate.

The downward arrows indicate a reduction while the upward arrows indicate a growth of signal intensity. The peak at 8.44 ppm designated by "f" is from the contaminant, formic acid.

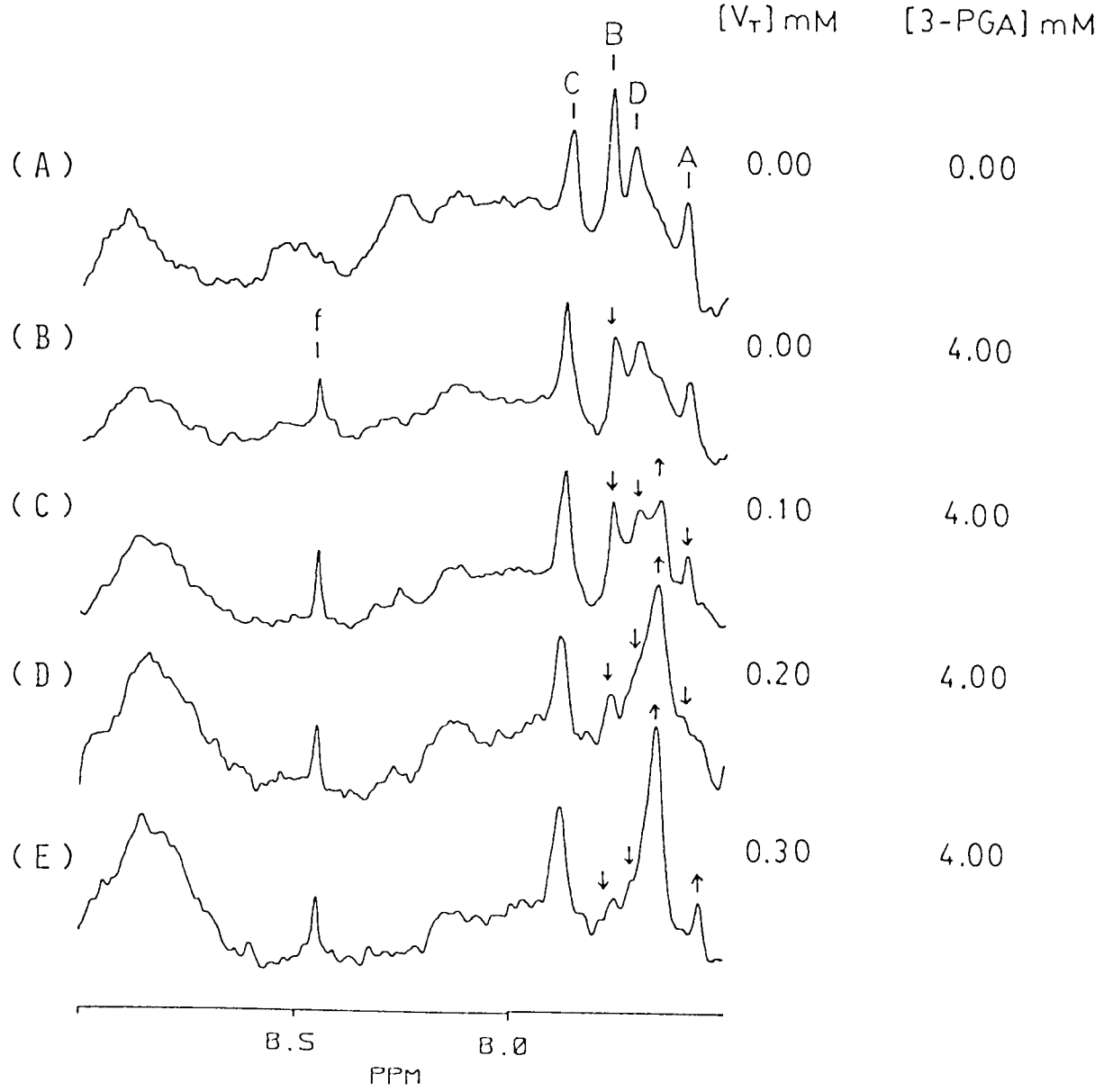

Figure II.13 The aromatic region of 400 MHz ^{1}H NMR spectra of 0.25 mM dPGM in 20 mM EDA buffer (99.8% D_2O) at pH* 8.50±0.06.

(A) Spectrum of free dPGM showing His A, B, C and resonance D.

(B) Spectrum illustrating the effects of addition of 4.0 mM 3-PGA to (A).

(C-E) Spectra illustrating the effects of successive additions of vanadate to (B).

The downward arrows indicate a reduction while the upward arrows indicate a growth of signal intensity. The peak at 8.44 ppm designated by "f" is from the contaminant, formic acid.

Table II.2 : Summary of ^1H NMR Binding Studies of Rabbit Muscle dPGM, Showing the Resonances in the Aromatic Region of the NMR Spectrum that are Affected upon the Binding of Various Ligand.

pH	ligands	His-A (7.63ppm)	His-B (7.76ppm)	His-C (7.86ppm)	Res.D (7.71ppm)	7.65 ppm	7.60 ppm
7.70 ±0.05	Vanadate	d	d	s	-	-	-
	Pyrophosphate	-	d	s	-	-	-
	2-PGA	-	d	s	-	-	-
	3-PGA	-	d	s	-	-	-
	Vanadate	d	d	s	-	-	-
	+2-PGA	u	o	s	o	i	i
	Vanadate	d	d	s	-	-	-
	+3-PGA	u	o	s	o	i	i
	3-PGA	-	d	s	-	-	-
	+Vanadate	u	o	s	o	i	i
	2-V-3PGA	u	o	s	o	i	i
	3-V-2PGA	u	o	s	o	i	i
	3-PMGA	-	d	s	-	-	-
	Vanadate	d	d	s	-	-	-
	+3-PMGA	u	o	s	d	i	i
	2,3-DPG	u	d	s	d	i	i

pH	ligands	His-A (7.63ppm)	His-B (7.76ppm)	His-C (7.86ppm)	Res.D (7.71ppm)	7.66 ppm	7.56 ppm
8.50 ±0.05	Vanadate	d	d	s	i	-	-
	3-PGA	-	d	s	-	-	-
	+Vanadate	o	o	s	d	i	i

Signal intensities are relative to the signal intensity of His C, which does not show any change in intensity upon additions of various ligands.

Abbreviation:
u = undetermined due to signals overlap.
- = no observed change in intensity.
d = signal decreases in intensity.
o = total disappearance of signal.
i = increase in signal intensity.
s = small change in chemical shift (0.01-0.02ppm).

buffer or change of ionic strength by adding KCl does not seems to have had any affect on the C-2H resonances. Under these experimental conditions, inactivated PGM was found not to bind vanadium and vanadate esters. No significant amount of nonspecific binding of ligands to dPGM was observed as at the end of each set of experiment a high concentration of 2,3-DPG, sufficient to displace essentially all the competetive inhibitors from the active site, was added and spectra similar to Figure II.11.b were observed.

In all cases, the signal from His C is shifted downfield by 0.02 ppm. This may be due to a change in local environment around the histidine side chain. Histidine C is now tentatively identified as a histidine residue that is remote from the active site of PGM. Resonance D, from an aromatic moiety other than histidine, completely disappears in the cases that vanadate esters of 3-PGA or 2-PGA are formed and binds to dPGM. It also disappears when 2,3-DPG binds to dPGM.

A general observation that has been made is that when high concentrations of 2,3-DPG or the vanadate ester of either 3-PGA or 2-PGA, buffered at pH* 7.70, is added to dPGM at pH* 7.70 (with 20 mM EDA buffer), the pH* reading from the pH meter shifts from 7.70 to a maximum of 8.50 depending on the concentration of the ligand added. This proton uptake might be caused by a disruption or formation of ionic bonds in the protein due to a conformational change

when vanadate ester or 2,3-DPG binds to dPGM. Additional support for the change of conformation of PGM has been provided by Winn et.al.,[46] who showed that crystals of yeast dPGM shatter when soaked in solution of 2,3-DPG. This indicates that the molecule undergoes a conformation change on phosphorylation which is not observed during binding of 3-PGA to dPGM. This supports the ideas that resonance D derives from a residue that is remote from the active site of PGM. It coincidently shifts under the new resonance that occurs when 2,3-DPG or vanadate esters are bound. This is a consequence of the change of the tertiary structure of the protein. The possibility that resonance D represents an amino acid that is in the active site of PGM and is only affected by the tight binding ligands, cannot be definitely excluded.

The results of these ^{1}H NMR studies, as encompassed by Table II.2 and Figure II.3, lead to a tentative identification of His A and B as histidines that occur in the active site of the enzyme and participate in the binding of the various ligands to rabbit muscle dPGM. However, there is no evidence that either His A or His B forms a covalent linkage with the phosphate group during the phosphoryl transfer process. Furthermore, there is no evidence to decide whether the phosphoryl transfer occurs through a double displacement or a triple displacement mechanism. It has been suggested by Rose that one of the

histidine residues in the active site may play a general acid-base role in the phosphoryl transfer.[30] To break the P-O bond, a positively charged histidine residue on the enzyme is needed to neutralize the charge on the bridging oxygen of the phosphoryl group that is to be transferred and a proton must be transferred to that oxygen to form the product. Thus, in the free enzyme, one histidine in the active site should be protonated while in the phosphoenzyme it should not be protonated. The second histidine should be unprotonated in the active free enzyme. The pH optimum for the PGM has been reported to be 5.9.[47] Based on the pK_a values determined in section II.C.1, at this pH histidine A will be primarily in the protonated form while histidine B will be in the unprotonated form. This is in agreement with a previous proposal that the positively charged histidine A will be available to neutralize the charge on the bridging oxygen of the phosphoryl group that is to be transfered and histidine B will be phosphorylated when binding of 2,3-DPG occurs as depicted in Figure II.14.[30] This arrangement would appear to offer the speed and ready reversibility required by the mutase.

The proton uptake shown by the addition of 2,3-DPG or vanadate ester of 3-PGA and 2-PGA to dPGM at pH 7.70 is consistent with the general acid-base role of the histidine residues as shown in Figure II.14. At pH 7.70, both imidazole rings of the histidine A and B are unprotonated.

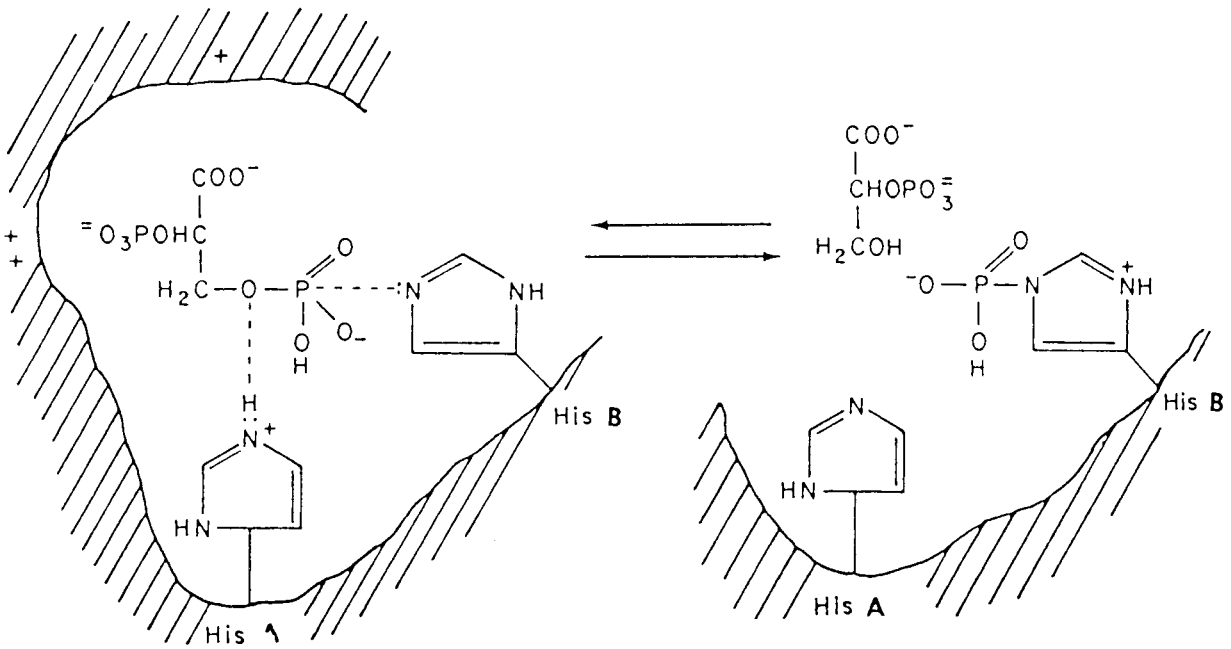

Figure II.14 Schematic diagram showing the possible role of two histidine residues in the phosphorylation of phosphoglycerate mutase by 2,3-DPG[30]. No specific geometry is implied for the two histidine residues.

In order to form the enzyme/substrate or enzyme/vanadate ester complex, a proton is absorbed into the enzyme active site. However, the ^{1}H NMR studies do not show a downfield C-2H resonance when the 2,3-DPG or the vanadate ester of 3-PGA or 2-PGA was added to the dPGM. This may indicate that the proton that is absorbed is incorporated into the substrate or substrate analogue instead of onto the histidine residue in the active site. Further investigation has to be carried out to study this proton uptake behaviour in the reaction of phosphoglycerate mutase.

CHAPTER III

^{51}V NMR STUDIES: BINDING OF INORGANIC VANADATE AND VANADATE ESTERS TO RABBIT MUSCLE PHOSPHOGLYCERATE MUTASE

III.A The Use of ^{51}V NMR Spectroscopy to Investigate Enzyme Mechanism

As indicated by its magnetic properties, vanadium is well suited for studies utilizing nuclear magnetic resonance spectroscopy.[1] Vanadium is nearly 100% abundant in the ^{51}V isotope and has nuclear spin of $^{7}/_{2}$. Because of the large nuclear moment of ^{51}V (5.1392, in units of nuclear magneton), the NMR sensitivity of this nucleus is about 0.38 that of the proton. NMR studies in solution are limited to diamagnetic vanadium(V) species. Paramagnetism greatly accelerates nuclear relaxation rates, which generally results in extemely broad NMR lines from the paramagnetic species. Vanadium(V) signals which occur at a resonance frequency of 105 MHz on our instrument are, in general, sufficiently well resolved to allow chemical assignment of all signals. High-field NMR spectrometers provide a distinct advantage over low field spectrometers since ^{51}V signals tend to be quite broad because of quadrupolar relaxation. Signal widths are typically 50-100 Hz for compounds of nominally tetrahedral symmetry about vanadium and much broader as lower symmetry is obtained.[49] ^{51}V NMR

spectroscopy has been used to study the oligomerization and the esterification reactions of vanadate in aqueous solutions.[49-53]

Most recently, the interaction between vanadate(V) and large biomolecules such as ribonuclease,[14] transferrin[54] and the peroxidase from A.nodosum,[55] have been investigated. The latter was the first ^{51}V NMR detection of an enzyme containing vanadium(V) as the prosthetic group.

The binding of inorganic vanadate to rabbit muscle PGM has also been studied by ^{51}V NMR spectroscopy.[33] It has been proposed that one divanadate ion will bind to each of the two identical subunits of PGM in a noncooperative manner. An extension of the model proposed will be made in order to analyze the results of the binding of vanadate esters to PGM.

III.B Experimental Procedure

For materials and preparation of vanadate stock solutions see sections II.B.1 and II.B.2 .

III.B.1 Instrumentation

^{51}V NMR spectra were obtained at 105 MHz by using the broad-band accessory of a Bruker WM-400 NMR spectrometer. Sweep widths of 40 KHz, 0.025 s acquisition times, 2K data sets and 60° pulse angles were used for all spectra. Doubling the acquisition times was found to have

no observable effect on signal intensities. A total of 20,000 transients was acquired for each spectrum. A line-broadening factor of 40 Hz was applied to all spectra before zero-filling to 8K and transforming to the frequency domain. The Fourier transforms for any particular series of compounds were done in the absolute intensity mode so that signal intensities were directly comparable between spectra. Chemical shifts reported are relative to the external reference standard, $VOCl_3$, which has been assigned to 0 ppm. All spectra were obtained at ambient temperature. Base-line roll was removed from all spectra before signal intensities were measured. The signal intensities were measured with the instrument manufacturer's software and no effort was made to obtain more accurate integrals.

III.B.2 Preparation of PGM for ^{51}V NMR Studies

A suspension of PGM in aqueous ammonium sulfate was centrifuged, the supernatant was discarded and the pellet was dissolved in sufficient buffer containg 20 mM HEPES, 6.0 mM KCl and 1.0 mM glycolate 2-phosphate to give a concentration of PGM of about 10 mg/ml. The resulting solution was then dialyzed for 4 hours at 4°C against 100 ml of the same buffer and then dialyzed overnight at 4°C against 100 ml of a similar buffer containing no glycolate 2-phosphate. Aliquots of 2 ml of this solution were used in the NMR studies.

III.B.3 Binding of Inorganic Vanadate(V_i) to PGM

With reference to methods as described by Stankiewicz et.al,[33] solutions were prepared by successive additions of small volumes of 0.1 M NaH_2VO_4 to 2.0 ml of a solution containg 0.12 - 0.2 mM PGM.

III.B.4 Binding of Vanadate Ester to PGM

Solutions were prepared by successive additions of small volumes of substrate or substrate analogues to 2.0 ml of a solution containing 0.17 - 0.22 mM PGM, 1 mM vanadate in 20 mM HEPES buffer and 6 mM KCl.

The pH adjustments were made by adding 0.05 - 0.1 N NaOH and 0.05 - 0.1 N HCl. The pH was measured both immediately before and immediately after obtaining the NMR spectra. If the difference in pH readings of a sample before and after recording a spectrum was greater than 0.1 pH units, the results were not accepted. In general the agreement was better than 0.05 pH units.

III.B.5 Concentration of Vanadate Ester

The equilibrium constant for the formation of 2-V-3PGA is 2.5 M^{-1} at pH 7.5 under the conditions of 1 M ionic strength with added KCl.[35] Therefore, the concentration of 2-V-3PGA can be calculated by Equation II.3 as shown in Section B.3. The studies of the interaction of vanadate with glyceric acid have shown that the formation of various

glyceric acid derivatives were similar to those of lactate.[10] The equilibrium constants for the formation of 2-vanado or 3-vanado glyceric acid are assumed to be equal to that of 2-vanado-lactate, 0.54 M^{-1}, determined at pH 7.5 with 1 M KCl ionic strength.[10] The equilibrium constant for the formation of 2-V-3PMGA has not been studied. However, it is expected that the interaction of vanadate with 3-PMGA will be very similar to either 3-PGA or lactate. Therefore, for the purposes of comparison, both values, 2.5 M^{-1} and 0.54 M^{-1}, were used for the calculation of the concentration of 2-V-3-PMGA.

III.B.6 Determination of Free and Bound Vanadium Concentration

Each ^{51}V NMR spectrum was transformed to the frequency domain and scaled identically so that a change in the integrated peak area of a given resonance from one spectrum to the next gave an accurate measure of the change in concentration of the species which gave rise to the resonance being observed. A search of 80 KHz (200 ppm) was carried out to ensure that all broad resonances were included. The relationship between the concentration of V_i and that of V_2 and V_4 is given by Equations III.1 and 2 where K_2 and K_4 are the formation constants for V_2 and V_4, respectively.

$$[V_i]^2 K_2 = [V_2] \qquad \text{III.1}$$

$$[V_i]^4 K_4 = [V_4] \qquad \text{III.2}$$

These two equilibrium constants were determined from a set of independent experiments carried out in solutions containing only buffer and vanadate at known total vanadium atom concentration. Under the conditions of these experiments, the concentrations of other vanadate oligomers are neglible so that the sum of vanadium atom concentrations of V_i, V_2, V_4 is equal to the total vanadium atom concentration. By obtaining spectra over a range of vanadium atom concentrations and plotting of $[V_2]/[V_i]^2$ and $[V_4]/[V_i]^4$, K_2 and K_4 at pH 7.0 were determined to be $(3.1\pm0.2)\times10^2$ M^{-1} and $(3.0\pm0.2)\times10^8$ M^{-3}, respectively.

When bound to the enzyme, the vanadium tumbles at the same rate as the enzyme, which is considerably slower than the tumbling rate of the vanadate free in solution. Since the ^{51}V nucleus has a rather large quadrupole moment, slower tumbling is expected to cause broadening of the ^{51}V resonance and the signal will be virtually unobservable on the ^{51}V NMR spectrum. The bound vanadate (V_B) is given by the difference between the total vanadate in solution (V_T) and the observed sum ($[V_i]$ + $[V_2]$ + $[V_4]$), as shown in Equation III.3.

$$V_B = V_T - ([V_i] + [V_2] + [V_4]) \qquad \text{III.3}$$

III.C Results and Discussion

III.C.1 Binding Study of Inorganic Vanadate to dPGM at pH 7.0

The investigation of the binding of V_2 to PGM has been repeated under conditions similar to those described by Stankiewicz et.al..[33] ^{51}V NMR spectra were obtained from solutions containing a fixed concentration of PGM and variable amounts of vanadium. A series of such spectra is shown in Figure III.1. The concentrations indicated are the total vanadium atom concentrations. The resonance occuring at -560 ppm arises from monomeric tetrahedral vanadate V_i, while those at -573 and -576 ppm are from divanadate (V_2) and tetravanadate (V_4), respectively. The results of the concentration study are tabulated in Table III.1 which gives the measured concentrations of the various vanadate species obtained as a function of total vanadate in solution.

Information concerning the stoichiometry of binding was obtained by plotting the various $[V_i]$ against the corresponding $[V_B]/[E_T]$ using the results in Table III.1. This plot is shown in Figure III.2.A where it is compared with the data of Stankiewicz et.al.[33] obtained under the same experimental conditions. Both curves show a sigmoidal dependence of $[V_B]/[E_T]$ on $[V_i]$. In an effort to obtain information concerning the stoichiometry of the reaction, $1/[V_B]$ vs $1/[V_i]$ was plotted. This graph shows lines of upward curvature as shown in Figure III.2.B.

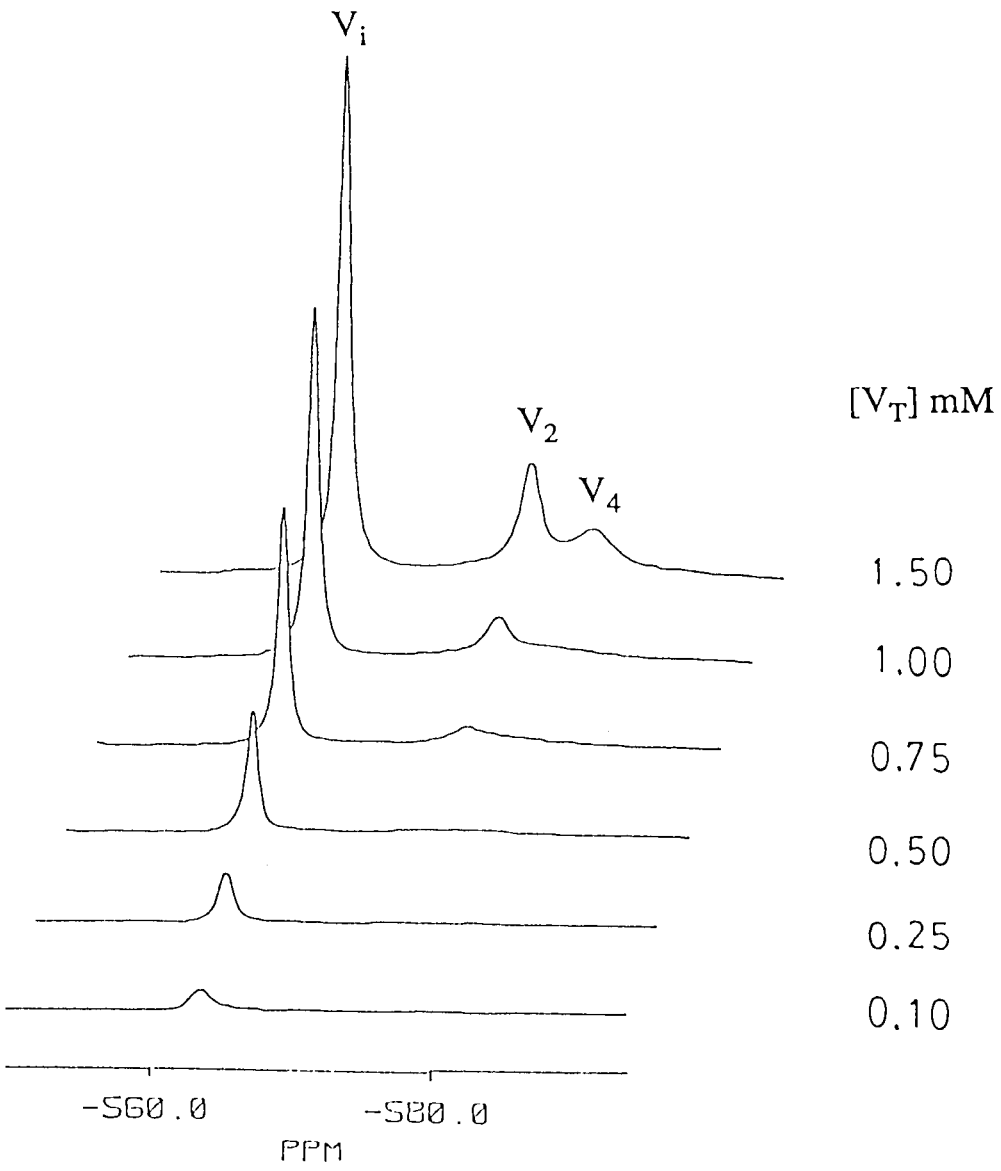

Figure III.1 The ^{51}V NMR spectra of various concentrations of vanadate in the presence of dPGM at pH 7.0. The solutions contained 0.13 mM dPGM, 20 mM HEPES, 6.0 mM KCl and total vanadium atom concentrations as indicated.

Table III.1 : Distribution of Vanadate among Free and Bound Forms in the Presence of dPGM at pH 7.0.

$[V_T]$	$[V_{vis}]$	$[V_i]$	$[V_2]$	$[V_4]$	$[V_B]$	$[V_{B,vis}]$	$[V_{B,inv}]$	$[V_B]/[E_T]$
0.10	0.086	0.030			0.070	0.056	0.014	0.539
0.25	0.211	0.071	0.003		0.176	0.137	0.039	1.359
0.50	0.338	0.134	0.011		0.355	0.193	0.162	2.738
0.75	0.581	0.251	0.039	0.005	0.456	0.286	0.169	3.514
1.00	0.798	0.384	0.091	0.027	0.498	0.296	0.202	3.842
1.50	1.282	0.603	0.225	0.161	0.511	0.293	0.218	3.940

$[E_T]$ = 0.130mM

Units are vanadium atom concentrations in mM.
Experimental conditions: 20 mM HEPES, 6 mM KCl and various concentrations of vanadate as indicated at pH 7.0.
The abbreviations are as follows:
$[V_i]$ = monomeric tetrahedral vanadate.
$[V_2]$ = divanadate, concentration calculated from equation III.1 with $K_2 = 0.31\ mM^{-1}$.
$[V_4]$ = tetravanadate, concentration calculated from equation III.2 with $K_4 = 0.30\ mM^{-3}$.
$[V_{vis}]$ = total observed vanadium concentration (including the intensity of the broad NMR signal).
$[V_{B,vis}]$ = the difference between the total free vanadium concentration and the total observed vanadium concentration, i.e. $[V_{vis}]-[V_i]-[V_2]-[V_4]$, which corresponds to the vanadium causing the broad signal in the NMR spectrum.
$[V_{B,inv}]$ = the difference between the total bound and visible bound vanadium concentration.
$[V_B]$ = the difference between total vanadate concentration and the observed sum of $[V_1]+[V_2]+[V_4]$, i.e. $V_T-([V_1]+[V_2]+[V_4])$
$[E_T]$ = Total concentration of PGM.

Figure III.2

(A) Dependence of the proportion of bound vanadium to total dPGM on free V_i concentration at pH 7.0. Curves shown are calculated from $K_{id}(V_2)$ obtained from the x-intercept of (C). The sigmoidal dependence of $[V_B]/[E_T]$ on $[V_i]$ is apparent.

(B) Plot of $1/[V_B]$ vs. $1/[V_i]$.

(C) Plot of $1/[V_B]$ vs. $1/[V_i]^2$.

The data were taken from Table III.1 and Reference 33.

(A)

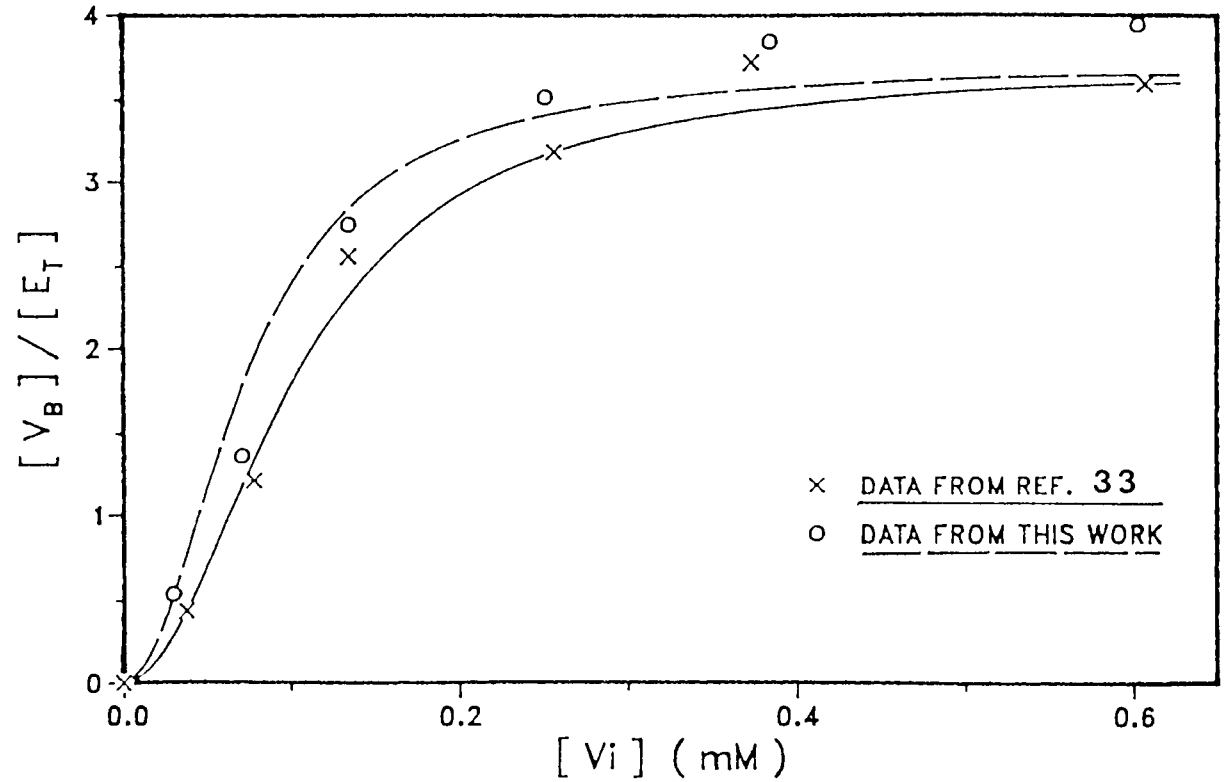
4
3
2
1
0
[V_B] / [E_T]
0.0
0.2
0.4
0.6
[Vi] (mM)
× DATA FROM REF. 33
○ DATA FROM THIS WORK

(B)

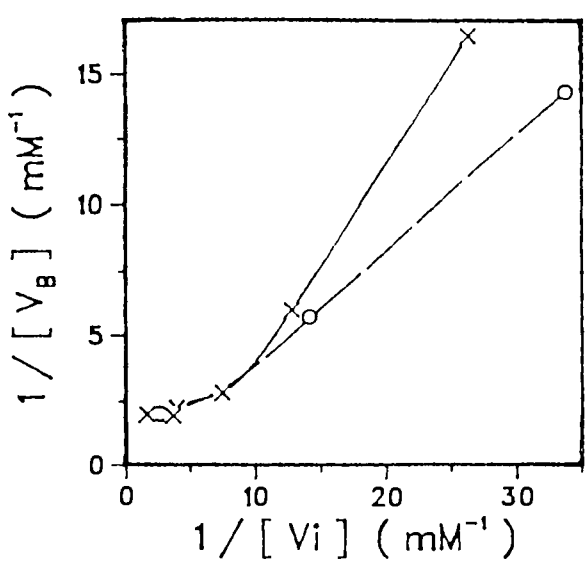
15
10
5
0
1 / [V_B] (mM^{-1})
0
10
20
30
1 / [Vi] (mM^{-1})

(C)

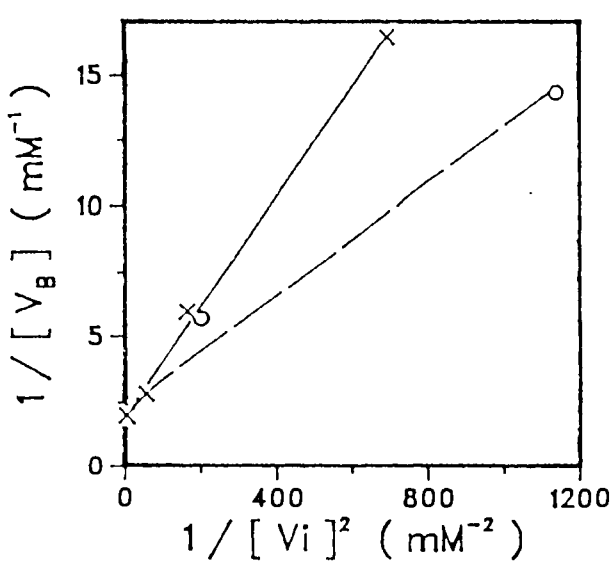
15
10
5
0
1 / [V_B] (mM^{-1})
0
400
800
1200
1 / [Vi]^2 (mM^{-2})

However, when $1/[V_B]$ is plotted against the reciprocal of vanadate concentration squared, straight lines are obtained as shown in Figure III.2.C. This indicated that two vanadate ions were simultaneously being incorporated into the PGM.

From the plot of Figure III.2.C, one obtains a vertical intercept of 2.28 which corresponds to 0.44 mM V_B per (0.13±0.01) mM PGM (determined from Lowry's method). A stoichiometry of 3.38±0.28 mole of bound vanadium atoms per mole of PGM was obtained. This corresponds to 4 atoms of vanadium bound if the PGM is 85% active. It was found that about 80% of the bound vanadium was released from the PGM by addition of 10 mM of 2,3-DPG at the end of the experiment. Under the conditions of this experiment, inactive PGM was found not to bind vanadium. These data are consistent with the assumption that the PGM is about 80% active and the loss of activity of PGM must due to the adjustment of pH by additions of acid or base to the enzymatic solution in the experimental procedure.

Using the horizontal intercept of $-248.0\ mM^{-2}$ from Figure III.2.C and the K_2 value of $(3.1\pm0.2)\times10^2\ M^{-1}$ in Equation III.1, a concentration for V_2 of $(1.3\pm0.3)\times10^{-6}$ M at half enzyme saturation is obtained. This value of $[V_2]$ corresponds to the intrinsic dissociation constant (K_{id}) of enzyme bound vanadium and describes the equilibrium between the free ligand, the free site of the enzyme, and the

enzyme-ligand complex for one site of the enzyme without regard to the other site on the same enzyme. The value of K_{id} previously obtained by Stankiewicz et.al.[33] was $4x10^{-6}$ M. The discrepancy between these values arises mainly from the double reciprocal plot method required for the analysis. The relatively few points at the high end of the $1/[V_i]^2$ scale (low $[V_i]$) do not allow a very accurate determination of the intercept. Moreover, it is these points at the lower concentrations of vanadate that are most heavily weighted in the subjective fitting of the line in the double reciprocal plot. Thus, the differences between the curves on Figure III.2.A are small but the K_{id} values show a remarkable difference.

The data are consistent with the model obtained by Stankiewicz et.al.[33] that one divanadate ion binds to each of the two subunits of PGM in a noncooperative manner as depicted in Equation III.4 with Equation III.5 and III.6 defining the two dissociation constants K_5 and K_6 respectively.

$$E \underset{V_2}{\overset{V_2\ K_6}{\rightleftharpoons}} E(V_2) \underset{V_2}{\overset{V_2\ K_5}{\rightleftharpoons}} E(V_2)_2 \qquad \text{III.4}$$

$$K_5 = [E(V_2)][V_2]/[E(V_2)]_2 \qquad \text{III.5}$$

$$K_6 = [E][V_2]/[E(V_2)] \qquad \text{III.6}$$

In terms of this model, the dissociation constants K_5 and K_6 are $(2.6\pm0.4)\times10^{-6}$ M and $(6.5\pm0.4)\times10^{-7}$ M, respectively. These values differ from each other because of the statistical factor deriving from the occurrence of two identical binding sites.

It has been observed that for PGM, the bound vanadium is divided approximately equally between NMR-visible and NMR-invisible forms.[32] Based on this, it was proposed that one of the two vanadate moieties in the bound V_2 is tetrahedral and the other is trigonal bipyramidal as shown in Figure III.3. It is because the ^{51}V nucleus has a rather large quadrupole moment and the enzyme bound vanadium tumbles at the same rate as the enzyme, which is considerably slower than the tumbling rate of free vanadium, quadrupole relaxation causes broadening of the ^{51}V resonances. However, because the tetrahedral structure is more symmetric than the trigonal bipyramidal structure, the quadrupole relaxation process is expected to be more efficient for the trigonal bipyramidal vanadium. In this case, the resonance from the latter species will be significantly broader than that from the former. The broad signal which was observed was assigned to the tetrahedral

bound vanadium and the signal intensity which was lost from the spectrum was assigned to the pentacoordinate moiety.

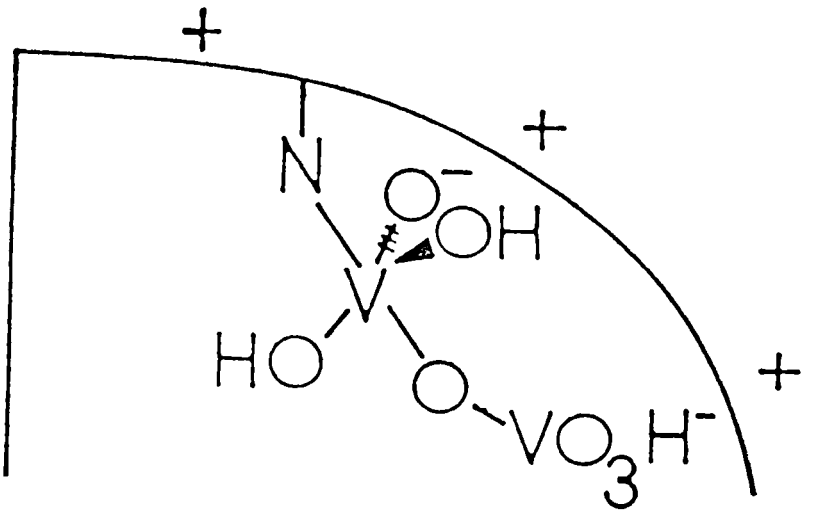

Figure III.3 Representation of divanadate bound at the catalytic site of PGM. (From Stankiewicz et.al.[33])

The visible bound and invisible bound vanadium concentrations are tabulated in Table III.1. In agreement with the previous work (Stankiewicz et.al.[33]) the $[V_{B,vis}]$ and $[V_{B,inv}]$ are equal within the experimental error. This division of $[V_B]$ into $[V_{B,vis}]$ and $[V_{B,inv}]$ is much less accurate than the measurement of $[V_B]$ since a "sharp" signal from V_i rather than the broad signal deriving from $V_{B,vis}$ is used to give $[V_B]$. The approximately equal division of V_B between visible and invisible forms is significant and is consistent with the tight binding of V_2 to PGM. The K_{id} of V_2 (1.3×10^{-6} M) is within a factor of 4 of the K_m for 2,3-DPG (3.26×10^{-7} M)[42], the cofactor for PGM. As was discussed

in the introduction, the transition state structure about the phosphorus in the phosphoryl transfer reaction is a pentacoordinate trigonal bipyramidal structure and vanadate adopts this structure very readily. Therefore it is not surprising that V_2, with a pentacoordinate moiety, binds very tightly to PGM.

III.C.2 Binding study of Inorganic Vanadate to dPGM at pH 8.0

The binding of inorganic vanadate to dPGM has also been studied at pH 8.0 by using ^{51}V NMR spectroscopy. Table III.2 gives the observed concentrations of the various vanadate species in solution. A plot of $[V_i]$ against the corresponding $[V_B]/[E_T]$ at pH 7.0 gave sigmoidal dependence of $[V_B]/[E_T]$ on $[V_i]$ but at pH 8.0 it was not as obvious as for that at pH 7.0 (Figure III.4.A). However, a plot of $1/[V_B]$ vs $1/[V_i]^2$ gave a straight line which agrees with the model depicted in Equation III.4. In agreement with the pH 7.0 results, the vertical intercept gave a limiting stoichiometry of 3.68±0.05 mole of vanadium atoms per mole of PGM. This corresponds to 4 atoms of vanadium bound if the PGM is 92% active. From the horizontal intercept the intrinsic dissociation constant of V_2 bound to dPGM, $K_{id}(V_2)$, is calculated to be $(1.3\pm0.3)\times10^{-7}$ M which corresponds to values for the experimental dissociation constants K_5 and K_6 of 2.6×10^{-7} and 6.5×10^{-8} M respectively.

Table III.2: Distribution of Vanadate among Free and Bound Forms in the Presence of dPGM at pH 8.0.

$[V_T]$	$[V_{vis}]$	$[V_i]$	$[V_2]$	$[V_4]$	$[V_B]$	$[V_{B,vis}]$	$[V_{B,inv}]$	$[V_B]/[E_T]$
0.10	0.015	0.011			0.089	0.004	0.085	0.456
0.25	0.154	0.030			0.219	0.124	0.095	1.130
0.50	0.250	0.054	0.001		0.445	0.195	0.250	2.195
0.75	0.332	0.080	0.003		0.667	0.249	0.418	3.443
1.00	0.457	0.186	0.014	0.001	0.799	0.256	0.543	4.119
1.50	1.024	0.560	0.128	0.070	0.742	0.266	0.476	3.825

$[E_T]$ = 0.194 mM

Units are vanadium atom concentrations in mM.
Experimental conditions: 20 mM HEPES, 6 mM KCl and various concentration of vanadate as indicated at pH 8.0.
The values of $[V_2]$ were calculated with K_2 = 0.20 mM^{-1}
The values of $[V_4]$ were calculated with K_4 = 0.18 mM^{-3}
For abbreviations used, Refer to Table III.1

Figure III.4
(A) Dependence of the proportion of bound vanadium to total dPGM on free V_i concentration at pH 8.0. Curves shown are calculated from $K_{id}(V_2)$ obtained from the x-intercept of (C).
(B) Plot of $1/[V_B]$ vs. $1/[V_i]$.
(C) Plot of $1/[V_B]$ vs. $1/[V_i]^2$.
The data were taken from Table III.2.

(A)

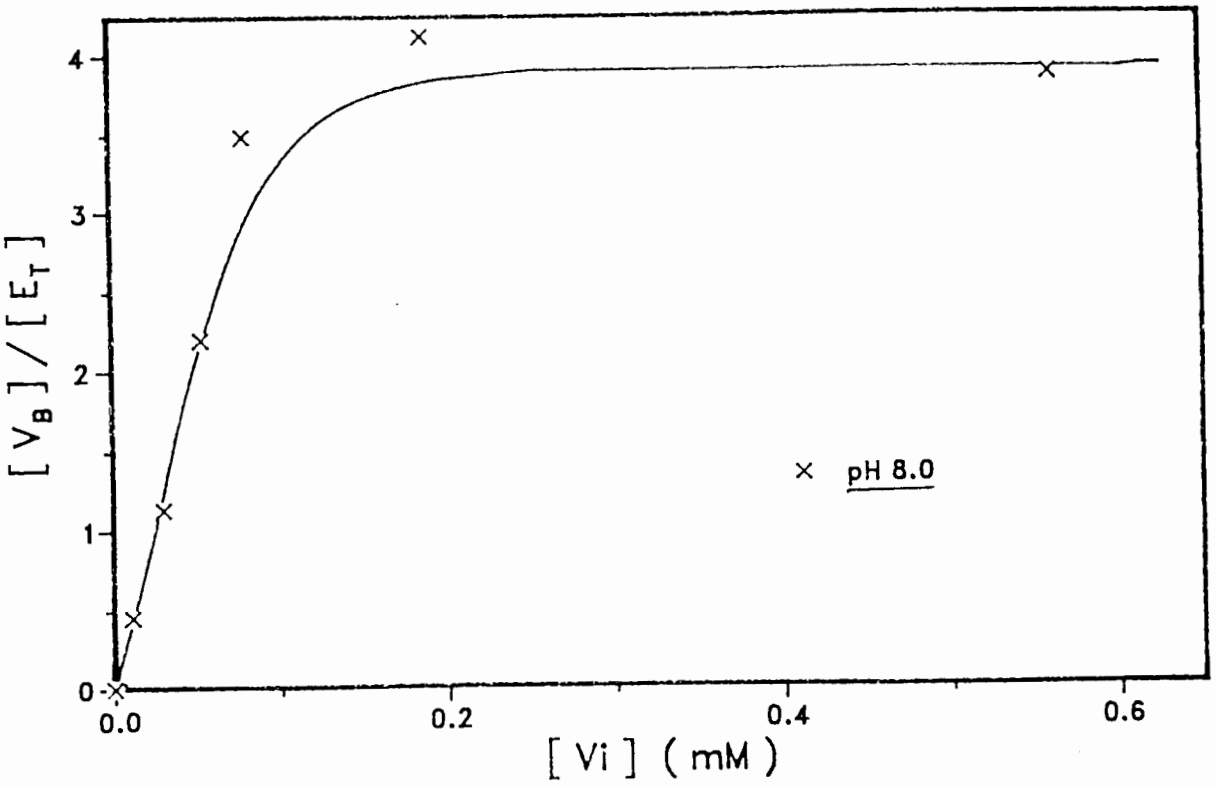
4
3
2
1
0
0.0
0.2
0.4
0.6
[V_B] / [E_T]
[Vi] (mM)
× pH 8.0

(B)

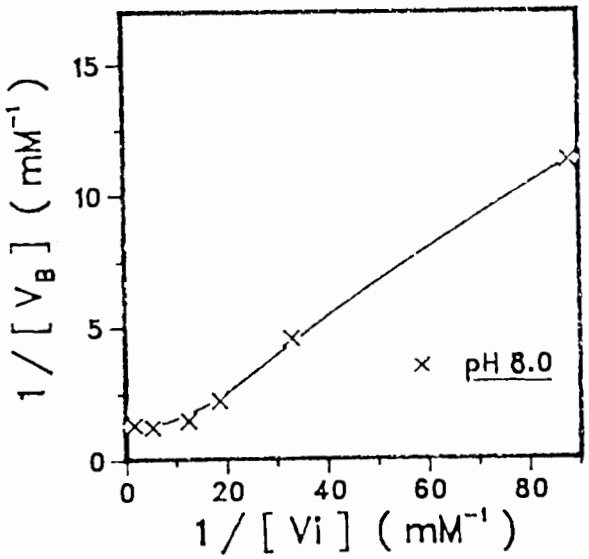
15
10
5
0
0
20
40
60
80
1 / [V_B] (mM^{-1})
1 / [Vi] (mM^{-1})
× pH 8.0

(C)

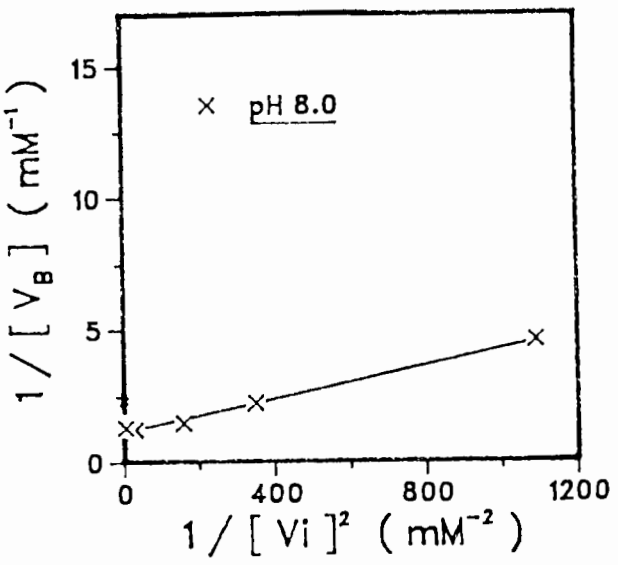
15
10
5
0
0
400
800
1200
1 / [V_B] (mM^{-1})
1 / [Vi]^2 (mM^{-2})
× pH 8.0

The noncooperative binding of one divanadate ion to the individual binding site of each of the two subunits which form the enzyme explains, in a logical and simple manner, both the limiting stoichiometry of four bound vanadium atoms per enzyme molecule and also the linear relationship between $1/[V_B]$ and $1/[V_i]^2$.

Table III.3 summarizes the intrinsic dissociation constants and the dissociation constants K_5 and K_6 as defined in Equation III.4, III.5 and III.6 at pH 7.0 and pH 8.0.

Table III.3: Summary of Dissociation Constants of V_2 Bound to dPGM

pH	intrinsic dissociation constants $K_{id}(V_2)$ (M)	dissociation constants of individual subunit K_5 (M)	K_6 (M)
*7.0	4×10^{-6}	8×10^{-6}	2×10^{-6}
7.0	$(1.3\pm0.3)\times10^{-6}$	$(2.6\pm0.4)\times10^{-6}$	$(6.5\pm0.4)\times10^{-7}$
8.0	$(1.3\pm0.3)\times10^{-7}$	$(2.6\pm0.4)\times10^{-7}$	$(6.5\pm0.4)\times10^{-8}$

* Data from Stankiewicz et.al.[33]
The data were taken from Table III.1 and III.2 and were calculated as described in the text.

About a factor of 10 between the K_{id} for pH 7.0 and 8.0 was observed. The difference is due to a significant amount of divanadate (pK_{a2} = 7.2)[53] in its trianion form, $HV_2O_7^{3-}$, at pH 8.0 when compared to that at pH 7.0. The electrostatic interaction between the highly negatively charged V_2 and the positively charged groups in the catalytic site cause V_2 to bind more favorably to dPGM at pH 8.0.

III.C.3 Binding Studies of Inorganic Vanadate to dPGM at pH 6.0

The binding of inorganic vanadate has also been studied at pH 6.0 by using ^{51}V NMR spectroscopy. Table III.4 gives the observed concentrations of the various vanadate species as a function of total vanadate in solution. A plot of $[V_i]$ against $[V_B]/[E_T]$ is shown in Figure III.5. It can be seen that at 1.5 mM of total vanadate, a concentration where at pH 7.0 and 8.0 binding has reached its limiting stoichiometry of four bound vanadium atoms per enzyme molecule, $[V_B]/[E_T]$ is close to 7 and has not yet reached the limiting stoichiometry. This result indicates very strongly that at this pH much of the observed binding of vanadium is nonspecific and vanadate binds to both the catalytic site and other groups of the enzyme molecule. This nonspecific binding behavior of inorganic vanadate to PGM might due to the fact that more

Table III.4 : Distribution of Vanadate among Free and Bound Forms in the presence of dPGM at pH 6.0.

$[V_T]$	$[V_{vis}]$	$[V_i]$	$[V_2]$	$[V_4]$	$[V_B]$	$[V_{B,vis}]$	$[V_{B,inv}]$	$[V_B]/[E_T]$
0.10	0.018	0.009			0.091	0.008	0.082	0.604
0.20	0.027	0.016			0.184	0.010	0.173	1.224
0.30	0.027	0.021			0.278	0.006	0.273	1.856
0.50	0.067	0.038	0.001		0.461	0.028	0.433	3.072
0.75	0.110	0.070	0.003		0.676	0.036	0.640	4.509
1.00	0.202	0.146	0.014	0.001	0.840	0.042	0.798	5.598
1.25	0.360	0.262	0.043	0.007	0.937	0.047	0.890	6.249
1.50	0.534	0.356	0.080	0.025	1.038	0.073	0.966	6.921

$[E_T]$ = 0.158mM

Units are vanadium atom concentrations in mM.
Experimental conditions: 20 mM HEPES, 6 mM KCl and various concentrations of vanadate as indicated at pH 6.0.
The values of $[V_2]$ were calculated with K_2 = 0.32 mM^{-1}.
The values of $[V_4]$ were calculated with K_4 = 0.39 mM^{-3}.
For abbreviations used, see Table III.1 .

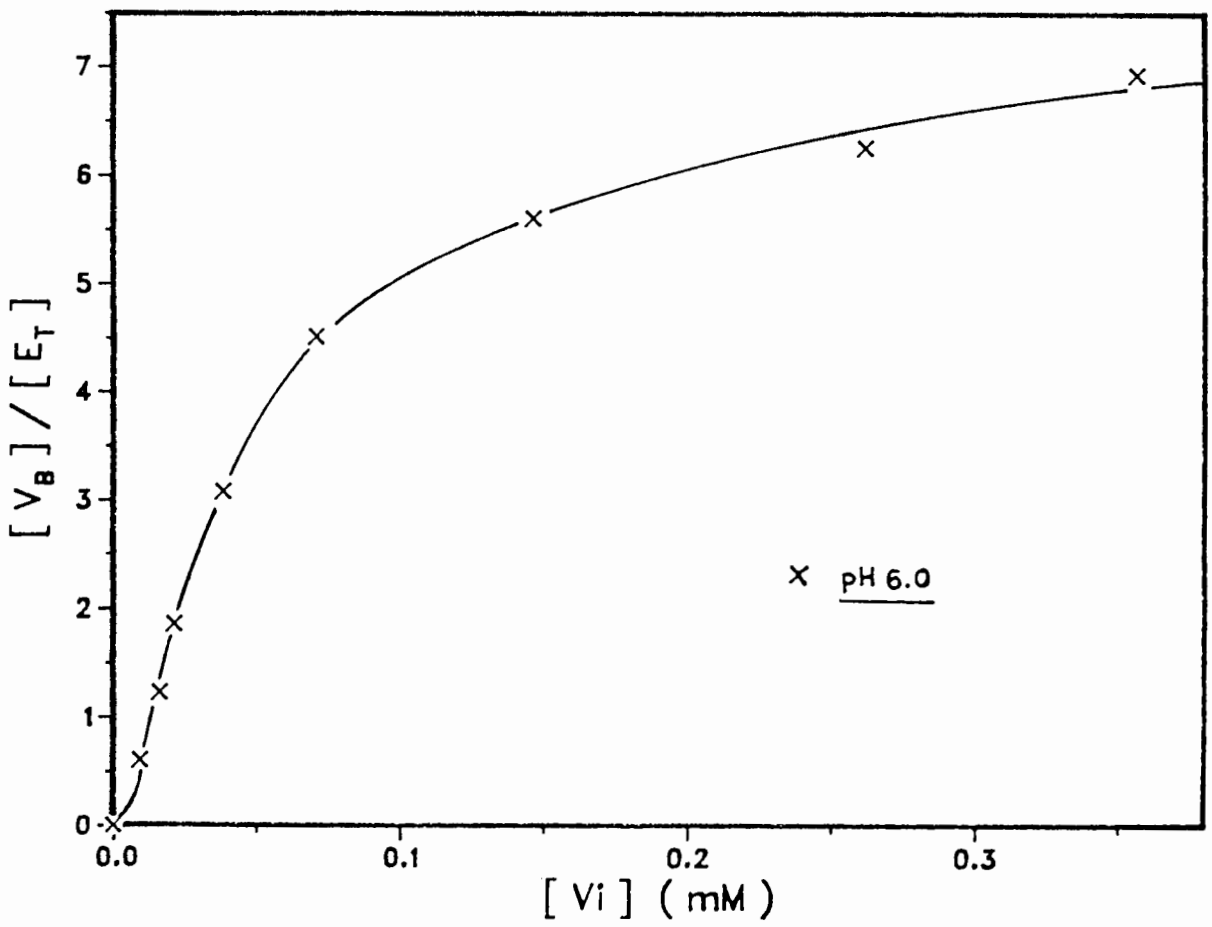

Figure III.5 Dependence of the ratio of bound vanadium to total dPGM concentration versus free V_i concentration at pH 6.0. The data were taken from Table III.3.

amino acid functional groups on the surface of the enzyme becomes protonated at pH 6.0 and interact with the negatively charged vanadate species. As a result, $[V_B]/[E_T]$ increased. This nonspecific binding behavior makes the quantitative analysis of the dissociation constant difficult. Further investigation has to be carried out to study the nonspecific binding of inorganic vanadate to PGM before making refinement of the model possible.

III.C.4 Studies of the Binding of Vanadate Esters to dPGM at pH 7.0

^{51}V NMR spectra were obtained from solutions containing a fixed concentration of dPGM, 1.0 mM V_T and varying concentrations of substrate or substrate analogue at pH 7.0. Under these conditions, binding of vanadate has reached its limiting stoichiometry of four bound vanadium atoms per enzyme molecule before the additions of substrate or substrate analogues. Once the substrate or the substrate analogue is added to the vanadate/enzyme solution, a vanadate ester of the substrate or the substrate analogue is expected to form spontaneously.[8-12] In the event that the vanadate derivative of the substrate analogue binds more tightly to dPGM than divanadate, then dependent on the stoichiometry, a net release of vanadate from the enzyme may occur. Figure III.6 demonstrates this for the case of 3-PGA. The bottom spectrum in this figure derives from a

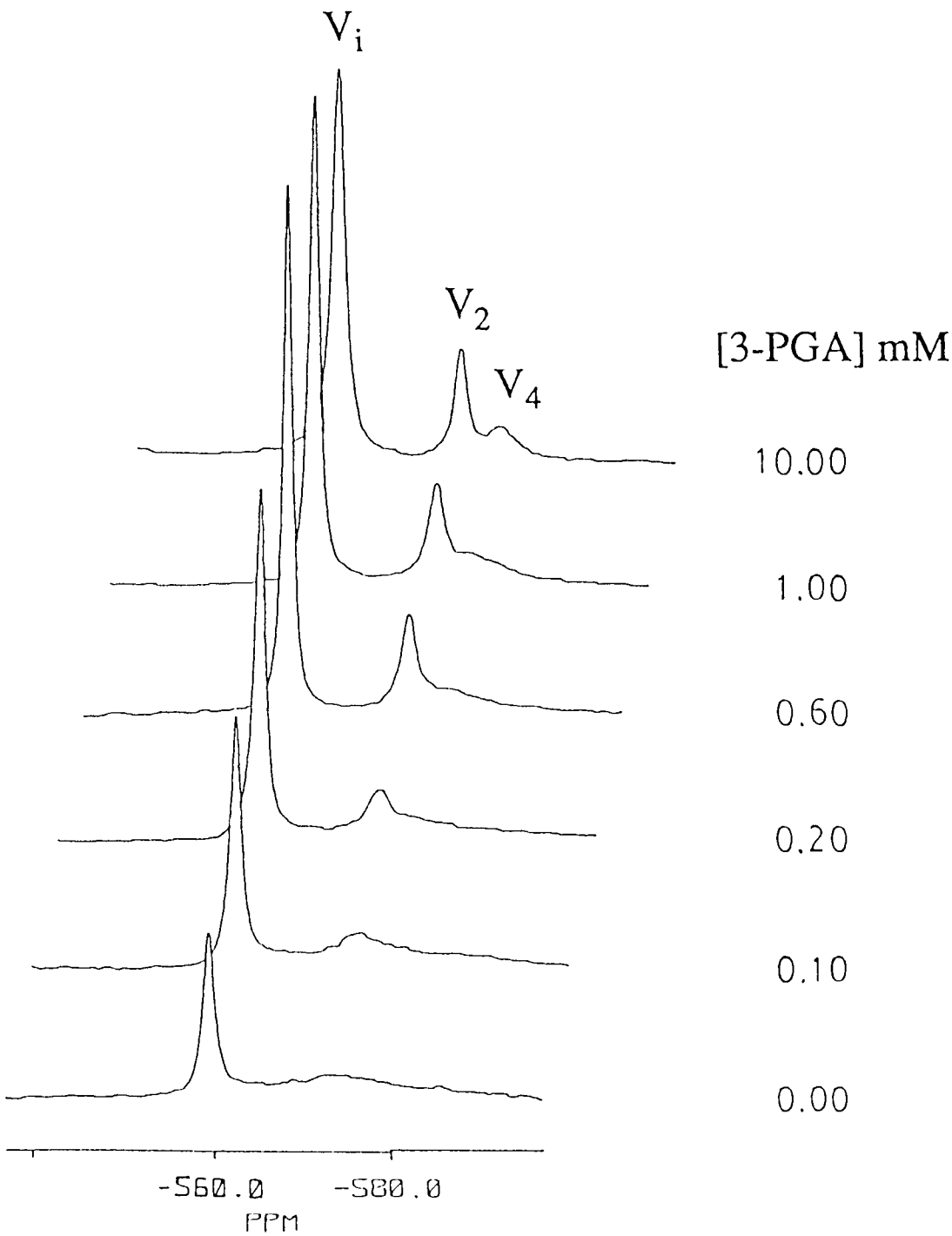

Figure III.6 The ^{51}V NMR spectra obtained from vanadate at a constant concentration but with varying concentrations of 3-PGA in the presence of a fixed concentration of dPGM at pH 7.0. The solution contained 0.21 mM dPGM, 20 mM HEPES, 6 mM KCl, 1 mM vanadate and 3-PGA concentrations as indicated.

solution containing no 3-PGA and since the spectra are plotted in the absolute intensity mode, the figure reveals that total observable vanadium atom concentration increased as the concentration of 3-PGA was increased. The resonances in these spectra are assigned similarly to those in Figure III.1. The distribution of vanadate among free and bound forms in the presence of a fixed concentration of PGM, V_T, and various amount of 3-PGA is tabulated in Table III.5. Similar studies with 3-PMGA, glyceric acid and glycolic acid have been done and the results are presented in Table III.6-8.

Information concerning the stoichiometry of binding was obtained by plotting the concentration of substrate or substrate analogue against the corresponding $[V_B]/[E_T]$. This plot is shown in Figure III.7. A stoichiometry of close to four bound vanadium atoms per enzyme molecule was obtained when no substrate or substrate analogue was present, a result in agreement with the vanadate binding studies and consistent with binding of one divanadate ion to each of the two subunits of dPGM. When 3-PGA or 3-PMGA was added, bound vanadate atoms were released and in the limit of excess added substrate a residual stoichiometry of 2.0±0.1 mole of bound vanadium atoms per mole of dPGM was obtained. It is not immediately obvious how to rationalize the plot of $[V_B]/[E_T]$ vs the concentration of substrate or substrate analogues. The simplest means to do so appears to be as described in the following. Noncooperative binding

Table III.5 : Distribution of Vanadate among Free and Bound Forms in the Presence of dPGM and Various Concentrations of 3-PGA at pH 7.0.

$[3\text{-PGA}]_T$	$[V_{vis}]$	$[V_i]$	$[V_2]$	$[V_4]$	$[V_{OC}]$	$[V_B]$	$[V_{B,vis}]$	$[V_{B,inv}]$	$[V_B]/[E_T]$
0.00	0.501	0.171	0.018	0.001		0.810	0.310	0.499	3.795
0.05	0.584	0.232	0.033	0.003		0.731	0.315	0.416	3.427
0.10	0.672	0.275	0.047	0.007		0.671	0.343	0.328	3.145
0.15	0.672	0.328	0.067	0.014		0.592	0.263	0.328	2.773
0.20	0.824	0.375	0.087	0.024		0.513	0.337	0.176	2.407
0.40	0.691	0.422	0.111	0.038		0.428	0.119	0.309	2.008
0.60	0.743	0.424	0.111	0.039		0.426	0.169	0.257	1.999
1.00	0.746	0.420	0.109	0.037		0.433	0.179	0.254	2.031
2.00	0.719	0.430	0.114	0.041	0.031	0.384	0.103	0.281	1.802
10.00	0.737	0.422	0.110	0.038	0.069	0.361	0.098	0.263	1.693

$[E_T] = 0.213$ mM

Concentrations are in units of mM.
Experimental conditions: 1 mM total vanadate, 20 mM HEPES, 6 mM KCl with 3-PGA concentrations as indicated at pH 7.0.
The values of $[V_2]$ were calculated with $K_2 = 0.310\ mM^{-1}$.
The values of $[V_4]$ were calculated with $K_4 = 0.300\ mM^{-3}$.
For abbreviation used: $[V_{OC}]$ = vanadium complex with octahedral coordinate about each vanadium nucleus assigned and described in Tracey et.al..[8]

Table III.6 : Distribution of Vanadate among Free and Bound Forms in the Presence of dPGM and Various Concentrations of 3-PMGA at pH 7.0.

$[3\text{-PMGA}]_T$	$[V_{vis}]$	$[V_1]$	$[V_2]$	$[V_4]$	$[V_{OC}]$	$[V_B]$	$[V_{B,vis}]$	$[V_{B,inv}]$	$[V_B]/[E_T]$
0.00	0.428	0.173	0.018	0.001		0.807	0.236	0.572	3.787
0.05	0.426	0.201	0.025	0.002		0.772	0.198	0.574	3.621
0.12	0.469	0.256	0.041	0.005		0.698	0.167	0.530	3.275
0.24	0.542	0.292	0.053	0.009		0.646	0.188	0.458	3.032
0.48	0.520	0.318	0.063	0.012		0.606	0.126	0.480	2.845
0.96	0.538	0.353	0.078	0.019	0.017	0.533	0.071	0.462	2.500
1.44	0.618	0.369	0.084	0.022	0.038	0.487	0.105	0.382	2.283
1.92	0.647	0.375	0.087	0.024	0.074	0.440	0.087	0.353	2.063
2.40	0.670	0.371	0.085	0.023	0.103	0.417	0.087	0.330	1.957
10.00	0.670	0.411	0.105	0.034	0.104	0.346	0.016	0.330	1.970

$[E_T]$ = 0.213 mM

Concentrations are in units of mM.
Experimental conditions: 1 mM total vanadate, 20 mM HEPES, 6 mM KCl with 3-PMGA concentrations as indicated at pH 7.0.

Table III.7 : Distribution of Vanadate among Free and Bound Froms in the Presence of dPGM and Various Concentrations of Glyceric Acid at pH 7.0.

$[Glyceric\ Acid]_T$	$[V_{vis}]$	$[V_i]$	$[V_2]$	$[V_4]$	$[V_{OC}]$	$[V_B]$	$[V_{B,vis}]$	$[V_{B,inv}]$	$[V_B]/[E_T]$
0.0	0.431	0.158	0.015	0.001		0.826	0.257	0.569	3.750
0.5	0.420	0.158	0.015	0.001		0.826	0.246	0.580	3.750
1.0	0.416	0.146	0.013	0.001		0.841	0.257	0.584	3.817
1.5	0.419	0.140	0.012			0.847	0.265	0.581	3.845
2.0	0.381	0.136	0.011			0.852	0.233	0.619	3.869
3.0	0.399	0.150	0.014	0.001		0.835	0.234	0.601	3.793
4.0	0.420	0.145	0.013	0.001		0.841	0.261	0.581	3.821
5.0	0.422	0.145	0.013	0.001		0.842	0.263	0.578	3.821
10.00	0.450	0.139	0.012		0.044	0.804	0.299	0.505	3.651
20.00	0.500	0.105	0.007		0.113	0.775	0.275	0.500	3.518

$[E_T]$ = 0.220 mM

Concentrations are in units of mM.
Experimental conditions: 1 mM total vanadate, 20 mM HEPES, 6 mM KCl with glyceric acid concentrations as indicated at pH 7.0.

Table III.8 : Distribution of Vanadate among Free and Bound Forms in the Presence of dPGM and Various Concentrations of Glycolic Acid at pH 7.0.

[Glycolic acid]	$[V_{vis}]$	$[V_1]$	$[V_2]$	$[V_4]$	$[V_B]$	$[V_{B,vis}]$	$[V_{B,inv}]$	$[V_B]/[E_T]$
0.00	0.495	0.276	0.047	0.007	0.670	0.164	0.505	3.715
0.05	0.568	0.288	0.051	0.008	0.652	0.220	0.432	3.617
0.10	0.542	0.290	0.052	0.009	0.649	0.190	0.459	3.600
0.20	0.604	0.293	0.053	0.009	0.645	0.249	0.396	3.579
0.30	0.548	0.287	0.051	0.008	0.654	0.203	0.452	3.631
0.40	0.553	0.291	0.052	0.009	0.648	0.201	0.447	3.596
0.60	0.545	0.290	0.052	0.009	0.649	0.194	0.455	3.602
1.00	0.599	0.305	0.058	0.010	0.627	0.226	0.401	3.478
1.50	0.565	0.296	0.054	0.009	0.641	0.206	0.435	3.557
2.00	0.589	0.289	0.052	0.008	0.651	0.240	0.411	3.614
4.00	0.611	0.286	0.051	0.008	0.655	0.266	0.415	3.637
10.00	0.585	0.278	0.048	0.007	0.667	0.252	0.415	3.702

$[E_T]$ = 0.180 mM

Concentrations are in units of mM.
Experimental conditions: 1 mM total vanadate, 20 mM HEPES, 6 mM KCl with glycolic acid concentrations as indicated at pH 7.0.

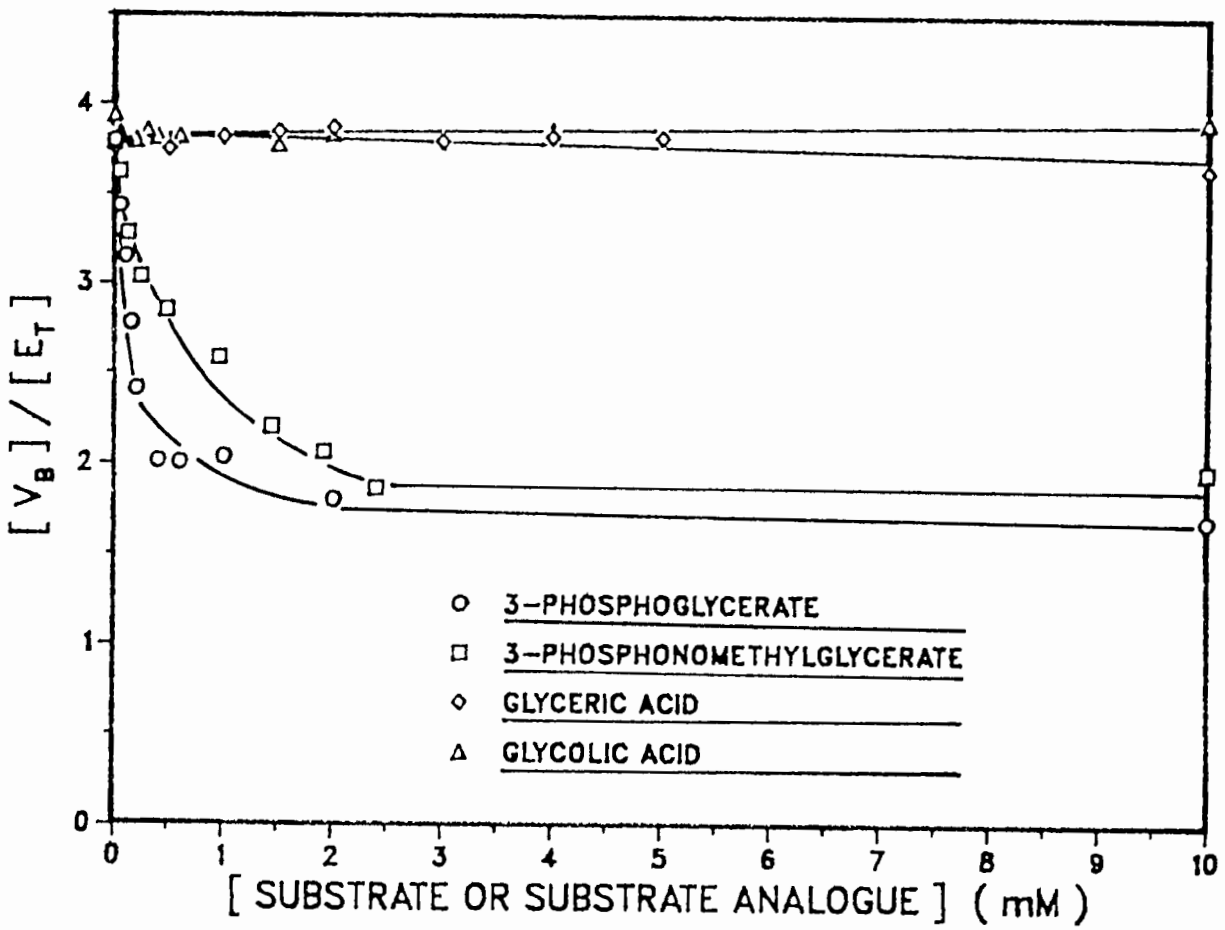

Figure III.7 Dependence of the ratio of bound vanadium to dPGM concentration versus the concentration of various ligands at pH 7.0. The solutions contained 0.17-0.22 mM dPGM, 20 mM HEPES, 6 mM KCl, 1.0 mM vanadate and ligand concentration as indicated.
The data are consistent with binding of one divanadate ion to each of the two identical subunits of PGM when no other ligand is present. With addition of 3-PGA or 3-PMGA, two vanadate ions are released from the enzyme while two remain bound. All points and curves shown are experimental data only.

of V_2 occurs to each of the two subunits of PGM. As the vanadate esters are formed, they compete with divanadate for the catalytic site. Since each vanadate ester contains only one vanadate, a total of two vanadium atoms are released from the enzyme while the remaining two are bound as a vanadate esters. The various equilibria to be considered are depicted in Figure III.8.

The equations that define the dissociation constants, the conservation equations and the iterative method that allows for the calculation of $[V_B]/[E_T]$ at various concentrations of 3-PGA are given in Appendix III. The assumption that had made in this model is that there is no cooperativity in the binding of divanadate (V_2), or vanadate ester (I), to the two binding sites of PGM (i.e. $K_5 = 4K_6 = 2K_{10}$ and $K_8 = 4K_7 = 2K_9$). The dissociation constants K_5 and K_6, K_8 and K_9 differ from each other because of the statistical factor arising from the assumption of two identical binding sites which display no cooperativity. Furthermore, it is assumed that the binding of V_2 or I to one site does not affect the affinity of the other for either V_2 or I.

Figure III.9 shows the results of the binding studies of PGM with constant concentration of vanadate and varied concentration of 3-PGA added. The experimental data are shown with a family of curves that were calculated from different values of K_7 by the iterative method given in

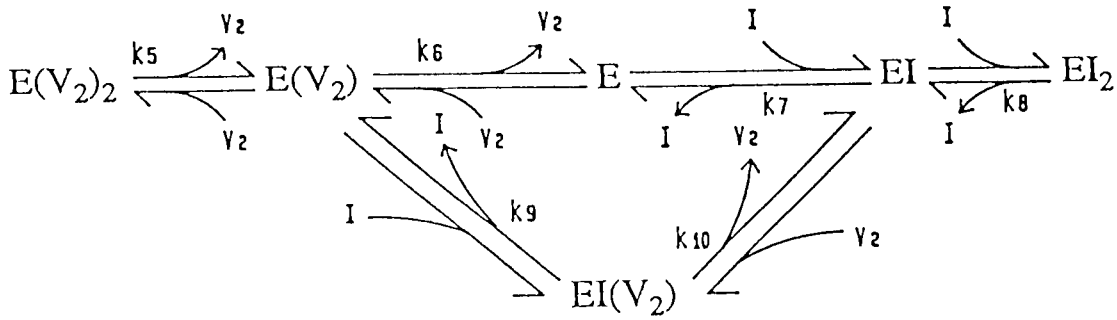

Figure III.8 Proposed scheme for the binding of divanadate and vanadate ester to dephosphorylated rabbit muscle PGM. Assumptions that have made in this model are (1) there is no cooperativity in the binding of V_2 or I to the two binding sites of PGM,

$$\text{i.e.} \quad K_5 = 4K_6 = 2K_{10}$$
$$K_8 = 4K_7 = 2K_9$$

(2) the binding of V_2 or I to one site of PGM does not affect the affinity of the other for either V_2 or I.

Abbreviations: E = free enzyme (with two empty active sites);
V_2 = divanadate;
I = inhibitor (vanadate ester).
Definition of the dissociation constants are shown in Appendix III.

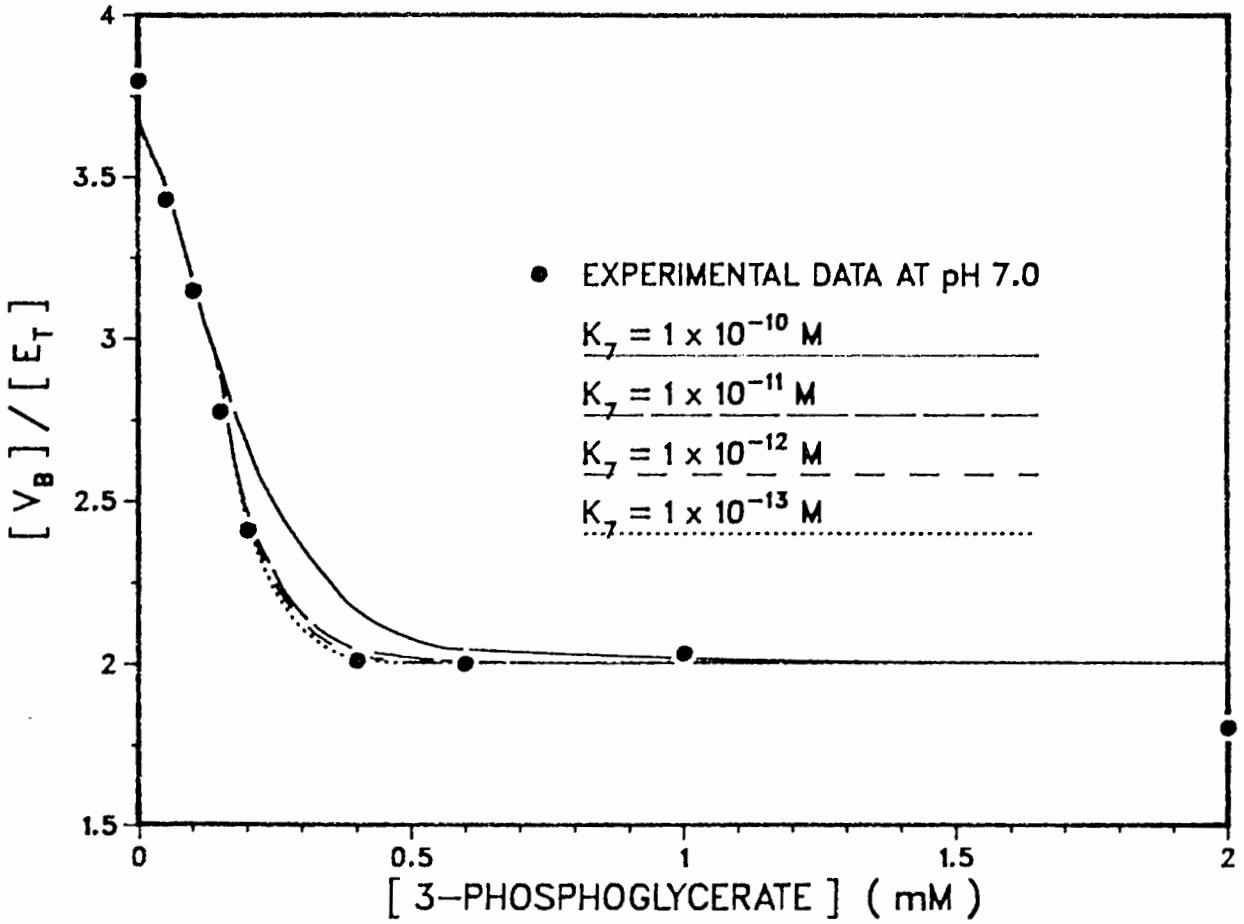

Figure III.9 Dependence of $[V_B]/[E_T]$ on the concentration of 3-PGA at pH 7.0. Experimental data from Table III.5 are shown with the calculated curves that are solved by the iterative method given in Appendix III by assuming various values of K_7 and $K_3 = 2.5\ M^{-1}$.

Appendix III. It can be seen from Figure III.9 that once the value of K_7 used for the calculated curves was smaller than $1x10^{-11}$ M, the curves were almost superimposed on one another. This behaviour probably results from the fact that the dissociation constant of the vanadate ester is about 10^6 fold lower than that for V_2. At such levels the binding of V_2 to dPGM is no longer comparable to that of 2-V-3PGA and consequently the amount of vanadate release is essentially equal to the amount of 3-PGA added, independent of the actual value of K_7. It can be seen that most of the experimental data lies on the curves for which the assumed K_7 are smaller than $1x10^{-11}$ M. This means that an upper limit of $1x10^{-11}$ can be placed on K_7, unfortunately no lower limit can be estimated.

Figures III.10.A and B show the results obtained from binding studies of dPGM with 1 mM of vanadate and varying concentration of 3-PMGA. The results are very similar to those obtained from the study of 3-PGA with two bound vanadate atoms being released from the enzyme while two remain bound. A family of curves calculated from various values of K_7 has been superimposed on a graph of the experimental data by assuming that the formation constants of the vanadate ester (K_3) is equal to 2.5 M^{-1}, the measured value for 2-V-3PGA. A similar plot has been made for K_3 = 0.54 M^{-1}, the formation constant for the formation of the lactate monoester. Figure III.10.A demonstrates this for K_3

Figure III.10 Dependence of $[V_B]/[E_T]$ on 3-PMGA concentration at pH 7.0. Experimental data from Table III.6 are shown with the calculated curves that are solved by the iterative method given in Appendix III by assuming various values of K_7.

(A) Curves are calculated by assuming that the formation constant of 2-V-3PMGA (K_3) is equal to that of 2-V-3PGA, 2.5 M^{-1}.

(B) Curves are calculated by assuming that K_3 is equal to that of 2-vanado-lactate, 0.54 M^{-1}.

(A)

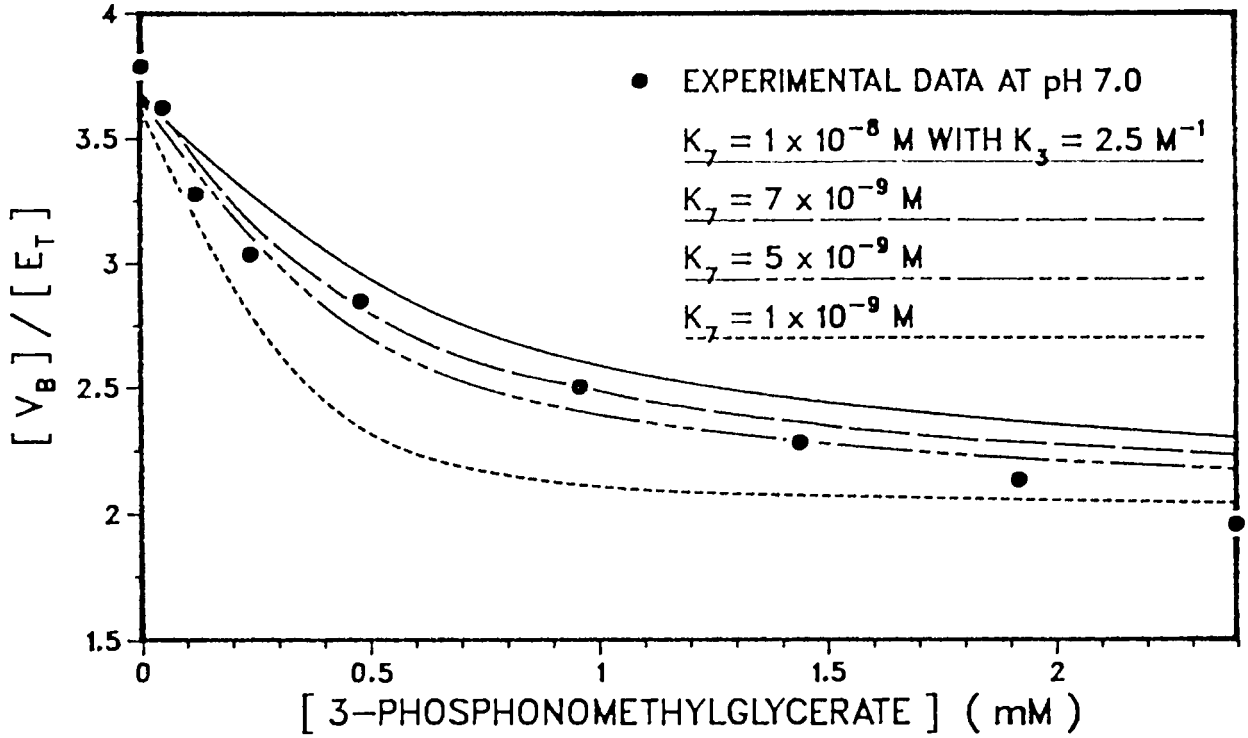
EXPERIMENTAL DATA AT pH 7.0
$K_7 = 1 \times 10^{-8}$ M WITH $K_3 = 2.5$ M^{-1}
$K_7 = 7 \times 10^{-9}$ M
$K_7 = 5 \times 10^{-9}$ M
$K_7 = 1 \times 10^{-9}$ M
$[V_B] / [E_T]$
[3–PHOSPHONOMETHYLGLYCERATE] (mM)

(B)

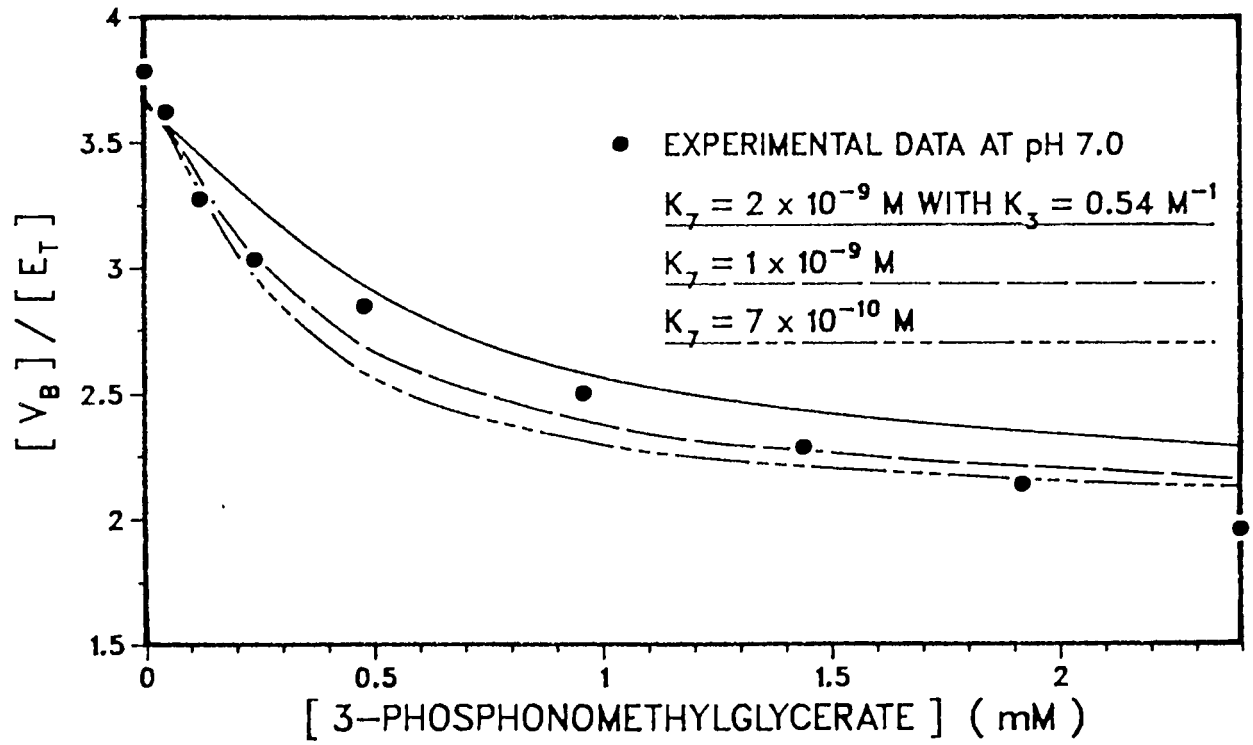
EXPERIMENTAL DATA AT pH 7.0
$K_7 = 2 \times 10^{-9}$ M WITH $K_3 = 0.54$ M^{-1}
$K_7 = 1 \times 10^{-9}$ M
$K_7 = 7 \times 10^{-10}$ M
$[V_B] / [E_T]$
[3–PHOSPHONOMETHYLGLYCERATE] (mM)

= 2.5 M^{-1}, and it can be seen that the calculated curve with K_7 = $5x10^{-9}$ M is the closest to the experimental data. When K_3 = 0.54 M^{-1}, as shown in Figure III.10.B, the calculated curve with K_7 = $1x10^{-9}$ M provides the closest fit to the experimental data.

Figure III.11 shows the studies of glyceric acid vanadate ester binding to PGM. It can be seen from the experimental data that with addition of 20 mM of glyceric acid, only a very small amount of bound vanadium atoms are released from the enzyme. As before, a family of curves was obtained for various values of K_7 and superimposed on the graph of the experimental data. As shown in Figure III.11, the calculated curve with K_7 = $7x10^{-7}$ M is the closest to the experiment data and therefore the K_7 is estimated to be $7x10^{-7}$ M.

The binding of the vanadate ester of glycolic acid to dPGM has also been studied. In this case, with the addition of aliquots of glycolic acid, no significant amount of bound vanadium was released as shown previously in Figure III.7. Therefore no estimation of the values for K_7 could be made. Calculations showed that once the K_7 becomes larger than the binding constant for V_2 ($1x10^{-6}$ M), the calculated curves are very similar. This results because the binding of the vanadate ester to dPGM does not effectively compete against the binding of V_2. The

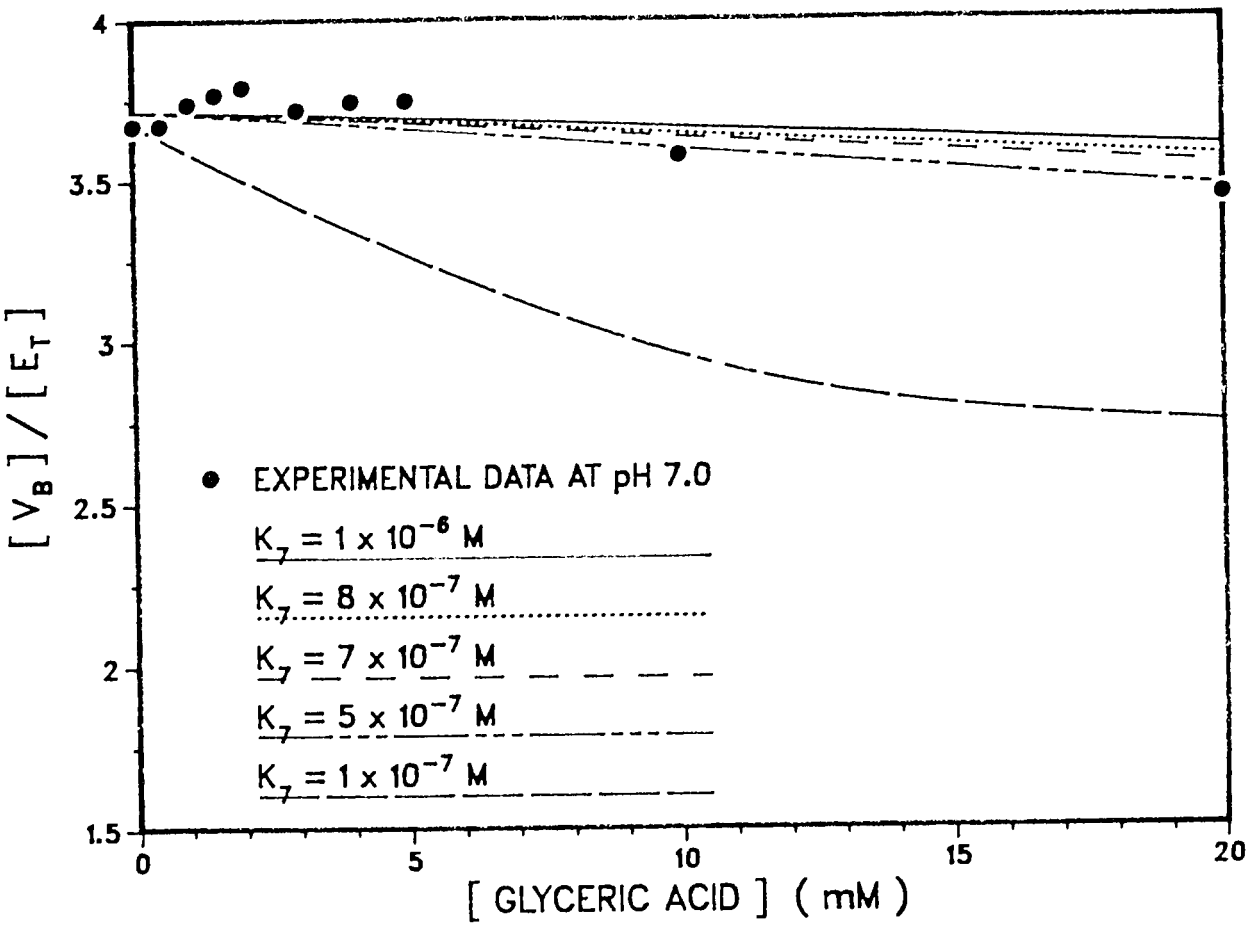

Figure III.11 Dependence of $[V_B]/[E_T]$ on glyceric acid concentration at pH 7.0. Experimental data from Table III.7 are shown with the calculated curves that are solved by the iterative method given in Appendix III by assuming K_3 = 0.54 M^{-1} and various values of K_7.

divanadate remains bound and no significiant amounts of vanadium are released from the enzyme.

Table III.9 tabulates the K_7's and dissociation constants estimated for various vanadate esters binding to dPGM.

Table III.9: Dissociation Constants of Various Vanadate Esters from dPGM at pH 7.0

Vanadate Ester of	K_3 (M^{-1})	K_7 (M)	K_8 (M)	K_9 (M)	K_{id} (M)
3-PGA	2.5	$1x10^{-11}$	$4x10^{-11}$	$2x10^{-11}$	$2x10^{-11}$
3-PMGA	2.5	$5x10^{-9}$	$2x10^{-8}$	$1x10^{-8}$	$1x10^{-8}$
	0.54	$1x10^{-9}$	$4x10^{-9}$	$2x10^{-9}$	$2x10^{-9}$
Glyceric acid	0.54	$7x10^{-7}$	$3x10^{-6}$	$1x10^{-6}$	$1x10^{-6}$
Glycolic acid	0.54		($<1x10^{-6}$)		

K_3 = formation constants of vanadate ester used for the determination of K_7.
Definitions of dissociation constants and method of calculation are shown in Appendix III with the model depicted in Figure III.8. The values of K_5 and K_6 that have been used for the determination of K_7 were obtained from Table III.3.

A comparison of the K_7 values of 3-PMGA that were obtained from the two different values of K_3, 2.5 and 0.54

M^{-1} shows about a 5 fold difference in the calculated values of K_7. The decrease in K_7 is roughly proportional to the decrease of the K_3 so that the actual value of K_7 is sensitive to the formation constant for the vanadate ester that is formed. Unfortunately not enough of this phosphono derivative was available to allow measurement of the formation constant. The value for K_3 is, however, not likely to be outside the range 0.5 to 2.5 M^{-1}.

A comparsion of the K_7 values obtained for 2-V-3PGA and 2-V-3PMGA shows that the K_7 value obtained for 2-V-3PGA is more than 10^3-fold higher than that for 2-V-3PMGA. The structural parameters for the DL-2-amino-4-phosphonobutanic acid monohydrate and barium D-3-phosphoglycerate dihydrate that have been obtained from X-ray diffraction studies have shown that the major structural differences between these two compounds are centered around the bond length (C_4-P_1 = 0.1807 nm in the phosphono analogue and O_4-P_1 = 0.1590 nm in 3-PGA) and the bond angle (C_3-C_4-P_1 = 111.5° in the phosphono analogue and C_3-O_4-P_1 = 123.2° in the 3-PGA)[56]. Thus, it may be the more acute C_3-C_4-P_1 bond angle and the longer C_4-P_1 bond distance which leads to a lost of a hydrogen bond on the bridging oxygen atoms, thus weaken the interactions of 3-PMGA to PGM when compared to that of 3-PGA. Another important difference is that the dissociation constants for the final deprotonation of alkyl phosphonates, in general, corresponds to higher pK_a values than for the

corresponding phosphates. In the present case the second of pK_a values for 3-PGA and 3-PMGA are 6.20 and 7.45, respectively.[57] Thus the net charge on 2-V-3-PMGA probably is quite different from that on 2-V-3-PGA at pH 7.0, assuming that the vanadate does not affect the pK_a values significantly. At pH 7.0, the phosphono group of 3-PMGA is essentially fully monoanionic while the phosphoryl group of 3-PGA is predominantly in the dianionic form. This suggests that a main contribution to the specificity of substrate binding for PGM is electrostatic in nature, the interaction between the dianionic phosphoryl group of the substrate and one or more positively charged groups on the enzyme will be prefered over the interaction between the monoionic phosphono group and the enzyme.

Studies of the interaction of vanadate and glyceric acid by ^{51}V NMR spectroscopy have shown that the complexity is even greater than that between lactate and vanadate.[10] No direct evidence for formation of acyclic esters of vanadate was obtained, mainly because of signal overlap complicated by the presence of other products, including pentacoordinate complexes similar to those formed between vanadate and ethylene glycol, propylene glycol and lactate. In the case of ethylene glycol, the acyclic esters formed are 2-hydroxyethyl vanadate and bis(2-hydroxylethyl)vanadate.[9] No evidence for a 1,2-cyclic tetrahedral vanadate ester was found. Thus in the case of glycerate, the acyclic glycerate

ester of vanadate that is expected to form will have only one vanadate atom attached to either the hydroxyl group in the C-2 or C-3 position of glyceric acid and the formation constant is estimated to be 0.54 M^{-1}, as for lactate. It can be seen from Figure III.10 that with the addition of up to 20 mM glyceric acid, only a small amount of V_8 is released per mole of enzyme. This might indicate that the vanadate ester of glycerate binds to dPGM about as strongly as V_2.

Glycolic acid has only one hydroxyl group at the C-2 position and is expected to form an ester with vanadate with a formation constant similar to that of lactate. From Figure III.7 and Table III.8, it can be seen that with the addition of 10 mM glycolic acid, no significant amount of bound vanadium was released from the enzyme. This indicates that the vanadate ester of glycolic acid binds very weakly to dPGM and is not competitive with the binding of V_2. The possibility that the formation of the ester is not favorable or that the ester formed does not bind to dPGM cannot be definitely excluded.

From the calculated curves it is apparent that a sigmoidal dependence of $[V_8]/[E_T]$ on the concentration of the substrate or the substrate analogue should be observable for $K_7 < 1x10^{-6}$ M. This derives from the assumption in the proposed mechanism that allows for the formation of the species, $EI(V_2)$, and requires that the binding of V_2 or I to

one site does not affect the affinity of the other site for either V_2 or I. There is a possibility that binding of a transition state analogue may prevent binding of divanadate in the active site of the second subunit. This possibility to an extent may be tested and Figure III.12 shows the experimental dependence of $[V_B]/[E_T]$ on [3-PGA] and two curves calculated with $K_7 = 1x10^{-11}$. One curve is obtained using the model depicted in Figure III.8 which allows for the formation of the species, $EI(V_2)$, while the second curve assumes a similar model but which excludes the existence of the species $EI(V_2)$. It is clear that the curve which allows for the formation of the species $EI(V_2)$ fits with the experimental data quite well while the second does not. This result suggests that the two subunits function independently of each other in agreement with the vanadate binding studies where neither positive nor negative cooperativity was observed.

It has been shown that the bound vanadium atoms were released from the PGM by addition of sufficient 2,3-DPG. This indicated strongly that the observed binding of vanadium or vanadate-ester occurred at the catalytic site of PGM and that the binding was neither nonspecific nor due to an impurity in the enzyme preparation. The enzyme preparation was highly purified, according to the supplier, and when it was assayed for mutase activity, it was found to

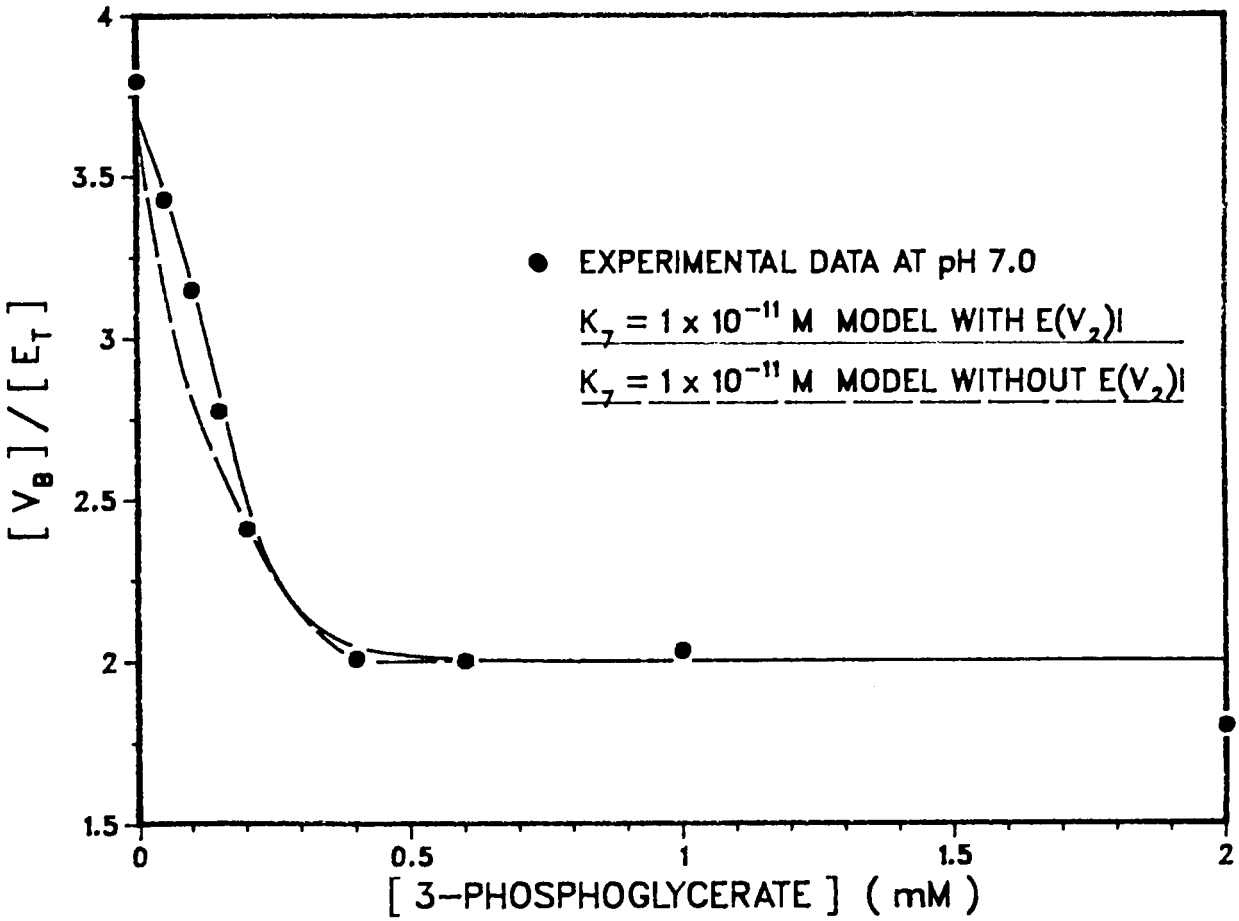

Figure III.12 Dependence of $[V_B]/[E_T]$ on 3-PGA concentration at pH 7.0. Experimental data from Table III.5 are shown with curves calculated with $K_7 = 1 \times 10^{-11}$ M and $K_3 = 2.5\ M^{-1}$. One curve is calculated from the model on Figure III.7, while the other one is calculated from the model as shown below:

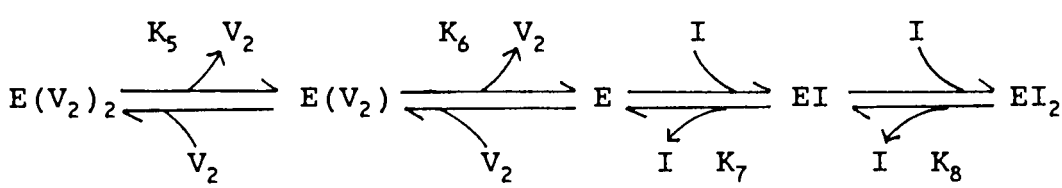

have a specific activity equal to the highest values reported in literature.[58]

III.C.5 Binding Studies of 2-Vanado-3-Phosphoglycerate to dPGM at pH 8.0

^{51}V NMR spectra were obtained from solutions containing a fixed concentration of dPGM and 1.0 mM V_T with varying concentration of 3-PGA at pH 8.0. The distribution of vanadate between the free and bound forms is tabulated in Table III.10 and the results displayed pictorially in Figure III.13. It can be seen from this table that when 3-PGA was added to the enzyme solution, the vanadate that was bound to PGM was released from the enzyme and a limiting stoichiometry of 2.0±0.1 mole of vanadate per mole of PGM was obtained in agreement with the value obtained at pH 7.0. These results are in accordance with the binding model developed for the pH 7.0 results (Figure III.8). That is, V_2 binds noncooperatively to each of the two subunits of PGM, and as vanadate ester is formed in aqueous solution and competes with divanadate for the catalytic site, two bound vanadate atoms are released from the enzyme while two remaining are bound as vanadate-ester. The experimental data of Figure III.12 are shown with the curves that were calculated as described in Appendix III. The agreement between calculated and experimental results is very good when K_7 equals to 7×10^{-11} M. This values corresponds to an

Table III.10 : Distribution of Vanadate among Free and Bound Forms in the Presence of dPGM and Various Concentrations of 3-PGA at pH 8.0.

$[3\text{-PGA}]_T$	$[V_{vis}]$	$[V_1]$	$[V_2]$	$[V_4]$	$[V_B]$	$[V_{B,vis}]$	$[V_{B,inv}]$	$[V_B]/[E_T]$
0	0.469	0.207	0.017	0.001	0.775	0.244	0.531	3.995
0.1	0.487	0.279	0.032	0.004	0.685	0.172	0.513	3.531
0.2	0.580	0.382	0.060	0.015	0.543	0.123	0.420	2.799
0.5	0.679	0.457	0.085	0.031	0.427	0.106	0.321	2.201
1.0	0.686	0.477	0.093	0.037	0.393	0.079	0.314	2.026
4.0	0.742	0.496	0.100	0.043	0.361	0.103	0.258	1.861
10.0	0.716	0.461	0.087	0.032	0.420	0.136	0.284	2.165

$[E_T]$ = 0.194 mM

Concentrations are in units of mM.
Experimental conditions: 1 mM vanadate, 20 mM HEPES, 6 mM KCl and various concentrations of 3-PGA as indicated at pH 8.0.

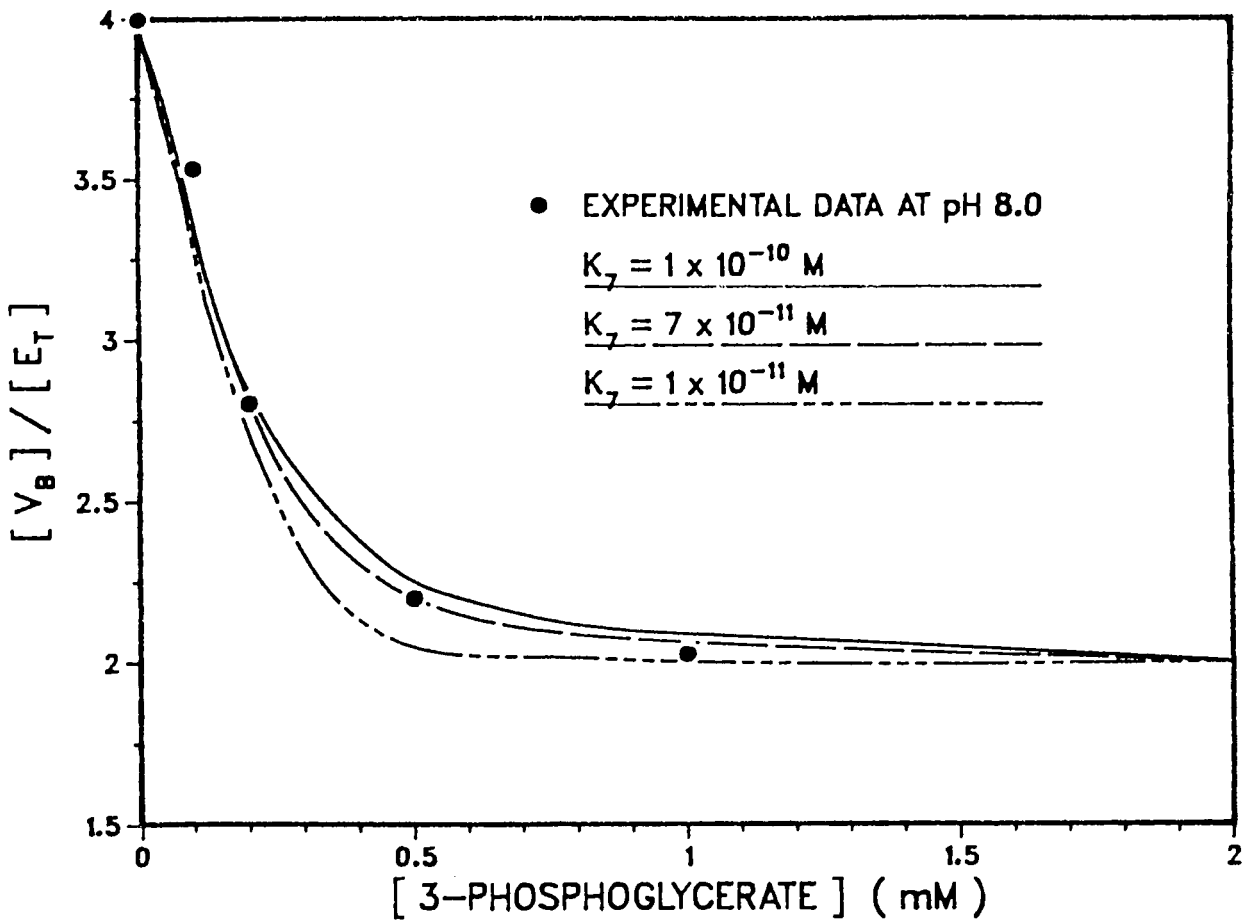

Figure III.13 Dependence of $[V_B]/[E_T]$ on the concentration of 3-PGA at pH 8.0. Experimental data from Table III.10 are shown with curves calculated with K_3 = 2.5 M^{-1} and various values of K_7.

intrinsic dissociation constant of $1x10^{-10}$ M and the values for the experimental dissociation constants K_8 and K_9 of $3x10^{-10}$ and $1x10^{-10}$ M, respectively. Table III.11 compares the K_7 values calculated and the corresponding dissociation constants for 2-V-3PGA binding to PGM at pH 7.0 and pH 8.0.

Table III.11: Dissociation constants of Binding 2-V-3PGA to dPGM at pH 7.0 and pH 8.0

pH	K_3 (M)	K_7 (M)	K_8 (M)	K_9 (M)	K_{id} (M)
7.0	2.5	$1x10^{-11}$	$4x10^{-11}$	$2x10^{-11}$	$2x10^{-11}$
8.0	2.5	$7x10^{-11}$	$3x10^{-10}$	$1x10^{-10}$	$1x10^{-10}$

Definations of dissociation constants and method of calculation are shown Appendix III with the model depicted in Figure III.8. K_3 is the formation constant of vanadate ester that used for the determination of K_7.

The interactions of vanadate with a variety alkyl alcohols have been studied in aqueous solution.[59] An interesting correlation between the pK_a values of the product esters and the pK_a of the parent alcohols was observed. It was found that below a pK_a for the alcohol of about 15 the pK_a values of the esters were essentially constant. However, above this value of 15, the pK_a of the

ester was found to increase rapidly with an increase in pK_a of alcohol. The pK_a value for the hydroxyl group of 3-PGA can be expected to be below 15 because of the electron withdrawing groups in adjacent positions. Thus the pK_{a2} values of 2-V-3PGA will be expected to be in the range of 8.0-8.5, not very much different from that of vanadate (pK_{a2} = 8.3) and vanadate ester formation (K_3) will be insensitive to pH. If the electrostatic interaction is a major factor that contributed to the binding of 2-V-3PGA to the active site of PGM at pH 7.0, then the 7 fold difference between the two K_7 values for pH 7.0 and pH 8.0 will not be expected since the ionization state of 2-V-3PGA will be similar for the two pH values. The increase in the value of K_7 at pH 8.0 over that at pH 7.0 probably does not correspond to a change in the net charge on the 2-V-3PGA. As previously discussed in Section II, a proton uptake was observed when high concentrations of either 2,3-DPG or the vanadate esters of 3-PGA or 2-PGA was added to the dPGM at a pH of about 7.0. This was explained by a disruption or formation of ionic bonds in the protein due to a conformational change as either vanadate ester or 2,3-DPG binds to dPGM. On the other hand, this increase of pH reading can be explained by a proton absorbed into the active site of PGM or the ligand in order to form a complex of E(2,3-DPG), E(2-V-3PGA) or E(3-V-2PGA). In this case, the formation of the enzyme complex is expected to be more favorable at the lower pH.

This clearly is what is observed, with the value of the dissociation constant at pH 8.0 increasing by a factor of about 7 over that at pH 7.0.

III.C.6 Source of Errors

A major source of error arises from the experimental procedure. Adjusting the pH of the enzyme containing solutions with acid or base can cause partial denaturing of the enzyme. This leads to a faulty determination of the bound vanadium and changes the value for E_T, the total enzyme in solution.

As mentioned previously, the formation constant of 2-V-3PGA (K_3) that was used for the calculation of the dissociation constants of 2-V-3PGA binding to PGM was obtained under the experimental condition of 1 M KCl ionic strength and pH 7.5.[35] As it has been shown in Table III.9, for the case of the binding of 2-V-3PMGA at pH 7.0 the value of K_7 obtained is directly proportional to the value of K_3 assumed, a small error in K_7 may arises by assuming the same value of K_3 (2.5 M^{-1}) for both pH 7.0 and pH 8.0.

The interaction between vanadate and 3-PMGA has not been studied. The formation constant of 2-V-3PMGA was assumed to be equal to that of 2-V-3PGA or 2-vanado-lactate. A small error in the value of K_7 may arise by assuming these values of K_3.

CHAPTER IV

SUMMARY AND FUTURE WORK

Binding of vanadate and vanadate esters to dephosphorylated rabbit muscle PGM has been studied by ^{1}H and ^{51}V NMR spectroscopy.

It has been shown by ^{1}H NMR studies that, upon pH titration, three C-2 protons of imidazole rings are freely accessible to solvent and show a change in chemical shift. From the pH dependence of the chemical shifts the pK_a values of these three histidine residues were determined. The values were 6.54, 5.24 and 5.20. Titration of a phosphoglycerate mutase enzyme solution with vanadate and with the vanadate esters of either 3-phosphoglycerate or its 3-phosphono analogue caused a decrease in intensity of two histidine signals. This decrease was accompanied by the appearance of two new signals. It is proposed that the signals which are affected by addition of transition state analogues originate from the two histidines at the active site of the enzyme and that these histidines participate in binding the substrate and analogues.

Investigation of the binding of inorganic vanadate to PGM shows a sigmoidal dependence of bound vanadate on the free vanadate concentration with a stoichiometry of four vanadium atoms per PGM molecule at saturating $[V_i]$. The data are consistent with binding of one divanadate ion to

each of the two identical subunits of PGM in a noncooperative manner with the intrinsic dissociation constants of 1.3×10^{-6} M and 1.3×10^{-7} M at pH 7.0 and 8.0, respectively. At pH 6.0, non-specific binding of vanadate to PGM was observed but at higher pH this non-specific binding is much less important.

Complexes formed from vanadate and 3-PGA have previously been studied by ^{51}V NMR spectroscopy.[35] The vanadate ester, 2-vanado-3-phosphoglycerate, was identified as one of the products formed. The binding of the dephosphorylated rabbit muscle PGM to the complex of 2-V-3-PGA, which is postulated to act as a transition state analogue to 2,3-DPG, has been studied. Two moles of vanadate atoms were found to be incorporated into each mole of dPGM when saturating amounts of vanadate and 3-PGA are available. The data are consistent with the binding of an individual 2-V-3-PGA to each of the two identical subunits of PGM in a noncooperative manner with an intrinsic dissociation constants of 2×10^{-11} M and 1×10^{-10} M at pH 7.0 and 8.0, respectively. Similar results were obtained using the phosphonate analogue of 3-PGA for which the intrinsic dissociation constants was estimated to be about 6×10^{-9} M (dependent on the assumed value of K_3) at pH 7.0. Weaker binding of a complex of vanadate and glyceric acid was observed, and no binding of a complex of vanadate and glycolic acid was observed.

The values of K_7 obtained dependend on the values of K_3 assumed. A study on the interaction of 3-PGA and 3-PMGA with vanadate under the same experimental condition used in the binding studies of the vanadate esters to PGM will be appropriate in order to obtain more accurate values of K_3 for the calculation of the dissociation constants of vanadate esters binding to dPGM.

Although two histidine residues are involved in the binding of the substrate and the substrate analogues, it is not possible to determine whether there is a convalent linkage to the bound moiety or whether it is bound by strong electrostatic interactions between the phosphate group and the histidine residues. If the crystalline rabbit muscle PGM/2-V-3PGA complexes could be formed, X-ray crystallography will be an appropriate technique for studying the binding of the transition state analogue to rabbit muscle PGM. Cloning of the DNA sequence and performing site directed mutagensis on the histidine residues at the active site will modify the enzyme. Studies of this modified enzyme by ^1H NMR spectroscopy may help to distinguish the role that each histidine plays in the mutase reaction.

APPENDIX I

Rates of the phosphoglycerate mutase reaction were measured as described by Carreras using a coupled assay containing enolase, pyruvate kinase, lactate dehydogenase to convert the products of mutase reaction to lactate as shown in Scheme 1.[53] Concentrations and conditions were: 20 mM imidazole buffer, pH 7.0, 5.0 mM KCl, 0.04 μg/ml PGM, 50 μg/ml enolase, 50 μg/ml pyruvate kinase (PK), 25 μg/ml lactate dehydrogenase(LDH), 50 μM NADH, 300 μM ADP and 1 mM 3-PGA at 23°C. Rates were found to be unaffected by increasing the concentration of coupling enzymes by 2-fold. All spectrophotometric assays were performed by using a Hewlett-Packard 8452A diode array UV/VIS spectrophotometer with the HP 9153B chemstation software package. In all cases, rates of the mutase reaction were monitored by the change in absorbance of NADH at 340 nm (ϵ_{340nm} = 6.22 mM^{-1} cm^{-1}) as a function of time. The enzyme assay was generally initiated by the addition of 2,3-DPG to a preincubation mixture of the PGM, coupling enzymes and the remaining reagents.

Scheme 1

coupling assay for PGM reaction

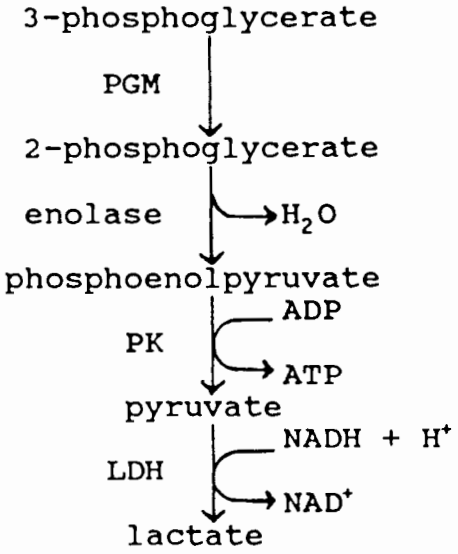

APPENDIX II

Since the exchange rates of protons on and off the nitrogen of the imidazole ring are fast (>2000 sec^{-1}) compared to the NMR chemical shift differences (100-400 Hz), the chemical shift (δ_{obs}) is a weighted average of the chemical shifts of the unprotonated (δ_A) and protonated (δ_{HA}) forms of the histidine. If the amounts of these forms are [A] and [HA] respectively; and the total amount is $[A_T]$, the two Equations A2.1 and A2.2 can be solved as followed:

$$|\delta| = \frac{[A]}{[A_T]} |\delta_A| + \frac{[HA]}{[A_T]} |\delta_{HA}| \qquad \text{A2.1}$$

$$[A_T] = [A] + [HA] \qquad \text{A2.2}$$

Thus we have,

$$\frac{[A]}{[A_T]} = \frac{|\delta_{HA}| - |\delta_{obs}|}{|\delta_{HA}| - |\delta_A|} \qquad \text{A2.3}$$

and

$$\frac{[HA]}{[A_T]} = \frac{|\delta_{obs}| - |\delta_A|}{|\delta_{HA}| - |\delta_A|} \qquad \text{A2.4}$$

If K_a is the acidity constant, i.e., $K_a = \frac{[H^+][A]}{[HA]}$,

then substitution of Equation A2.3 and A2.4 that for K_a will give Equation A2.5.

$$K_a = [H^+] \frac{|\delta_{HA}| - |\delta_{obs}|}{|\delta_{obs}| - |\delta_A|} \qquad \text{A2.5}$$

Taking the logarithm of both sides of Equation A2.5 and rearranging provides a linearized version of the titration curve (Henderson-Hasselbalch equation) and a plot of pH vs the chemical shift term in Equation A2.8 will give a line of unit slope with a y-intercept equal to the value of pK_a.

$$\log K_a = \log [H^+] + \log \frac{|\delta_{HA}| - |\delta_{obs}|}{|\delta_{obs}| - |\delta_A|} \qquad \text{A2.6}$$

$$-pK_a = -pH + \log \frac{|\delta_{HA}| - |\delta_{obs}|}{|\delta_{obs}| - |\delta_A|} \qquad \text{A2.7}$$

$$pH = pK_a + \log \frac{|\delta_{HA}| - |\delta_{obs}|}{|\delta_{obs}| - |\delta_A|} \qquad \text{A2.8}$$

The experimental points were fitted to theoretical titration curves using a least-squares fit program on an IBM computer.

APPENDIX III

The definitions of the equilibrium constants required in the development of the proposed mechanism for vanadate ester inhibition of rabbit muscle PGM (as shown in Figure III.8) are listed in the following equations:

$$K_2 = \frac{[V_2]}{[V_i]^2} \qquad \text{A3.1}$$

$$K_3 = \frac{[I]}{[PGA][V_i]} \qquad \text{A3.2}$$

$$K_4 = \frac{[V_4]}{[V_i]^4} \qquad \text{A3.3}$$

$$K_5 = \frac{[E(V_2)][V_2]}{[E(V_2)_2]} \qquad \text{A3.4}$$

$$K_6 = \frac{[E][V_2]}{[E(V_2)]} \qquad \text{A3.5}$$

$$K_7 = \frac{[E][I]}{[EI]} \qquad \text{A3.6}$$

$$K_8 = \frac{[EI][I]}{[EI_2]} \qquad \text{A3.7}$$

$$K_9 = \frac{[E(V_2)][I]}{[EI(V_2)]} \qquad \text{A3.8}$$

$$K_{10} = \frac{[EI][V_2]}{[EI(V_2)]} \qquad \text{A3.9}$$

The conservation equations are:

$$[V_B] = 4[E(V_2)_2] + 2[E(V_2)] + [EI] + 2[EI_2] + 3[EI(V_2)] \qquad \textbf{A3.10}$$

$$[E_T] = [E(V_2)_2] + [E(V_2)] + [E] + [EI] + [EI_2] + [EI(V_2)] \qquad \textbf{A3.11}$$

$$[V_T] = [V_i] + 2[V_2] + 4[V_4] + [I] + 4[E(V_2)_2] + 2[E(V_2)] + [EI] + 2[EI_2] + 3[EI(V_2)] \qquad \textbf{A3.12}$$

$$[PGA_T] = [PGA] + [EI] + 2[EI_2] + [I] + [EI(V_2)] + [I] \qquad \textbf{A3.13}$$

From the definitions of the equilibrium constants in Equation A3.1 to A3.9, the following expressions were obtained for substitution into the conservation equations in Equations A3.10 to A3.12.

$$[V_2] = K_2[V_i]^2 \qquad \textbf{A3.14}$$

$$[V_4] = K_4[V_i]^4 \qquad \textbf{A3.15}$$

$$[I] = K_3[PGA][V_i] \qquad \textbf{A3.16}$$

$$[E(V_2)] = \frac{[E][V_2]}{K_6} = \frac{K_2[E][V_i]^2}{K_6} \qquad \textbf{A3.17}$$

$$[E(V_2)_2] = \frac{[E(V_2)][V_2]}{K_5} = \frac{K_2^2[E][V_i]^4}{K_5K_6} \qquad \textbf{A3.18}$$

$$[EI] = \frac{[E][I]}{K_7} = \frac{K_3[E][PGA][V_i]}{k_7} \qquad \textbf{A3.19}$$

$$[EI_2] = \frac{[EI][I]}{K_8} = \frac{K_3^2[E][PGA]^2[V_i]^2}{k_7 K_8} \qquad \textbf{A3.20}$$

$$[EI(V_2)] = \frac{[E(V_2)][I]}{K_9} = \frac{K_2 K_3[E][PGA][V_i]^3}{k_6 K_9}$$

$$= \frac{[EI][V_2]}{K_{10}} = \frac{K_2 K_3[E][PGA][V_i]^3}{K_7 K_{10}} \qquad \textbf{A3.21}$$

By making the appropriate substitutions into Equations A3.11 to A3.13 (including $K_5 = 4K_6$ and $K_8 = 4K_7$, which are required if the binding of V_2 and I are to be noncooperative) and rearranging, Equation A3.22 can be obtained from Equation A3.13, Equation A3.23 from Equation A3.11 and Equation A3.24 from Equation A3.12.

$$\frac{K_3^2[E][PGA]^2[V_i]^2}{2K_7^2} + [PGA]\left\{1+K_3[V_i]\left(1 + \frac{[E]}{K_7} + \frac{[E][V_i]^2 K_2}{K_6 K_9}\right)\right\}$$

$$- [PGA_T] = 0 \qquad \textbf{A3.22}$$

where [E] is defined as:

$$[E] = \frac{4K_6^2 K_7^2 K_9 [E_T]}{\{4K_6^2 K_7^2 K_9 + 4K_6^2 K_7 K_9 K_3[PGA][V_i] +}$$

$$(4K_2 K_6 K_7^2 K_9 + K_6^2 K_9 K_3^2[PGA]^2)[V_i]^2 +$$

$$4K_6 K_7^2 K_2 K_3[PGA][V_i]^3 + K_2^2 K_7^2 K_9[V_i]^4\} \qquad \textbf{A3.23}$$

$$4[V_i]^4\left(K_4 + \frac{K_2^2[E]}{4K_6^2}\right) + 3[V_i]^3\left(\frac{K_2K_3[E][PGA]}{K_6K_9}\right)$$

$$+ 2[V_i]^2\left(K_2 + \frac{K_2[E]}{K_6} + \frac{K_3^2[E][PGA]^2}{4K_7^2}\right)$$

$$+ [V_i]\left(1 + K_3[PGA] + \frac{K_3[PGA][E]}{K_7}\right) - [V_T] = 0$$

A.24

These equations can be used, given values for the equilibrium constants and $[V_T]$, $[E_T]$ and $[PGA]_T$, to calculate equilibrium values of $[V_i]$ and $[PGA]$, these can then be used in Equation A3.25, which was obtained from Equation A3.10, to calculate $[V_B]/[E_T]$.

$$\frac{[V_B]}{[E_T]} = \frac{\dfrac{4K_2^2[V_i]^4}{4K_6^2} + \dfrac{2K_2[V_i]^2}{K_6} + \dfrac{K_3[PGA][V_i]}{K_7} + \dfrac{2K_3^2[PGA]^2[V_i]^2}{4K_7^2} + \dfrac{3K_2K_3[PGA][V_i]^3}{K_6K_9}}{\dfrac{K_2^2[V_i]^4}{4K_6^2} + \dfrac{K_2[V_i]^2}{K_6} + 1 + \dfrac{K_3[PGA][V_i]}{K_7} + \dfrac{K_3[PGA]^2[V_i]^2}{4K_7^2} + \dfrac{K_2K_3[PGA][V_i]^3}{K_6K_9}}$$

A3.25

The iterative procedure is as follows:

Step 1: Assume a reasonable value of $[V_i]$ for a given value of $[PGA_T]$. The experimental value can then be used

as a reasonable first approximation. [PGA] can then be solved quadratically from Equation A3.22. A value of [PGA] which gives a value of zero, to within ±0.001 mM, for the left hand side of Equation III.22 will then be obtained.

Step 2: The value of [PGA] obtained in Step 1 and the value of $[V_i]$ used in Step 1 will be used to calculate the left hand side of Equation A.24. If zero, within ±0.001 mM, is not obtained from Equation A3.24, the value $[V_i]$ has to be changed in the appropriate direction, and this value of $[V_i]$ will be used in the next execution of Step 1.

Step 3: The sequence of Step 1, 2, 1, 2, ... will be continued until the values of [PGA] and $[V_i]$, which satisfy both Equations A3.22 and A3.24 to within ±0.001 mM, are obtained. These [PGA] and $[V_i]$ values will then be substituted into Equation A3.25 for calculation of $[V_B]/[E_T]$.

REFERENCES

1. Chasteen, N.D., (1983) Structure and Bonding (Berlin) 53, p105-138.

2. Ramasarma, T. and Crane, F.L., (1981) Current Topic in Cell. Reg. 20, p247-301.

3. "Merck Index (1976)" 9th edition, Merck & Co., New Jersey, U.S.A.

4. Nicholls, D., (1979) "Complexes and First Row Transition Elements", Macmillan Press, London.

5. Lindquist, R.N., Lynn, J.L. Jr. and Lienhard, G.E., (1973) J. Am. Chem. Soc. 95, p8762-8768.

6. Pope, M.T., Still, E.R., Williams, R.J.P., (1980) "A Comparison Between the Chemistry and Biochemistry of Molybdenum and Related Elements in Molybdenum Containing Enzyme", Pergamon Press, New York, p1-40.

7. Knowles, J.R., (1980) Ann. Rev. Biochem. 49, p877-919.

8. Gresser, M.J. and Tracey, A.S., (1985) J. Am. Chem. Soc. 107, p4215-4220.

9. Gresser, M.J. and Tracey, A.S., (1986) J. Am. Chem. Soc. 108, p1935-1939.

10. Tracey, A.S., Gresser, M.J. and Parkinson, K.M., (1987) Inorg. Chem. 26, p629-638.

11. Tracey, A.S. and Gresser, M.J., (1988) Inorg. Chem. 27, p2695-2702.

12. Tracey, A.S., Gresser, M.J. and Liu, S., (1988) J. Am. Chem. Soc. 110, p5869-5874.

13. Ninfali, P., Aecorsi, A., Fazi, A., Palma, F. and Farnaini, G., (1983) Arch. Biochem. Biophys. 226, p441-447.

14. Borah, B., Chen, C.-W., Egan, W., Miller, M., Wlodawer, A. and Cohen, J.S., (1985) Biochemistry 24, p2058-2067.

15. Wlodawer, A., Miller, M. and Sjölin, L., (1983) Proc. Natl. Acad. Sci. U.S.A. 80, p3628-3631.

16. Nour-Eldeen, A.F., Craig, M.M. and Gresser, M.J., (1985) J. Biol. Chem. 260, p6836-6840.

17. Blattler, W.A. and Kowles, J.R., (1980) Biochemistry 19, p738-743.

18. Ray, W.J. and Peck, E.J., (1972) "The Enzymes" 3rd edition, edited by Boyer, P.D., New York: Academic Press, 6, p407-477.

19. Forthergill, L.A. and Harkin, R.N., (1982) Proc. R. Soc. Lond. B215, p19-24.

20. Campbell, J.W., Watson, H.C. and Hodgson, G.I., (1974) Nature 250, p301-303.

21. Rose, Z.B., (1970) Archs. Biochem. Biophys. 140, p508-513.

22. Forthergill, L.A. and Haggarty, N.W., (1980) FEBS LETTERS 109, p18-20.

23. Forthergill, L.A.and Harkins, R.N., (1982) Proc. R. Soc. Lond. B215, p19-24.

24. Carne, T.J., McKay, D.J. and Flynn, T.G., (1976) Can. J. Biochem. 54, p307-320.

25. Sheibley, R.H. and Hass, F.L., (1976) J. Biol. Chem. 251, p6699-6704.

26. Czok, R. and Bücher, Th., (1960) Adv. Protein Chem. 15, p377.

27. Winn, S.I., Watson, H.C. and Harkins, R.N., (1981) Phil. Trans. R. Soc. Lond. B293, p121-130.

28. Rose, Z.B., (1971) Arch. Biochem. Biophys. 146, p359-360.

29. Laforet, M.T., Butterfield, J.B. and Alpers, J.B., (1974) Arch. Biochem. Biophys. 165, p179-187.

30. Rose, Z.B., (1980) in "Advances in Enzymology", edited by Meister, A., John Wiley & Sons, New York, 51, p211-253.

31. Vives-Corrons, J.L., Jou, J.M., Ester A., Ibars. M., Carreras, J., Bartons, R., Climent, F. and Grisolia, S., (1981) Biochem. Biophys. Res. Commun. 103, p111-117.

32. Poillon, W.N., Robinson, M.D. and Kim, B.C., (1985) J. Biol. Chem. 260, p13897-13900.

33. Stankiewicz, P.J., Gresser, M.J., Tracey, A.S. and Hass, L.F., (1987) Biochemistry 26, p1264-1269.

34. Stankiewicz, P.J., Gresser, M.J., and Hass, L.F., in press.

35. Tracey, A.S. and Gresser, M.J., unpublished result.

36. Wuthrich, K., (1986) "NMR of Proteins and Nucleotides", Wiley, New York.

37. Jardetzky, O. and Roberts, G.C.K., (1981) "NMR in Molecular Biology", Academic Press, New York.

38. Wuthrich, K., (1976) "NMR in Biological Research: Peptides and Proteins", North-Holland Publishing Company.

39. Campbell, I.D., Dobson, C.M. and Williams, R.J.P., (1975) Proc. R. Soc. Lond. A. 345, p23-40.

40. Lowry, O.H., Rosebrough, N.J., Farr, A.L. and Randall, R.J., (1951) J. Biol. Chem. 193, p265.

41. Fersht, A., (1985) "Enzyme Structure and Mechanism", 2nd edition, W.H. Freeman and Company, New York, Chapter 5, p.170.

42. Stankiewcz, P.J. and Hass, L.F., (1986) J. Biol. Chem. 261, p12715-12721.

43. McAleese, S.M., Forthergill-Gilmore, L.A. and Dixon, H.B.F., (1985) Biochem. J. 230, p535-542.

44. Yount, R.G., (1975) "Advances in Enzymology (and Related Areas of Molecular Biology)", John Wiley & Sons, New York, 43, p1-51.

45. Pizer, L.I. and Ballou, C.E., (1959) J. Biol. Chem. 234, p1138-1142.

46. Winn, S.I., Watson, H.C., Forthergill, L.A. and Harkins, R.N., (1977) Biochem. Soc. Trans. 5, p657-659.

47. Rodwill, V.W., Towne, J.C. and Grisolia, S., (1957) J. Biol. Chem. 228, p875-885.

48. Roberts, G.C.K., Dennis, E.A., Meadows, D.H., Cohen, J.S. and Jardetzky, O., (1969) Biochemistry 62, p1151-1158.

49. Rehder, D., (1982) Bull. Magn. Reson. 4, p33-83.

50. O'Donnell, S.E. and Pope, M.T., (1976) J. Chem. Soc. Dalton Trans., p2290-2297.

51. Habayeb, M.A., Hileman, O.E. Jr., (1980) Can. J. Chem. 58, p2255-2261.

52. Borgen, O., Mahmoud, M.R. and Skauvik, I., (1977) Acta Chem. Scan. A31, p329.

53. Heath, E. and Howarth, O.W., (1981) J. Chem. Soc. Dalton Trans., p1105-1110.

54. Butler, A. and Danzitz, N.J., (1987) J. Am. Chem. Soc. 109, p1864-1865.

55. Vilter, H. and Rehder, D., (1987) Inorg. Chem. Acta 136, p107.

56. Kamiya, K., Cruse, W.B.T. and Kennard, O., (1983) Biochem. J. 213, p217-223.

57 Orr, G.A. and Kowles, J.R., (1974) Biochem. J. 141, p721-723.

58. Grisolia, S., (1962) Methods in Enzymology 5, p236.

59. Tracey, A.S., Galeffi, B. and Mahjour, S., (1988) Can. J. Chem. 66, p2294-2298.